Aus dem Institut für Neuropathologie
der Medizinischen Fakultät Charité – Universitätsmedizin Berlin

DISSERTATION

Characterization of the nature and consequence of the microglia response to high fat diet

zur Erlangung des akademischen Grades
Doctor of Philosophy (PhD)

vorgelegt der Medizinischen Fakultät
Charité – Universitätsmedizin Berlin

von

Caroline Baufeld
aus Berlin

Datum der Promotion: 09.09.2016

Table of contents

1 Abstract

Obesity is a disease affecting millions of people worldwide. In adipose tissue, obesity leads to chronic low-level inflammation mediated by infiltrating macrophages, which ultimately results in insulin resistance. Recent work exploring the effects of obesity and metabolic disease on the central nervous system (CNS) revealed that long-term high fat diet (HFD) leads to brain inflammation and leptin resistance in the hypothalamus. Microglia, the brain's intrinsic immune cells, play an essential role in physiological brain functions, including pruning of neuronal synapses and regulation of brain development, and respond to disease or injury to the CNS. Fitting with the notion that diets high in fat content are harmful to the brain, an altered microglia phenotype was detected in the hypothalamus of rats as early as 3 days after the start of HFD. The first aim of this thesis was to further elucidate the response of microglia to short-term and prolonged HFD exposure. The analyses of whole hypothalamic tissue and isolated microglia of HFD-fed mice revealed a distinct response of microglia to diet, including a shift in the microglia gene expression profile from pro-inflammatory in response to short-term HFD exposure to an anti-inflammatory or rather subdued phenotype following prolonged HFD. To dissect the role hypothalamic microglia might play in the regulation of body weight homeostasis, the CD11b-HSVTK mouse model was used, which allows for a specific and inducible depletion of microglia. Following microglia depletion, endogenous microglia are replaced by bone marrow-derived myeloid cells. This process appears to induce metabolic changes in CD11b-HSVTK mice that are independent of the diet such that microglia-depleted CD11b-HSVTK mice displayed a reduced body weight compared to wild-type mice when fed with either chow or HFD. From the performed analyses it can be concluded that the body weight phenotype is due to the phenomenon of myeloid cell repopulation that is taking place in microglia-depleted mice.

Taken together, the response of microglia to diets high in fat is not solely pro-inflammatory, but changes over prolonged exposure to HFD, which may represent a neuroprotective response. This shift in the microglia response should be further explored, and kept in mind when devising CNS-targeted treatment strategies for obesity. Moreover, the function microglia may exert in the regulation of body weight homeostasis in the hypothalamus remains unclear and requires further investigation.

2 Zusammenfassung

Übergewicht ist weltweit eines der größten Gesundheitsprobleme und ein Risikofaktor für chronische Krankheiten wie Diabetes, Herz-Kreislauf-Erkrankungen und Krebs. Untersuchungen der letzten Jahre haben gezeigt, dass bei Übergewicht durch Makrophagen ausgelöste Entzündungsprozesse in metabolisch aktiven Organen eine entscheidende Rolle spielen und zu Insulin- und Leptinresistenz führen können. Neben der Entzündung in der Peripherie konnte auch eine mit Übergewicht assoziierte Entzündung im zentralen Nervensystem (ZNS), speziell im Hypothalamus, detektiert werden. Mikroglia, die intrinsischen Immunzellen des Gehirns, spielen eine wesentliche Rolle in der Gehirnentwicklung und bei physiologischen Gehirnfunktionen, einschließlich der Bildung von neuronalen Synapse, und reagieren auf pathologische Prozesse oder Verletzungen des ZNS. Entsprechend der Vorstellung, dass fettreiche Ernährung schädlich für das Gehirn ist, wurde eine Reaktion der Mikroglia bereits 3 Tage nach Beginn einer fettreichen Diät (high fat diet, HFD) im Hypothalamus von Ratten beobachtet. Das erste Ziel dieser Arbeit war es, aufzuklären, auf welche Weise Mikroglia auf HFD reagieren. Die Analyse von Hypothalamusgewebe sowie isolierter Mikroglia aus dem Hypothalamus von HFD gefütterten Mäusen offenbarte eine deutliche Antwort der Mikroglia auf die fettreiche Ernährung. Diese war anfänglich (nach 3 Tagen) geprägt von der Expression pro-entzündlicher Marker, die sich bei längerer Fütterung (8 Wochen) zu einem anti-entzündlichen Expressionsprofil veränderte. Um bestimmen zu können, ob hypothalamische Mikroglia eine Rolle bei der Regulation des Körpergewichts spielen, wurde das CD11b-HSVTK Mausmodell genutzt, welches eine spezifische Depletion der Mikroglia ermöglicht. Das Ausschalten der Mikroglia führt zu einem Einwandern von aus dem Knochenmark stammenden myeloiden Zellen, die die endogenen Mikroglia ersetzen. Dieser Prozess scheint Stoffwechselveränderungen in den CD11b-HSVTK Mäusen auszulösen, die dazu führten, dass diese Mäuse ein geringeres Körpergewicht aufwiesen als die transgen-negativen Kontrolltiere und zwar unabhängig davon, ob sie mit HFD oder Kontrollfutter gefüttert wurden. Aus den durchgeführten Analysen lässt sich schließen, dass der Phänotyp der Veränderung des Körpergewichts auf die Einwanderung der peripheren myeloiden Zellen in das ZNS nach Depletion der endogenen Mikrogliazellen zurückgeführt werden kann.

Zusammengefasst zeigen die Ergebnisse dieser Arbeit, dass die Reaktion der Mikroglia auf eine fettreiche Ernährung nicht ausschließlich pro-entzündlich, sondern dass sie

sich im Laufe einer längeren fettreichen Ernährung verändert und letztlich eine neuroprotektive Rolle übernehmen könnte. Diese funktionelle Verschiebung der Mikroglia-Aktivität gilt es in künftigen Studien weiter zu untersuchen und dies gleichermaßen zu beachten, wenn es darum geht, Behandlungsstrategien zu entwickeln, die darauf abzielen, Mikroglia bei HFD zu manipulieren. Darüber hinaus ist eine mögliche Beteiligung der Mikroglia im Hypothalamus an der Regulation des Körpergewichts weiterhin unklar und sollte Gegenstand weiterer, dezidierter Untersuchungen sein.

3 Introduction

3.1 Obesity

Obesity is a major health problem worldwide that contributes to chronic diseases, such as diabetes, cardiovascular diseases and cancer. According to the World Health Organization (WHO), the worldwide prevalence of obesity has more than doubled since 1980 (Figure 1) with approximately 1.9 billion adults being overweight worldwide in 2014; 600 million of these were obese. Body mass index (BMI), which is defined as the weight in kilograms divided by the square of the height in meters (kg/m^2), represents a classical way to judge whether a person is overweight or obese. Persons with a BMI>25 are classified as overweight and >30 as obese. A BMI above 25 is already associated with a higher mortality [1-3] and is a risk factor for various diseases, e.g. cardiovascular diseases, type 2 diabetes, certain types of cancer and musculoskeletal disorders. Over the next 20 years, obesity is predicted to comprise 16 % of the total health care costs in Western countries [4].

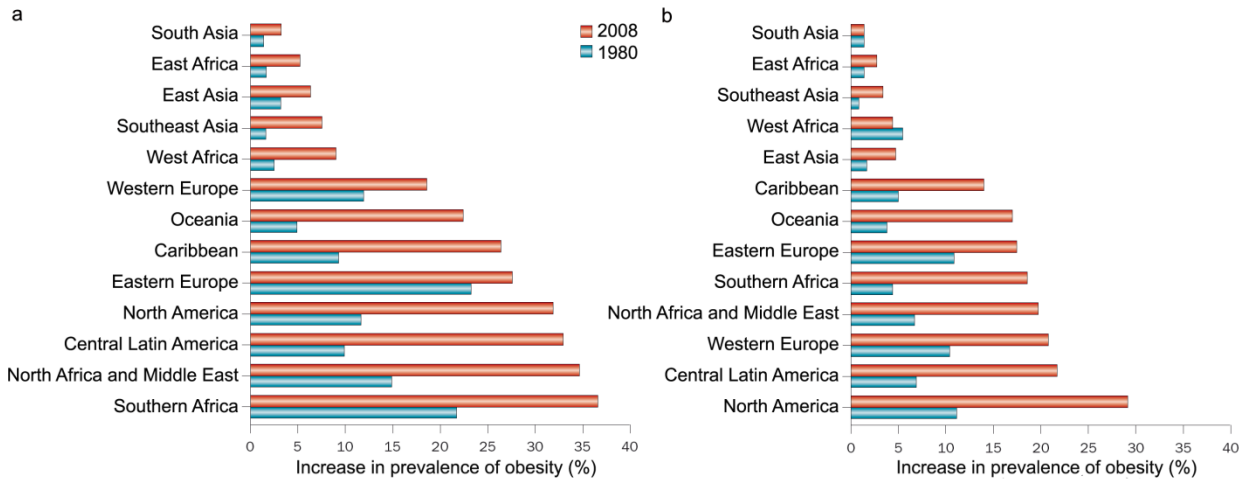

Figure 1: Percentage of overweight and obese (a) women and (b) men with a BMI over 25 in 1980 and 2008 by regions of the world (reprinted by permission from Macmillan Publishers Ltd: Nature Reviews Endocrinology [5], copyright (2013)).

The reasons for this epidemic might be environmental factors supporting the positive imbalance between energy intake and energy expenditure. Studies indicate that an increase in the quantity and energy density of food consumption, the increase in dietary fat intake in particular, as well as a decrease in physical activity account for the increase

in adiposity [6-8]. Along the same lines epidemiological studies revealed a positive correlation between increased fat contents in the diet and increased incidence of obesity [9–11]

Furthermore, a genome-wide association (GWA) study identified a SNP in the fat mass and obesity-associated gene (FTO) that is associated with a 1.67 fold increased risk of obesity compared to individuals without the allele [6, 12]. Lastly, social factors might also play an important role as a person's risks of becoming obese is increased by 57 % if a friend became obese or 37-40 % if the person had a sibling or spouse who became obese [6].

As a result of these startling statistics, great efforts are required to prevent and treat obesity as well as to gain a better understanding of the physiological processes underlying this disease.

3.2 Central regulation of body weight

Energy homeostasis is a process that adjusts food intake and energy expenditure over time to secure stability in the amount of stored body energy [13]. This process is tightly regulated by hormones (e.g. leptin, insulin or ghrelin; see Figure 2 a), which are secreted by metabolically active organs. In addition to their direct actions on the metabolic tissues themselves, their signaling to the CNS controls important aspects of metabolism [14]. The most important ones to be mentioned here are insulin and leptin. Leptin is secreted by adipocytes and insulin by the pancreatic β-cells. Both of their blood concentrations have been found to be elevated with increasing adiposity, and deficiency of either hormone promotes obesity [14]. These factors enter the CNS in proportion to their plasma levels [15] and can thus inform the brain of changes in fat mass [16, 17] and initiate an adjustment of energy balance.

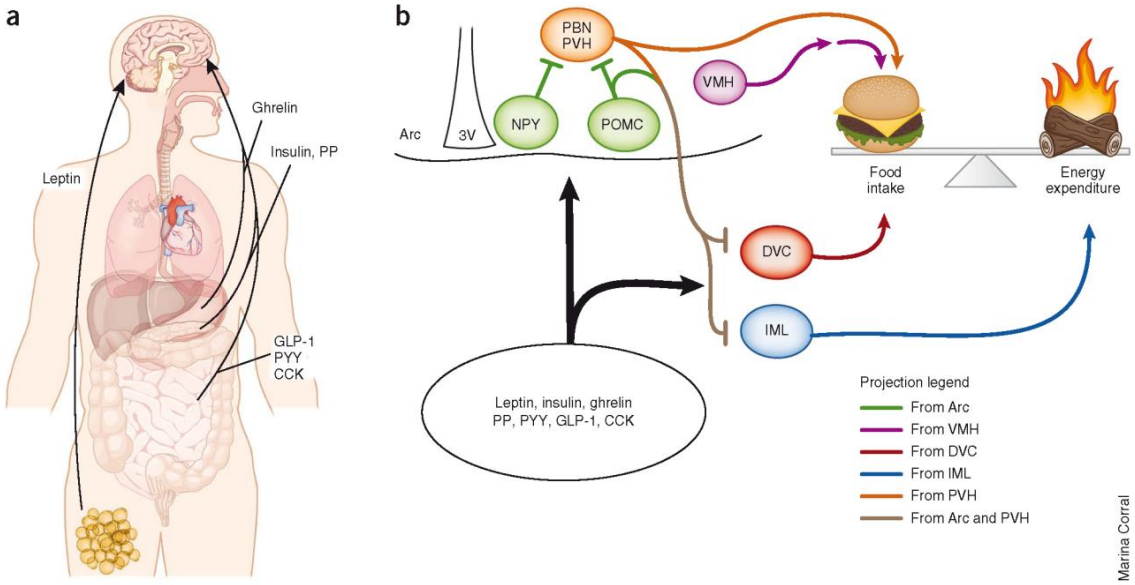

Figure 2: Central regulation of food intake and energy expenditure. (a) Various factors produced by peripheral metabolically active organs inform the CNS about the nutrient status of the body. (b) These factors modulate food intake and energy expenditure by activation or inhibition of proopiomelanocortin (POMC) and neuropeptide Y (NPY) neurons in the arcuate nucleus (Arc). Paraventricular nucleus of the hypothalamus (PVH) and ventromedial hypothalamus (VMH) neurons, as well as hindbrain DVC interneurons, parabrachial nucleus (PBN) and spinal cord intermediolateral cell column (IML) neurons, also regulate or counter-regulate these activities. Abbreviations: PP, pancreatic polypeptide; PYY, peptide YY; GLP-1, Glucagon-like peptite-1; CCK, Cholecystokinin; 3V, third ventricle. (reprinted by permission from Macmillan Publishers Ltd: Nature Neuroscience [18], copyright (2012)).

The key regulators of energy balance, namely the pro-opiomelanocortin (POMC)- and neuropeptide-Y/agouti-related peptide (NPY/AgRP) neurons, can be found in the medial basal hypothalamus, more specifically in the arcuate nucleus (arc) [19] (Figure 2 b). The pro-hormone POMC is cleaved to produce α-melanocyte stimulating factor (α-MSH), which binds to melanocortin-3 and melanocortin-4 receptors to stimulate energy expenditure and suppress food intake. AgRP and NPY oppose α-MSH actions [14]. Insulin and leptin regulate POMC and NPY/AgRP expression by binding to their respective receptors expressed by both types of neurons. Thereby, leptin inhibits NPY/AgRP neurons and excites POMC neurons. Additionally, leptin abrogates inhibition of POMC neurons through collaterals from NPY/AgRP neurons [20]. Knocking out insulin or leptin receptors exacerbates obesity in mice [16, 21–24]. Although, restricting the leptin receptor knock-out to POMC-expressing neurons causes only mild obesity

suggesting that also other sites of leptin action must be important for leptin's regulation of energy homeostasis [25].

The neuronal leptin and insulin receptor signaling cascades can be seen in Figure 3. Upon binding of leptin to its receptor, the janus kinase (JAK) is recruited and phosphorylates the leptin receptor. This leads to activation and phosphorylation of STAT3, which in turn stimulates *Pomc* and inhibits *Agrp* expression by binding to the respective promoters [26]. Another signaling pathway activated by leptin is the phosphatidylinositol 3 kinase (PI3K) pathway. Similarly, the same signaling cascade is also activated through binding of insulin to its receptor. In this context, PI3K activates pyruvate dehydrogenase kinase (PDK1), which activates protein kinase B (PKB, also known as AKT). AKT regulates the activation of various proteins and transcription factors, e.g. FoxO1, AMPK and mTOR which are all implicated in the hypothalamic regulation of food intake and energy expenditure [26].

In addition to the induction of *Pomc*, STAT3 stimulates the expression of suppressor of cytokine signaling (*Socs3*), an inhibitor of leptin and insulin signaling [27]. High fat diet feeding increases SOCS3 expression and conversely, neuronal SOCS3 deficiency elevates leptin sensitivity and reduces obesity [28].

Obesity has long been associated with insulin or leptin resistance in peripheral tissues, but recently it has been shown that the hypothalamus also develops resistance to these hormones [29–31]. Increased SOCS3 expression in hypothalamic neurons is likely to be the cause of this resistance [32, 33] and might be linked to hypothalamic inflammation [33, 34]. This inflammation has recently gained considerable attention as a potential key event in the sustained imprinting (and 'set point' defining) of environmentally-induced obesity and will be discussed in the next chapters.

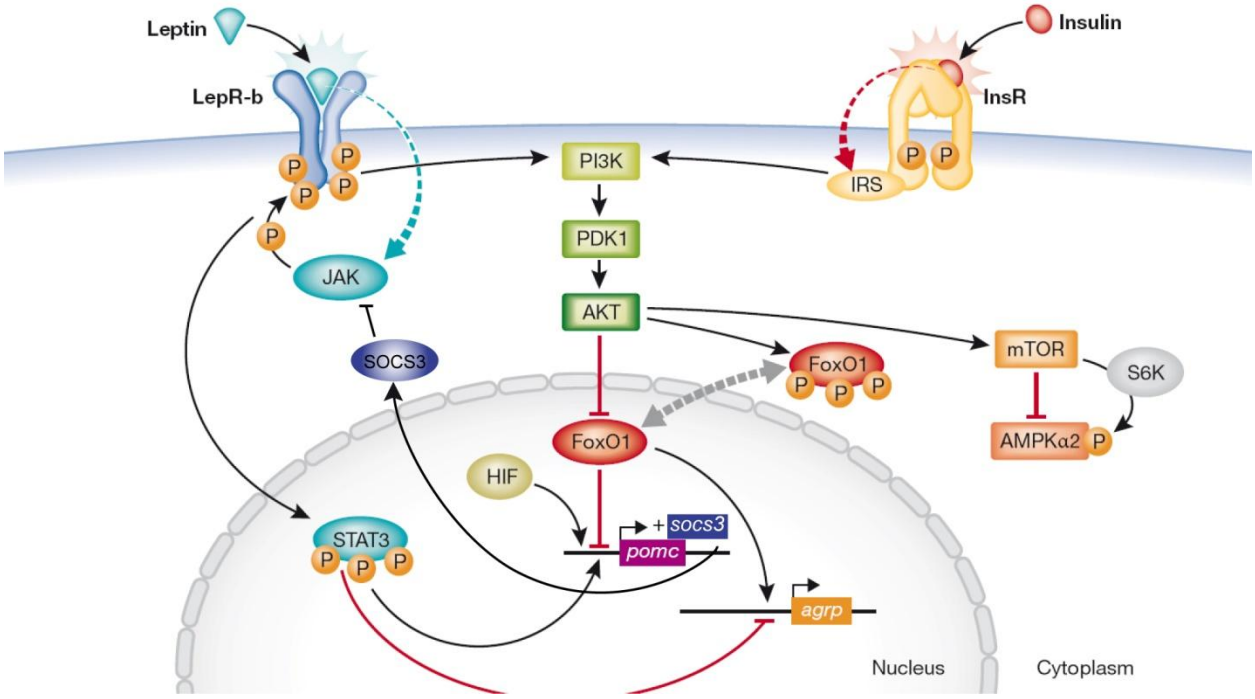

Figure 3: Insulin and leptin receptor signaling. Binding of leptin to its receptor activates the JAK/STAT or PI3K/AKT signaling cascade. Similarly, insulin receptor activation induces PI3K/AKT signaling. Both pathways activate various proteins and transcription factors, e.g. FoxO1, AMPK and mTOR, which activate or inhibit gene expression of genes involved in body weight homeostasis (e.g. *npy* or *pomc*). In addition, induction of *socs3* expression serves as a negative feedback of leptin receptor signaling. Abbreviations: JAK, janus kinase; STAT, Signal Transducers and Activators of Transcription; PI3K, phosphatidylinositol 3 kinase; AKT, protein kinase B; FoxO1, Forkhead box protein O1; AMPK, 5' AMP-activated protein kinase; mTOR, mammalian target of rapamycin. (reprinted by permission from John Wiley and Sons: EMBO Reports [26], copyright (2012))

3.3 Obesity-induced peripheral inflammation

It is well established that obesity causes inflammation in metabolic active organs [35-37]. However, it has to be emphasized that this is not a traditional type of inflammation as is induced by injury, but rather a ‘low-grade’ or ‘chronic’ inflammation triggered by nutrients and metabolic homeostatic changes over a long period of time, which is mediated by similar molecules and signaling pathways as classical inflammation [38].

The white adipose tissue is a major source of the inflammatory response in the progression of obesity [39, 40]. This is due to the fact that adipocytes themselves are a source for inflammatory molecules [41], but also due to the composition of the adipose tissue itself where adipocytes are surrounded by tissue resident immune cells,

especially macrophages [42]. Chronic overnutrition causes expansion of adipose tissue and release of cytokines from adipocytes (Figure 4). These cytokines not only activate tissue resident immune cells, but also recruit neutrophils, eosinophils and macrophages to the tissue [43, 44].

Macrophages are the most abundant leukocytes in the adipose tissue and their role in obesity-induced inflammation has been studied extensively [45]. In the lean adipose, tissue they express characteristic markers of anti-inflammatory macrophages, e.g. arginase-1 and IL-10 [46]. Impairing this anti-inflammatory activation of macrophages by deleting the peroxisome proliferator-activated receptor gamma (PPAR-γ) predisposes animals to diet-induced obesity [47]. When the adipose tissue expands, macrophage numbers increase and the population shifts towards a pro-inflammatory state producing cytokines such as TNF-α and IL-6 [46]. This shift is rather due to the pro-inflammatory polarization of the infiltrating monocytes and to a lesser extent to a transformation of the resident anti-inflammatory macrophages [48]. Weight loss reduces macrophage numbers and pro-inflammatory gene expression in the adipose tissue [49].

Based on the finding that inflammation plays a central role in obesity, anti-inflammatory treatment strategies were designed and tested, but were only able to counteract inflammation-mediated insulin resistance, while body weight and obesity were not influenced [40]. This indicates that the inflammatory processes in the periphery are not causal or the driving force of weight gain, but rather a consequence [50]. These findings emphasize the importance of studying the effects of obesity on the CNS, where peripheral signals are integrated and body weight is regulated.

3.4 Obesity-induced CNS inflammation

Since plasma cytokine levels are elevated in obesity and inflammation occurs in peripheral organs, it is not surprising that the CNS, especially the hypothalamus that is critical for the regulation of food intake and energy expenditure, is also susceptible to nutrient excess. De Souza et al. were among the first to show a pro-inflammatory response in the hypothalamus of high fat diet fed animals [30]. This CNS inflammation is in general, like the peripheral inflammation, a ‘low-grade’ inflammation occurring over a long period of time. However, in contrast to peripheral inflammation, this central

reaction to nutrient excess could be the cause of obesity rather than the consequence as it might modulate the 'set point' of body weight of the individual [51, 52].

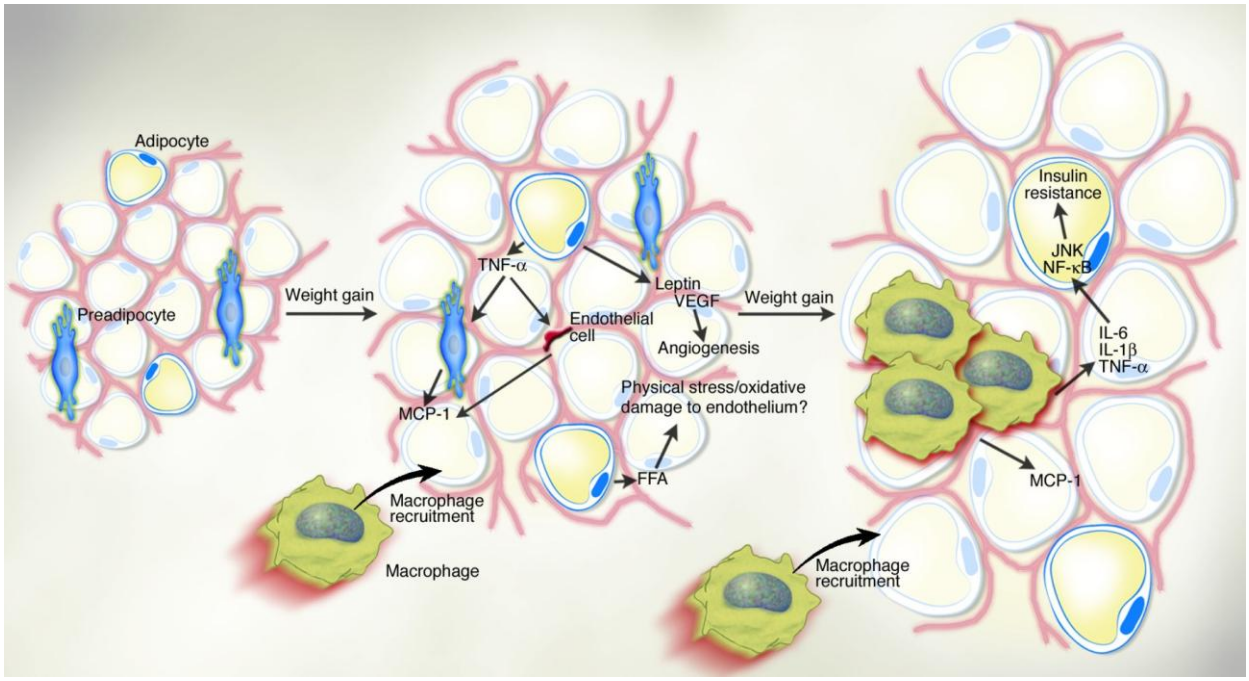

Figure 4: Obesity leads to inflammation and infiltration of macrophages in the adipose tissue. Chronic overnutrition causes expansion of the adipose tissue and release of tumor necrosis factor α (TNF-α) and monocyte chemotactic protein 1 (MCP-1) from adipocytes. MCP-1 recruits circulating monocytes, which mediate a pro-inflammatory reaction causing insulin resistance in the adipose tissue. Abbreviations: VEGF, Vascular Endothelial Growth Factor; FFA, Free Fatty Acids; IL, Interleukin; JNK, c-Jun N-terminal Kinase; NF-κB, Nuclear factor-κB. (republished with permission of the American Society for Clinical Investigation, from [37]**,** copyright (2003); permission conveyed through Copyright Clearance Center, Inc.)

Chronic overnutrition has various effects on the CNS (Figure 5). Specifically, it induces an Ikkβ (inhibitor of nuclear factor kappa-B kinase subunit beta)/NF-κb (nuclear factor 'kappa-light-chain-enhancer' of activated B-cells) dependent inflammatory response [33, 53], activates toll-like-receptor 4 (TLR4) and myeloid differentiation primary response gene 88 (MyD88) signaling [54, 55], causes ER and oxidative stress and impairs autophagy. Together, these changes impair neurogenesis [56], induce leptin resistance [30, 50, 57] and cause apoptosis of hypothalamic neurons [58, 59]. Brain-specific knock-out of *MyD88* as well as neuron-specific deletion of *Ikkb* prevents leptin resistance and dietary obesity [33, 54]. The same is true for blocking TLR4 or Ikkb with specific antibodies [55, 57]. This suggests that hypothalamic inflammation is indeed an

important, potentially reversible cause of diet-induced obesity (DIO). But the question remains which cell type(s) mediate this inflammatory response. Since microglia, the innate immune cells of the brain, mediate CNS inflammation in various settings and diseases, it is tempting to speculate that they also play a critical role in obesity, in line with recent reports indicating their potential involvement [59].

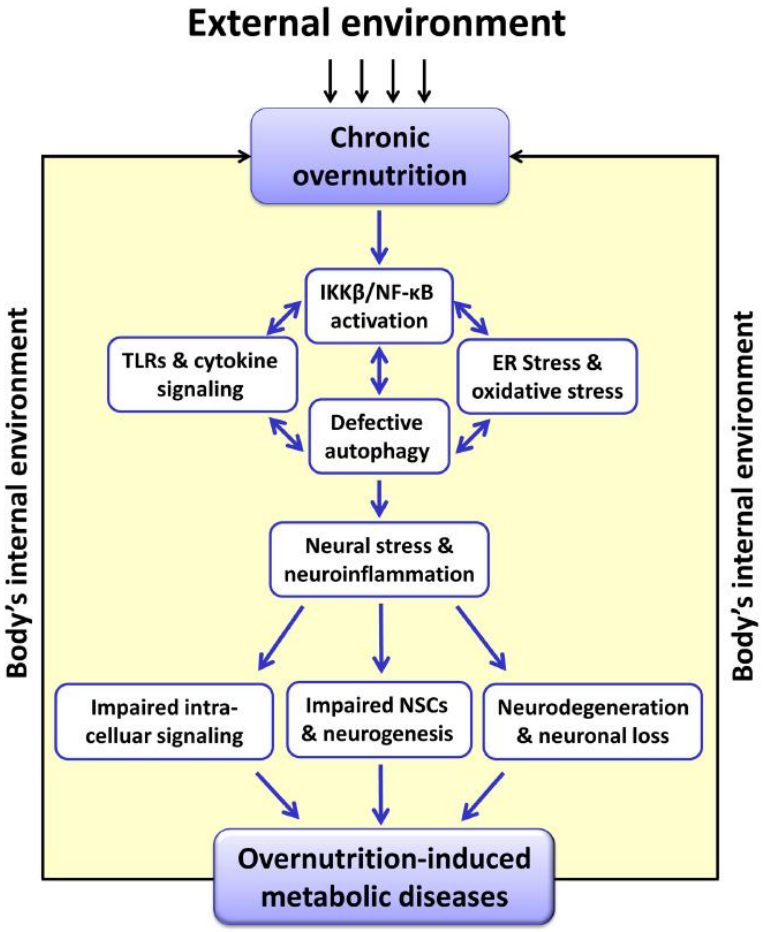

Figure 5: Role of neuroinflammation in overnutrition-induced diseases. Chronic overnutrition leads to IKKβ/NF-κB-directed inflammatory response and several intracellular organelle stresses in the mediobasal hypothalamus (MBH). Many of these cellular and molecular components promote each other, resulting in overnutrition-related neuroinflammation. Such neuroinflammation impairs intracellular hormonal signaling of regulatory neurons, disrupts neurogenesis through depletion of NSCs and leads to neurodegeneration and neuronal loss. The progression of overnutrition-related diseases such as obesity and diabetes secondarily leads to pathophysiological overnutrition in the body's internal environment and exacerbates this mechanism. Abbreviations: TLRs: toll-like receptors; NSCs: neural stem cells. (reprinted from [60], Copyright (2013), with permission from Elsevier)

3.5 Microglia

Glia cells make up about 90 % of all cells in the brain. The most prominent are astrocytes, oligodendrocytes and microglia. Microglia are the immune cells of the CNS and thus responsible for the innate immune response. They represent about 10 % of all glial cells and can be found in all brain regions, with highest densities in the hippocampus, olfactory telencephalon, basal ganglia and substantia nigra [61]. Microglia belong to the monocytic-macrophage lineage [62] and thus have similar functions alike other tissue macrophages such as phagocytosis, antigen presentation and production of cytokines [63]. As other cells of the myeloid lineage microglia are dependent on the transcription factor PU.1 for their development [64]. Furthermore, they express numerous macrophage markers such as CD11b, F4/80, Iba1 and CX3CR1 making it so far impossible to discriminate between microglia and myeloid cells in the periphery [64, 65]. However, it has to be emphasized that microglia form an autonomous population independently of circulating blood monocytes, as they are not derived from hematopoietic stem cells, but originate from the extra-embryonic yolk sac and populate the developing brain already 9.5 days past conception [64, 66–68]. In the CNS they are maintained by self-renewal without exchange with the periphery [62]. Only under inflammatory conditions peripheral myeloid cells were reported to enter the brain [69, 70].

In their homeostatic state, microglia cells display a ramified morphology with long and highly branched processes that serve to monitor their microenvironment enabling these cells to maintain homeostasis and react to alterations in the brain such as infection, trauma, ischemia, neurodegenerative disease or altered neuronal activity [61, 63, 71].

In the homeostatic state microglia can be identified by a unique gene signature [72], which is altered in a mouse model of familial amyotrophic lateral sclerosis leading to a suppression of their biological function, including phagocytosis [73]. Similarly, in the context of Alzheimer’s disease, microglia appear to be impaired or even dysfunctional and thus unable to clear the pathological Aβ [74].

Furthermore, the microglia reaction to homeostatic alterations involves proliferation, upregulation of cell surface molecules and production of chemokines and cytokines [63, 75]. In addition to inflammatory and immune-activating factors, microglia produce trophic factors that support the development and normal function of neurons and glia and help to promote axon growth [76–78].

3.6 Glial response to high fat diet and obesity

Since it was suggested that diets high in fat induce an inflammatory response in the hypothalamus, the glia cells attracted the interest of obesity research as they are likely to be major players in this response. In general, glia cells, especially astrocytes, were found to play a role in the physiological regulation of metabolic homeostasis. Astrocytes transport metabolites and nutrients into and within the brain and express metabolic receptors and regulators [79–81]. Furthermore, it was shown that leptin regulates glutamate and glucose transporters in hypothalamic astrocytes [82]. Microglia, too, express leptin receptors and this hormone can modify their activation state [83, 84]. However, a specific physiological role for microglia in the hypothalamus, with respect to the regulation of metabolic processes has not been brought forward so far.

3.6.1 Astroglial response

Apart from the physiological role of astroglia cells in the maintenance of hypothalamic homeostasis, their reaction in the context of obesity has come into focus. Fatty acids were shown to induce reactive gliosis and release of pro-inflammatory cytokines in cultured astrocytes [85, 86]. *In vivo*, increased circulating leptin levels and increased body weight due to neonatal overnutrition change astrocyte structure and morphology [87]. Furthermore, high fat diet feeding causes cleavage of caspase-3 in rat astrocytes already 3 days after the start of the diet, which however, does not lead to apoptosis of these cells. The morphological changes, as well as the hypothalamic inflammatory reaction, appear to be dependent on the type of diet, as they were not apparent in mice that gained body weight due to high sucrose intake [88].

3.6.2 Microglial response

Even though the physiological role of microglia in the regulation of metabolism has not been described thus far, their reaction to diets high in fat has been studied intensely during the last years. High fat diet was shown to lead to an increase in saturated fatty acids in the CNS, which are capable of inducing microglial activation by stimulation of toll-like receptor 4 [55]. Indeed, similar to the astroglial response, microgliosis only

occurs upon high fat diet, but not in mice that become obese due to leptin (*ob/ob*) or leptin receptor (*db/db*) deficiency [89]. The latter study also emphasized the role for leptin in the induction of hypothalamic microgliosis by its 'rescue' in *ob/ob* mice through subcutaneous leptin injection [89]. In addition, leptin was shown to induce IL-1 and IL-6 expression in microglia cells *in vitro* [83, 90].

Thaler et al. demonstrated that the glial activation upon HFD in rodents occurs in two phases [59]. A first phase of activation and inflammation, detectable as early as 24 hours after initiating HFD, was characterized by elevated gene expression levels of pro-inflammatory cytokines such as *Il6* and *Tnfa*, and microglia markers, such as *Emr1* and *Cd68*. While this first phase subsided after a few days of treatment, a second phase of sustained glial reaction was noted after 4 weeks of HFD in the hypothalamus of rats [59].

Whereas blood-borne factors from high fat diet serum exacerbate gliosis *in vitro* [85], exercise and replacement of HFD with normal chow have been shown to reduce the diet-induced change in microglia phenotype *in vivo* [91, 92].

As mentioned earlier, in addition to their role in CNS inflammation, microglia also exert numerous functions that serve to regulate CNS homeostasis under physiological conditions, amongst them supporting neurogenesis as *in vitro* experiments suggest [63]. In contrast, microglia-mediated inflammation has been implicated in suppression of neurogenesis [93]. This point is of major interest for energy balance, since neurogenesis occurs in the hypothalamus and has been reported to contribute to energy homeostasis and weight balance [94]. As a consequence of an altered microglia phenotype, this neurogenesis-based remodeling process may be inhibited by diet-induced obesity [95].

3.7 Obesity mouse models

Obesity is a risk factor for various chronic diseases, e.g. diabetes type 2, cardiovascular diseases and cancer and is associated with respiratory difficulties, musculoskeletal problems, skin problems and infertility [96]. Insights about obesity-related health problems are mainly derived from epidemiological studies of human subjects. However, animal models are indispensable for studying the molecular mechanism behind the development of obesity and its associated problems. This chapter will focus on the

available mouse models of obesity. In general, there are two types of models: genetic and diet-induced obesity models.

The first reported genetic mouse model for obesity was the *agouti* mouse. A deletion of genomic DNA in the *agouti* gene which is transiently expressed in follicular melanocytes to induce the production of red/yellow pheomelanin pigment and to inhibit black/brown pigment, leads to its ubiquitous overexpression due to loss of the tissue-specific promoter element [97]. Among other phenotypes, *agouti* mice exhibit mature-onset obesity, type-II diabetes and hyperleptinemia [97]. Another key discovery was the leptin-deficient *ob/ob* mouse in 1949 [98]. Due to the role of leptin in appetite control, these mice exhibit uncontrollable food intake and thus become obese and develop type-II diabetes. Similar to the *ob/ob* mouse, the *db/db* mouse becomes obese due to a mutation in the leptin receptor gene, which also impairs leptin signaling in the hypothalamus [97].

In addition to the genetic mouse models, diet-induced obesity mouse models are used to analyze how changes in the diet can influence or even rescue the obesity phenotype [97]. Numerous diet compositions with varying fat or sugar content are available to mimic the human situation. Due to the fact that diets high in fat have been shown to induce obesity in humans, and a positive correlation exists between dietary fat intake and obesity incidence [7, 8, 10, 11], most studies focus on high fat diets. Moreover, a number of studies mentioned in the previous chapter suggest a specific microglia response to a diet high in fat content [59, 89, 99], which is why the diet-induced obesity model was chosen for this thesis using a diet containing 60 % calories from fat.

3.8 Depletion of microglia and replacement by peripherally-derived myeloid cells in the CD11b-HSVTK mouse model

To determine whether microglia play a role in the regulation of body weight homeostasis under physiological conditions and in the context of high fat diet, the CD11b-HSVTK mouse model was used which allows for an inducible ablation of microglia [100]. In this mouse model, a gene of the human herpes simplex virus (HSV) encoding the thymidine kinase (TK) was cloned under the control of the monocyte, macrophage and microglia-specific CD11b promoter. This enzyme catalyzes an important step for DNA synthesis: the conversion of thymidine to thymidine-monophosphate. Addition of the drug

ganciclovir (GCV), which mimics the native substrate of the enzyme, leads to a monophosphorylation of the drug by the TK and an addition of further phosphate groups by endogenous host kinases. The product, gcv-triphosphate, cannot be integrated in the DNA and thus leads to cell cycle arrest and apoptosis of the respective cells. To achieve a specific depletion of microglia cells, ganciclovir is delivered intracerebroventricularly (icv) directly into the brain [101, 102].

Since the generation of the CD11b-HSVTK model it has been used to study the role of microglia in different diseases, e.g. Experimental autoimmune encephalomyelitis, Alzheimer's disease and stroke [100, 103, 104]. Furthermore it has been discovered that the depletion of microglia in this model leads to a robust infiltration of peripherally-derived myeloid cells replacing the endogenous microglia [101, 102]. Whether these cells can functionally replace the microglia remains to be elucidated and may depend on the specific context.

Recently, other microglia depletion models have been established using either the CX3CR1-CreER transgene to drive diphtheria toxin receptor expression in microglia, which makes it possible to deplete microglia upon diphtheria toxin administration [78], or a pharmacological inhibitor of the CSF-1 receptor, which is important for microglia survival [105]. Similar to the CD11b-HSVTK model, repopulation upon depleting resident microglia has been observed when treatment with the pharmacological inhibitor is stopped, though the source and origin of the repopulating cells in the latter model appears to be proliferating precursor cells within the brain, while in CD11b-HSVTK mice peripherally-derived myeloid cells replace the depleted microglia [102, 105, 106].

3.9 Aims of this study

Obesity has become one of the major health problems worldwide affecting millions of people and contributing to various secondary diseases such as diabetes, cardiovascular diseases and cancer. For this reason, research has focused heavily on elucidating the mechanisms behind the development of obesity with the aim to find possible treatments to combat this epidemic. Thus far, these efforts have not led to the ultimate cure of obesity. The problem remains that following weight loss, there is a high chance of weight regain once medication or dieting is stopped. This is hypothesized to occur because the central set point for body weight might be changed in obese persons and

thus the regulation of food intake and energy expenditure is impaired. For this reason, the brain has become a focus of obesity research. It has been shown that not only do changes in neuronal activity occur in diet-induced obesity animal models [107, 108], but a low-grade inflammatory response can also be detected as is the case in the peripheral metabolically active organs [59]. In this context microglia, the innate immune cells of the brain, were found to react to diets high in fat, though the precise nature of this response, especially to prolonged high fat diet exposure, *in vitro* and *in vivo* is still in need of thorough characterization and will be addressed in the first part of this thesis. In addition, the glial response in obese humans will be analyzed histologically, which is, to our knowledge, the first analysis of this kind.

Microglia are known to play a role not only in pathological conditions, but also in physiological brain functions, including pruning of neuronal synapses and regulation of brain development [63]. Nevertheless, it is not yet known whether they are also involved in supporting physiological processes of the hypothalamus, the brain region regulating appetite, food intake and energy expenditure. The second and third part of this thesis are thus aimed at determining whether microglia play a role in body weight homeostasis under physiological conditions as wells as in the context of high fat diet.

The specific aims of this thesis were:

1. Characterize the nature of the glial response to high fat diet in the hypothalamus of mice and humans.
2. Determine whether microglia play a role in body weight homeostasis under physiological conditions using the CD11b-HSVTK mouse model allowing depletion of resident microglia.
3. Determine whether microglia play a role in body weight homeostasis in the context of high fat diet using the CD11b-HSVTK mouse model to deplete resident microglia in combination with a diet-induced obesity model.

4 Methods

4.1 *In vivo* experiments

4.1.1 Mice

Adult male mice aged at least 100 days were used for all experiments. For the depletion of microglia, CD11b-herpes simplex virus thymidine kinase (CD11b-HSVTK) mice [100] were used together with transgene negative littermates as controls. C57Bl6/J mice were utilized for studying the effects of HFD in general.

All mice were kept under specific pathogen-free conditions on a 12-hour light-dark cycle, with *ad libitum* access to food and water. Animals were fed either a HFD (60 % kcal % fat, Research Diets, D12492) or recommended low-fat diet (10 % kcal % fat, Research Diets, D12450B).

All animal experiments were performed in accordance with the national animal protection guidelines approved by the regional office for health and social services in Berlin (G0154/08, G0390/12, LaGeSo).

4.1.2 Metabolic cages

For phenotypic characterization mice were placed in PhenoMaster cages (TSE Systems) for 48 h. The first 24 h were regarded as acclimatization and not used for analyses. Apart from food and drink consumption locomotor activity and energy expenditure were determined with the use of the PhenoMaster cages. Locomotor activity was determined by the interruptions of laser beams across the cage in x and in y direction. Each interruption was counted by the system and the combined counts per hour were displayed over one day or as mean activity. Energy expenditure was calculated from the respiratory quotient (RER) and gas exchange data [energy expenditure = (3,815+(1,232*RER)*VO2)] and normalized to lean mass [109] as measured using a body composition analyzer (minispec LF50, Bruker).

4.1.3 Genotyping

Genotyping was performed using ear or tail biopsies from individual mice which were digested over night at 55 °C with 0.1 mg/ml proteinase K in 300 µl lysis buffer (100 mM Trizma®Hydrochloride (Tris-HCl, pH = 9), 500 mM potassium chloride (KCl), 5 % nonoxinol (NP)-40, 5 % Tween20). The enzyme was heat inactivated for 10 min at 95 °C the next day and the lysate was centrifuged for 10 min at 13.000 x g.

The PCR reaction was carried out as follows: A reaction mix with 0.75 µl of the forward primer (100 pmol/µl), 0.75 µl of the reverse primer (100 pmol/µl) (Table 1) and 10 µl GoTaq Red Master Mix (STRATEC Molecular) was prepared for every reaction. To this mix, 2 µl of DNA was added and the PCR reaction was run with the parameters listed in Table 2.

Table 1: Primer sequences used for genotyping of CD11b-HSVTK mice.

Forward	5′-GACTTCCGTGGCTTCTTGCTGC-3′
Reverse	5′-GTGCTGGCATTACAGGCGTGAG-3′

Table 2: Parameters used for genotyping of CD11b-HSVTK mice.

step	temperature	duration
denaturation	94 °C	90 sec
denaturation (35 cycles)	94 °C	30 sec
annealing	53 °C	30 sec
elongation	72 °C	30 sec
final elongation	72 °C	5 min

The PCR products were separated on 2 % (w/v) agarose gels (1x TAE, 0.5 µg/ml ethidium bromide) at 120 mV.

4.1.4 Generation of bone marrow chimeric mice

For the generation of bone marrow chimeras $1x10^7$ bone marrow cells obtained from tibia and femur of Tg(ACTbEGFP)1Osb mice (GFP, Jackson Laboratories) were injected into the tail vein of C57BL/6 mice exposed to 10 gray whole-body irradiation. Mice were housed in individually ventilated cages and treated with antibiotic (0.01 %

Enrofloxacin, Baytril®, Bayer Vital) for four weeks. After another four weeks of recovery, mice were fed with high fat diet or low-fat chow for 20 weeks. For the analysis of proliferation of microglia cells upon HFD, animals received a weekly i.p. injection of 50 mg/kg Bromodeoxyuridine (BrdU), a thymidine analog that integrates into the DNA during replication.

4.1.5 Implantation of mini-osmotic pumps

Mini-osmotic pumps (model 2001 or 2004, 1.0 or 0.25 µl/h, respectively; Alzet®) were filled with a 2 mg/ml solution of ganciclovir (Sigma) in sterile filtrated artificial cerebrospinal fluid (aCSF) or aCSF alone one day before use and primed at 37 °C in aCSF. To implant minipumps, mice were anesthetized with isoflurane gas and received an i.p. injection of 5 mg/kg Rimadyl (Carprofen, Pfizer GmbH). A small cut was made in the scalp and a pocket was formed under the skin of the back of the mouse. The pump was inserted into the subcutaneous space and a brain infusion cannula was implanted into the right lateral ventricle (from Bregma: AP: +0.1 mm, ML: +1.0 mm and DV: -3.0 mm). The wound was sutured and treated with Zylocain® gel (AstraZeneca GmbH). Additionally, the mice were given paracetamol (ben-u-ron®; 0.1 mg/ ml) in their drinking water for 3 days after the surgery. [102]

4.1.6 Tissue processing and perfusion

Mice were sacrificed and terminal blood collection was performed from the heart to collect serum. White and brown adipose tissue was harvested and frozen in liquid nitrogen for further analysis. Mice were then transcardially perfused with PBS and the brain was removed for histology (4.2), microglia isolation (4.3.1), RNA isolation (4.4.1) or protein analysis (4.4.4).

4.2 Immunohistochemical evaluations

4.2.1 Histology

Brains were removed and stored in 4 % paraformaldehyde (PFA) overnight. The next day, PFA was replaced by 30 % sucrose for at least 24 h. Brains were cut coronally at

30 µm on a cryostat and stored at 4 °C in cryoprotectant (30% ethylenglycol, 20% glycerol, 50 mM sodium phosphate buffer, pH 7.4). For immunohistochemical and immunofluorescent stainings, sections were washed with PBS and blocked in PBS with 0.3 % Triton X-100 and 10 % serum for one hour at room temperature followed by an incubation with primary antibodies: Iba1 (1:500, Wako Chemicals), GFAP (1:5000, Dako) GFP (1:1000, Abcam) or anti-BrdU (1:500, AbD Serotec) at 4 °C over night. For BrdU-labeling, sections were pre-treated with 50 % formamide in 2 x standard saline citrate (SSC) for 2 h at 65 °C, washed 2 x 5 min in 2 x SSC at room temperature, incubated in 2 N HCl for 30 min at 37 °C and washed in 0.1 M borate buffer for 10 min prior to immunostaining. The following day sections were washed in PBS and incubated with the respective peroxidase-coupled secondary antibody (1:200, Dianova) for one hour at room temperature. For immunofluorescent staining, sections were incubated with Alexa Fluor® 488 anti-rabbit (1:200, Dianova) or anti-rat-Cy3 (1:200, Dianova). For GFAP and GFP immunostaining, sections were treated with 0.5 %, 1 % and again 0.5 % H_2O_2 in H_2O for 30 min each to quench endogenous peroxidase activity before incubation with secondary antibody. Then sections were developed with 3,3′-Diaminobenzidine (DAB) solution, mounted on glass slides (SuperfrostTM Plus, R.Langenbrinck), counterstained with hematoxylin and coverslipped with Roti® Histokitt II (Roth) mounting medium. Fluorescent sections were imaged using a confocal laser-scanning microscope (Leica).

4.2.1 Stereological and stereomorphometric analysis

For the assessment of Iba1+ and GFP+ cells, Stereoinvestigator® software (MBF Bioscience, Version 10) was used. Cells were counted using the Optical Fractionator method in a total of 8-10 sections per mouse collected at an interval of 6 sections apart. BrdU labeled cells were counted using the Meander Scan method. For analysis of GFAP staining in mouse brains as well as GFAP and Iba1 staining in human brains, pictures of 6-8 sections were analyzed with the CellSense software (Olympus) using the phase analysis tool to determine the percentage of area covered with staining within a defined area that was the same for all analyzed sections [110].

4.2.2 Collection and processing of human autopsy material

Brain autopsies were performed following written consent for pathological examination according to the law of Berlin. Following routine diagnostic neuropathological examination and the hypothalamus and parts of the frontal cortex were obtained and used for sectioning and immunohistochemical stainings. This procedure was approved by the Charité's ethics commission (EA1/019/13). Cases with infectious or inflammatory disease, psychotrophic drug use, history of substance addiction, chronic anti-inflammatory or immunosuppressive therapy, clinically or pathologically symptomatic brain edema, intracerebral hemorrhage, brain irradiation, chemotherapy, hypoxic or ischaemic damage were excluded from the analysis. Information about gender, age and BMI of the analyzed cases is given in Table 3. The formalin-fixed tissue was placed in 30 % sucrose for at least one day and then cut frozen on a cryostat in 50 µm thick sections, which were stored in cryoprotectant at 4 °C until use. The sections were then stained using the same procedure used for the mouse tissue.

Table 3: Summary of human cases.

	Non-obese (BMI < 25)	**Obese (BMI ≥ 30)**
#	9	12
Gender	7 m/ 2 f	9 m/ 3 f
Age [yr]	65 +/- 17,16	69 +/- 12

4.3 *In vitro* experiments

4.3.1 Isolation of murine CD11b^{+} brain cells

For the analysis of isolated murine microglia, mice were anaesthetized and perfused with PBS. Hypothalamus was dissected from the brain and manually dissociated in hanks buffered saline solution (HBSS; Life Technologies). The neural dissociation kit (Miltenyi Biotech) was used to create a single-cell suspension, which was then incubated with anti-CD11b microbeads (Miltenyi Biotech) and CD11b+ cells were isolated using MACS MS columns (Miltenyi Biotech).

4.3.2 Stimulation of isolated adult murine microglia

For plasma stimulation, sorted murine microglia cells were plated in a 24-well plate. For each condition 3 wells were prepared with $5x10^5$ cells per well containing DMEM supplemented with 10% FBS and 50 U/ml PenStrep and maintained at 37°C in a 5% CO_2 humidified atmosphere. The next day, the medium was replaced with medium containing 10 % plasma of mice fed HFD or chow for 16 weeks. After 5 hours this medium was exchanged with fresh medium, which was collected for analysis one hour later.

For stimulation with LPS isolated primary hypothalamic microglia were plated in 96-well plates with $5x10^5$ cells per well and 3 wells per condition. The next day, cells were stimulated with 1 µg/ml LPS and the medium was collected for cytokine analysis 24 hours later.

4.4 Molecular analysis

4.4.1 RNA isolation

RNA from hippocampal tissue was isolated with the InviTrap® Spin Tissue RNA Mini Kit (STRATEC Molecular). Isolation was carried out according to the manufacturer's instructions. Tissue was homogenized with gentleMACS™ M Tubes (Miltenyi Biotech). As a variation to the manual, 2-Mercaptoethanol was used in the lysis solution instead of Dithiothreitol (DTT).

TRIzol® (Life Technologies) was used for isolation of RNA from white and brown adipose tissue. Tissue was placed in 1000 µl TRIzol® reagent in gentleMACS™ M Tubes (Miltenyi Biotech) and homogenized using the gentleMACS Dissociator (Miltenyi Biotech). Tubes were centrifuged at maximum speed for 10 min and the solution was transferred to a 1.5 ml Eppendorf tube. Then 200 ml chloroform was added and the tubes were shaken vigorously for 15 s. After another centrifugation at 13,000 rpm for 15 min, the upper aqueous phase was transferred into a new 1.5 ml Eppendorf tube and mixed with 500 µl isopropanol. The mixture was incubated on ice for 10 min, and centrifuged again at 13,000 rpm for 10 min. The supernatant was discarded and the pellet washed with 1000 µl 75 % ethanol and centrifuged once more at 13,000 rpm for

10 min. Again the supernatant was discarded and the pellet was dried for 20-30 min until all ethanol had evaporated and the RNA was dissolved in RNAse-free water.
The concentration of total RNA was measured using a Nanodrop 2000 spectrophotometer (TECAN Infinite 2000).

4.4.2 Quantitative NanoString nCounter gene expression analysis

For NanoString analysis of gene expression of isolated microglia, RNA of sorted microglia cells was isolated using the PicoPure® RNA Isolation Kit (Life Technologies) according to the manufacturer's instructions. Quantitative gene expression analysis of the 42 genes plus 6 housekeeping genes listed in Table 4 was performed on each sample. Results were analyzed using the nSolver™ analysis software.

Table 4: Accession Number and name of genes analyzed using NanoString nCounter.

Accession Number	**Gene name**		**Accession Number**	**Gene name**
NM_019741	Slc2a5		NM_011313	S100a6
NM_009151	Selplg		NM_009115	S100b
NM_178706	Siglech		NM_213659.2	Stat3
NM_008479	Lag3		NM_010548.1	Il10
NM_001164034	ntf3		NM_008361.3	Il1b
NM_009917.5	CCr5		NM_031168.1	Il6
NM_007651.3	Cd53		NM_007707.2	Socs3
NM_011905.2	tlr2		NM_011577.1	Tgfb1
NM_021297.2	tlr4		NM_009367.1	Tgfb2
NM_001042605.1	CD74		NM_009368.2	Tgfb3
NM_011146.1	Pparg		NM_009369.4	Tgfbi
NM_008352.1	Il12b		NM_009370.2	Tgfbr1
NM_031252.1	il23a		NM_009371.2	Tgfbr2
NM_008625	mrc1		NM_031254.2	Trem2
NM_008689.2	Nfkb		NM_011662.2	Tyrobp
NM_010546.2	Ikbkb		NM_008746	TrkC
NM_010745.2	ly86		NM_007540	Bdnf
NM_008320.4	Irf8		**Housekeeping genes:**	
NM_001291058.1	CD68		NM_020559.2	Alas1
NM_009987.4	Cx3cr1		NM_026007.4	Eef1g
NM_009142.3	Cx3cl1		NM_008062.2	G6pdx
NM_001111275.1	Igf1		NM_001001303.1	Gapdh
NM_146162.2	Tmem119		NM_010368.1	Gusb
NM_027571.3	P2ry12		NM_013556.2	Hprt
NM_013693.1	Tnf			

4.4.3 Quantitative real-time PCR (qRT-PCR)

For quantitative RT-PCR, cDNA is synthesized using the QuantiTect® Reverse Transcription Kit (Qiagen). Synthesis was performed according to the manufacturer's instructions. In brief, 1 µg of RNA was incubated with gDNA elimination buffer at 42 °C for 5 min. Next, buffer, primer mix and enzyme were added and the reaction was incubated for another 15 min at 42 °C. The reaction was stopped by incubating at 95 °C for 5 min, and cDNA was stored at -20 °C until use. For qRT-PCR analysis cDNA was diluted 1:100 in ddH_2O and 10 µl were added to 1 µl TaqMan® Gene Expression Assay and 9 µl TaqMan® Fast Universal PCR Master Mix (2x) (both Applied Biosystems) in a 96-well plate. The plate was centrifuged at 4000 rpm for 2 min and placed into the qRT-PCR machine (ABI 7900HT, Applied Biosystems). QRT-PCR results were analyzed using the delta-delta C_t method and *Gapdh* gene expression for normalization of relative gene expression [111].

4.4.4 Tissue homogenization

For the analysis of protein expression, hypothalami were homogenized on ice in 600 µl PBS with 1 % Triton-X 100 using needles with descending gauge sizes (20, 23, and 25 G). After complete homogenization, the samples were incubated on ice for 30 min with short vortexing every 5-10 min. The incubation was followed by a centrifugation at maximum speed for 30 min at 4 °C. The supernatant was aliquoted, frozen in liquid nitrogen and stored at -80 °C.

4.4.5 Bicinchoninic acid (BCA) protein assay

Protein content of the homogenized samples was measured using the Pierce® BCA Protein Assay Kit. The reaction was performed according to the manufacture's manual. A serial dilution (1:2) of albumin in PBS was prepared from a 2 mg/ml stock solution supplied with the assay. 10 µl of sample and standard (2000 - 3.125 µg/ml) were incubated with 200 µl of BCA solution (50 parts reagent A, 1 part reagent B) for 30 min at RT in the dark. Then absorption was measured at 562 nm using a microplate reader (Infinite® M200, Tecan) and analyzed with the software Magellan™ (Tecan).

4.4.6 Meso Scale

Serum parameters and cytokines were measured with the Meso Scale Discovery (MSD) 96-Well system (Mouse Metabolic Kit, V-PLEX Plus Proinflammatory Panel 1 (mouse) Kit) according to the manufacturer's instructions. Samples were analyzed undiluted in duplicates. All plates were analyzed on a MS6000 (MSD) machine.

4.5 Statistical analysis

Differences between groups were analyzed using GraphPad® Prism. For pairwise comparisons of experimental groups, student's t-test was used. One- or two-way ANOVA with Bonferroni's post-hoc analysis was used for comparison of more than two groups. Results were displayed as mean values +/- standard errors of the mean (SEM). Significance was considered as follows: *$p < 0.05$, **$p < 0.01$, and ***$p < 0.001$.

5 Results

During the last years the attention of obesity research included more and more its effect on the CNS, since it plays a key role in regulating body weight homeostasis. In the periphery, innate immune cells play a central role in the progression of obesity. The innate immune cells of the brain, namely microglia, might have a similarly important role in the CNS. The aims of this thesis are thus to characterize the glial response to high fat diet in the hypothalamus and to determine whether hypothalamic microglia are important for regulating of body weight.

5.1 Characterization of the glial response to high fat diet in the hypothalamus of mice and humans

5.1.1 Gliosis in the mouse hypothalamus in response to short-term and prolonged high fat diet

As described previously, a number of studies have been reported in which the authors analyze the glial reaction to HFD [59, 106, 112]. Since different time courses, animal models, diet compositions and measures of glial responses were used in these studies, the first aim of this thesis was to independently establish the time course of glial activation in response to a high fat diet with 60 % calories from fat. To assess the effect of short-term high fat diet feeding, mice were fed for 3 days and for 4 weeks. The effect of prolonged HFD was analyzed after 8 weeks, when increased body weight and insulin and leptin resistance had been demonstrated in high fat diet fed animals [58, 113]. Gliosis in the hypothalamus was analyzed histologically using Iba1 as a marker for microglia and GFAP for astrocytes. After 3 days of HFD no morphological alterations or increase in microglia cell number were detected (Figure 6 A, B) in contrast to previously published results [59]. After 4 weeks of HFD, a slight trend towards a higher number of Iba1+ myeloid cells in the hypothalamus was detected, while after 8 weeks of HFD the number of Iba1+ cells was significantly higher than in chow fed mice (Figure 6 B). Similarly, the area covered by GFAP-positive astrocytes was significantly increased after 8 weeks of HFD (Figure 6 C, D).

These results emphasize that there is a specific response of glial cells in the hypothalamus upon HFD, which can be detected histologically. Other brain regions were not affected by this gliosis at the analyzed time points (data not shown).

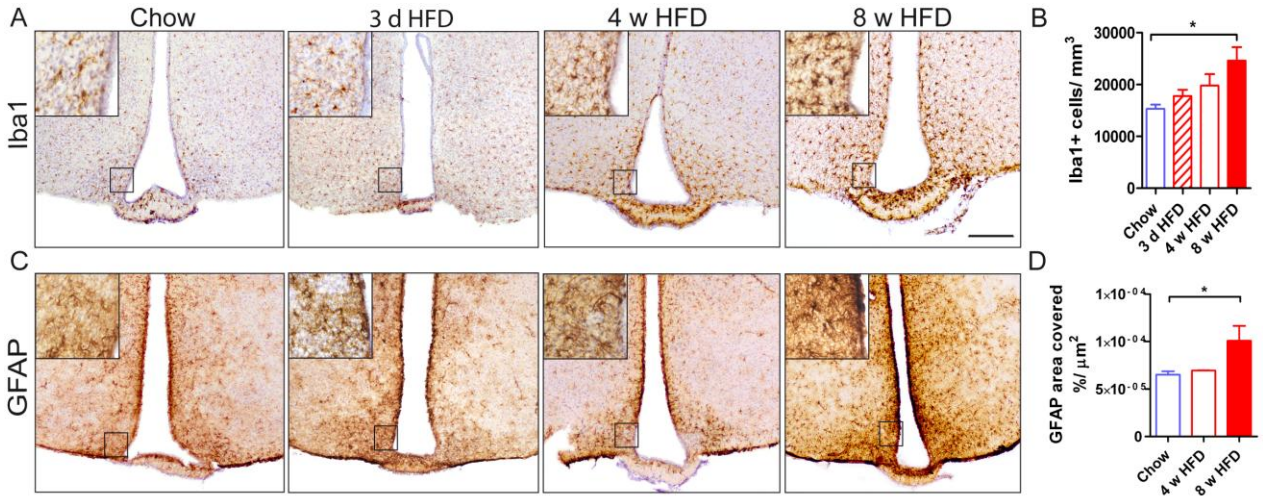

Figure 6: Gliosis in the mouse hypothalamus in response to short-term and prolonged HFD. (A) Iba1 immunoreactivity in the hypothalamus of HFD- and chow-fed wild-type mice. (B) Quantification of Iba1-positive cells in the hypothalamus of HFD- vs. chow-fed wild-type mice. Chow: n=5, HFD: n=5 (3 d), n=3 (4 w), n=7 (8 w). (C) GFAP immunoreactivity in the hypothalamus of HFD- and chow-fed wild-type mice. (D) Quantification of GFAP-positive cells in the hypothalamus of HFD- vs. chow-fed wild-type mice. Chow: n=5, HFD: n=3 (4 w), n=3 (8 w). *p<0.05 based on Two-Way ANOVA with Bonferroni's post-hoc test. Scale bar, 200 µm. Data represents means +/- s.e.m. HFD, high fat diet; d, days; w, weeks.

5.1.2 Gliosis in the hypothalamus of obese humans

To determine whether a similar glial response occurs in the brains of obese humans as was observed in the brains of HFD-fed mice, post-mortem hypothalamic and cortical brain tissue from normal weight individuals with BMI<25 and obese individuals with BMI>30 was analyzed histologically using the same markers used in the mouse study; Iba1 and GFAP. Analysis of the hypothalamic area of obese individuals revealed Iba1+ cells with morphological alterations, including enlarged cell bodies and shortened, deramified processes adjacent the third ventricle in the hypothalamic area (Figure 7 A, top panels), whereas Iba1+ cells in the cortex exhibited an inconspicuous, homeostatic morphology characterized by small cell bodies and delicate, ramified processes (Figure 7 A, bottom panels). To quantify the degree of microglia changes, the area covered by Iba1+ cell bodies in the hypothalamus was normalized to that of the cortical Iba1 area

covered for each individual. Not only was the ratio of hypothalamic/cortical Iba1 covered area significantly increased from 1.2 in individual with BMI<25 to 2.8 in individuals with BMI>30, but correlated significantly overall with the BMI (Figure 7 B, C) revealing altered hypothalamic microglia reactivity in association with increased BMI.

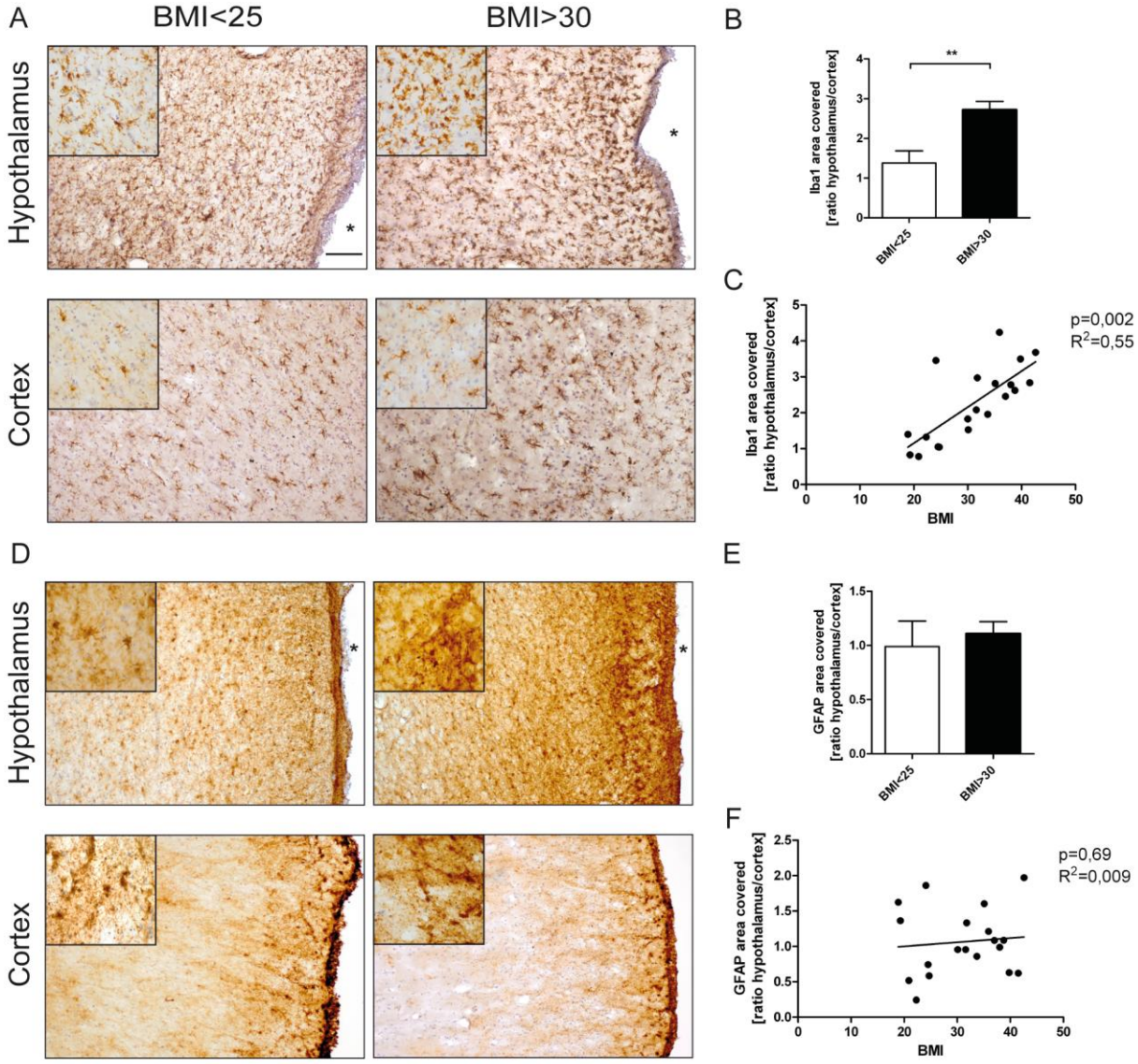

Figure 7: Gliosis in the hypothalamus of human individuals with BMI>30. (A) Iba1 immunoreactivity in the hypothalamus region of individuals with BMI<25 vs. BMI>30. (B) Ratio of Iba1 covered area in the hypothalamus versus cortex of individuals with BMI<25 vs. BMI>30. (C) Correlation of hypothalamus/cortex Iba1 covered area to BMI. (D) GFAP immunoreactivity in the hypothalamus of individuals with BMI<25 vs. BMI>30. (E) Ratio of GFAP covered area in the hypothalamus versus cortex of individuals with BMI<25 vs. BMI>30. (F) Correlation of hypothalamus/cortex GFAP covered area to BMI. n=9 (BMI<25), 12 (BMI>30). **p<0.01 based on student's t-test. Scale bar, 100 µm. Asterisk (*) marks the third ventricle. Data represents means +/- s.e.m.; BMI, body-mass index.

The astrocytic response was not as robust as the microglial response to BMI, as the observed increase in the ratio of hypothalamic to cortical GFAP did not differ significantly between individuals with BMI<25 compared to those with BMI>30 (Figure 7 D-F).
This data reveals a similar response of microglia cells in the hypothalamic areas of obese individuals as it was seen in the hypothalamus of mice fed HFD.

5.1.3 Contribution of peripheral monocytes to the hypothalamic response to high fat diet

Peripheral macrophages infiltrate the adipose tissue and induce inflammation as a result of HFD. To determine the source of the increased number of Iba1+ cells in the hypothalamus, bone marrow chimeric mice harboring actin-GFP bone marrow were generated and fed HFD for 20 weeks. This allows for discrimination between the endogenous (GFP negative) and the infiltrating peripheral (GFP positive) myeloid cells in the brain. After 20 weeks mice were sacrificed, serum was taken for analysis of the hormones insulin and leptin and the brain was prepared for histological analysis of GFP and Iba1. At this time point, the mice exhibited significant weight gain equivalent to approximately 60 % of their starting body weight, whereas the weight of chow fed mice only increased by 10 % (Figure 8 A). In addition, HFD-fed bone marrow chimeras exhibited elevated serum insulin and leptin levels, indicators of typical diet-induced leptin and insulin resistance (Figure 8 B, C).
When analyzing the number of myeloid cells in the brain, significantly more Iba1+ cells were found in the hypothalamus of chimeric animals fed HFD (Figure 8 D, E), confirming earlier findings (Figure 6 A, B). In contrast, there was no quantitative difference in the number of peripherally-derived GFP+ myeloid cells in the hypothalamus of mice fed HFD compared to chow (Figure 8 G), which is also evident in histological images (Figure 8 F). Moreover, analysis of the total number of GFP+ cells throughout the whole brain did not reveal a significant difference in the number of CNS infiltrating myeloid cells between HFD and chow fed bone marrow chimeric mice (Figure 8 H, I). Therefore, these results demonstrate that in this experimental setup, infiltrating peripheral cells do not account for the increase in hypothalamic Iba1+ cells in mice fed HFD (Figure 8 E).

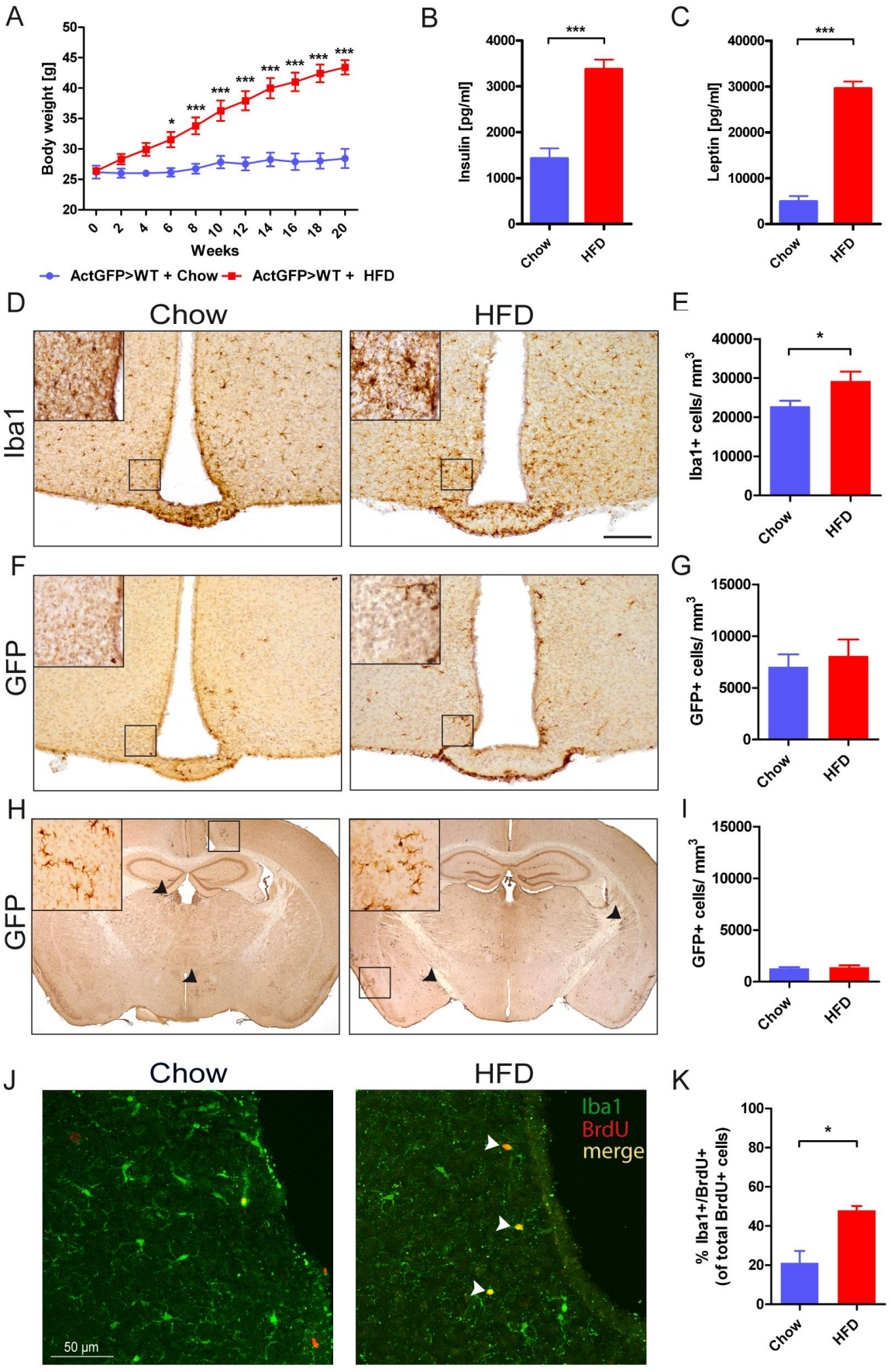
A
Body weight [g]
Weeks
ActGFP>WT + Chow
ActGFP>WT + HFD
B
Insulin [pg/ml]
Chow
HFD
C
Leptin [pg/ml]
Chow
HFD
D
Chow
HFD
Iba1
E
Iba1+ cells/ mm3
Chow
HFD
F
GFP
G
GFP+ cells/ mm3
Chow
HFD
H
GFP
I
GFP+ cells/ mm3
Chow
HFD
J
Chow
HFD
Iba1
BrdU
merge
50 µm
K
% Iba1+/BrdU+ (of total BrdU+ cells)
Chow
HFD

Figure 8: HFD leads to proliferation of endogenous microglia in the hypothalamus. (A) Body weight development of Actin-GFP bone marrow chimeric mice fed either HFD or chow for 20 weeks. (B) Serum insulin and (C) serum leptin levels of Actin-GFP bone marrow chimeric mice fed either HFD or chow for 20 weeks. (D) Iba1 immunoreactivity in the hypothalamus of Actin-GFP bone marrow chimeras fed HFD or chow for 20 weeks. (E) Quantification of Iba1-positive cells in the hypothalamus of Actin-GFP bone marrow chimeras fed HFD or chow for 20 weeks. (F) GFP immunoreactivity in the hypothalamus of Actin-GFP bone marrow chimeras fed HFD or chow for 20 weeks. (G) Quantification of GFP-positive cells in the hypothalamus of Actin-GFP bone marrow chimeras fed HFD or chow for 20 weeks. (H) GFP immunoreactivity in the whole brain of Actin-GFP bone marrow chimeras fed HFD or chow for 20 weeks. (I) Quantification of GFP-positive cells in the whole brain of Actin-GFP bone marrow chimeras fed HFD or chow for 20 weeks. Scale bar, 200 µm. (J) Iba1 (green)/BrdU (red)-immunoreactivity in chow and HFD-fed Actin-GFP bone marrow chimeras. (K) % of Iba1+/BrdU+ cells of all BrdU+ cells in the hypothalamus of chow and HFD-fed Actin-GFP bone marrow chimeras. n=7 chow, n=8 HFD. ***p<0.001, *p<0.05, based on unpaired student's t-test. Data represents means +/- s.e.m. HFD, high fat diet.

Hence, proliferation of endogenous microglia upon HFD was assessed by weekly pulsing of Bromodeoxyuridine (BrdU), a thymidine analogue that integrates into the DNA during replication and can be made visible using an antibody in an immunofluorescent staining. Quantification of Iba1/BrdU double positive cells revealed a higher percentage of proliferating microglia (% Iba1+ cells of total BrdU+ cells) in the hypothalamus of HFD-fed mice (Figure 8 J, K). These results confirm a specific response of resident microglia to HFD and identify the specific cellular origin of the increase in microglia number in response to HFD feeding.

5.1.4 Prolonged HFD exposure reverses acute hypothalamic pro-inflammatory responses

As a contribution of peripheral myeloid cells to the hypothalamic response to HFD was excluded (5.1.3), the next aim was to analyze the microglia response to prolonged HFD in more detail. The results of previous studies hint towards an early pro-inflammatory response to HFD in the hypothalamus of rats, which manifests after 28 days of HFD feeding [59].

For this analysis, mice were fed HFD for 3 and 7 days and also for 4 and 8 weeks. The hypothalamus was taken for analysis of gene expression of pro- and anti-inflammatory markers using qRT-PCR. Even though no morphological signs of gliosis were visible in

mice fed HFD for 3 days (Figure 6) a selective 2.6-fold upregulation of the pro-inflammatory cytokine interleukin-1b (Il1b) was detected (Figure 9 A). However, neither after 4 weeks nor even after 8 weeks of HFD feeding elevation in pro-inflammatory cytokine mRNA levels were observed. In contrast, changes in anti-inflammatory molecules Il-10 (*Il10*), CD206 (*Cd206*) and Arginase1 (*Arg1*) were evident (Figure 9 B), revealing a significant 2.5-fold increase in *Il10* expression levels.

To assess whether these changes in gene expression translate into a change in protein level, wild-type mice were fed either with chow or HFD for 3 days and 8 weeks, the time points where cytokine gene expression has been assessed (Figure 9 A, B). The hypothalami of these mice were taken, homogenized and cytokine protein expression was analyzed using Meso Scale® V-PLEX Plus Proinflammatory Panel.

Analysis of cytokine protein levels at 3 days and 8 weeks did not confirm the previously detected mRNA changes, as neither IL-1b nor TNF-a were increased in the hypothalamus after 3 days of high fat diet compared to chow feeding (Figure 9 C). Similarly, no increase in IL-10 protein was detected after 8 weeks of high fat diet, as was seen on the mRNA level. However, IL12p70 protein was decreased in the hypothalamus of mice fed high fat diet for 8 weeks compared to mice fed chow (Figure 9 D).

Taken together, these data confirm the finding of the study by Thaler et al. [59] revealing an increase in pro-inflammatory cytokine expression. However, this pro-inflammatory response subsides and switches to a rather anti-inflammatory pattern upon prolonged HFD feeding. Analysis of the protein expression of the respective cytokines at the given time points, revealed no significant differences detectable at the protein level. Only the pro-inflammatory cytokine IL-12 was downregulated in the hypothalamus of mice fed HFD exemplifying the overall anti-inflammatory pattern of hypothalamic microglia upon prolonged HFD, though gene expression of its subunit Il12a was not changed and Il12b could not be determined in whole hypothalamic tissue (data not shown).

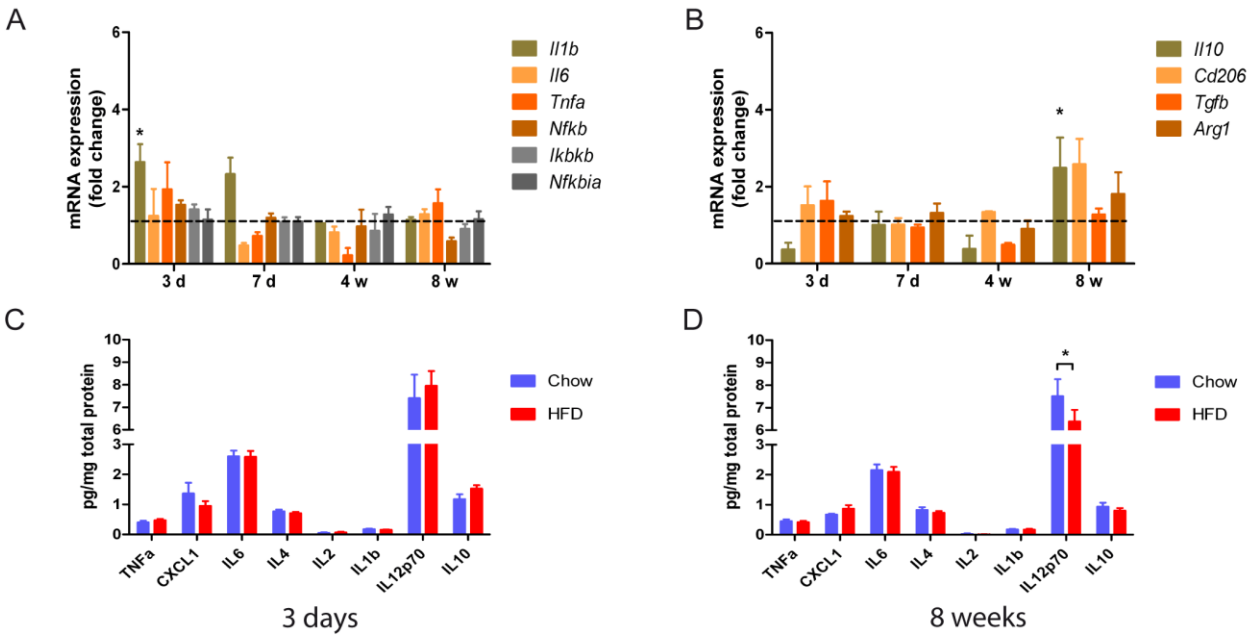

Figure 9: Pro- and anti-inflammatory gene and protein expression in the hypothalamus of HFD- and chow-fed mice. (A) Pro-inflammatory and (B) anti-inflammatory cytokine expression in the hypothalamus of mice fed HFD for 3 days, 7 days and for 4 and 8 weeks normalized to hypothalamic gene expression of chow fed mice. n=6-7 per group. Protein levels of cytokines in the hypothalamus of mice fed HFD or chow for (C) 3 days and (D) 8 weeks. n=10 per group. *p<0.05 based on Two-Way ANOVA with Bonferroni's post-hoc test. Data represents means +/- s.e.m. HFD, high fat diet; d, days; w, weeks.

5.1.5 Gene expression pattern of isolated microglia cells exposed to short-term and prolonged high fat diet

The effects of HFD upon hypothalamic cytokine expression have thus far only been assessed in whole hypothalamic tissue, within the framework of this thesis as well as in all published studies. Therefore, the aim of the presently discussed experiment was to specifically assess the reaction of a specific cell type of the CNS, namely microglia, to diet without potential confounding influences from other cell types present in whole CNS tissue preparations. For this purpose, hypothalamic microglia were isolated from mice fed chow or HFD for 3 days and 8 weeks using CD11b+ magnetic beads. Following cell isolation, RNA was analyzed to quantify the gene expression of 42 selected genes using the NanoString nCounter® Technology. This method allows for the analysis of multiple gene targets in one reaction with the sensitivity of one RNA copy per cell. Targets for this analysis included typical inflammatory genes (e.g. *Il1b*, *Il6*, *Tnf*, *Il10*,

Tgfb) as well as genes that have been shown to be specifically enriched in microglia cells [72, 114] (e.g. *P2ry12*, *Selplg*, *Siglech*, *Tmem119*, *Ccr5*) (see methods Table 4). The data were analyzed using nSolver® software and target gene expression was normalized to the 6 housekeeping genes that were included in the analysis. Hierarchical clustering of the normalized gene expression using nSolver® software showed that after 3 days, the expression profile of microglia from mice fed HFD was not distinct from microglia from chow-fed mice (Figure 10 A). In contrast, 8 weeks of HFD induced a change in the microglial gene expression pattern that is clearly distinguishable from that of microglia isolated from chow-fed mice (Figure 10 B). Despite a lack of overall expression profile difference, analysis of mRNA counts of microglia from mice experiencing HFD for 3 days compared to chow-fed mice confirmed the previous findings (Figure 9 A), namely that short-term exposure to a diet high in fat induces a pro-inflammatory reaction. The gene expression of the cytokines IL-1β (*Il1b*) and IL-6 (*Il6*) was increased by 50 % in microglia from HFD-fed mice compared to those isolated from chow-fed animals. In addition, gene expression of CD74 (*Cd74*), a factor involved in MHCII transport and formation, was increased by 56 % (Figure 10 C). After 8 weeks of HFD, the expression of the pro-inflammatory molecules IL-6 and IRF-8 was decreased by 21 %. Furthermore, expression of microglia specific 'sensing' genes, including *P2ry12*, *Selplg*, *Slc2a5* and *Trem2*, was reduced between 10 and 17 % (Figure 10 D). Instead *Pparg* expression was highly increased (160 %) in microglia from HFD-fed mice compared to microglia from chow-fed mice.

These results obtained from isolated hypothalamic microglia cells support the impression from the analysis of whole hypothalamus tissue, that HFD induces an early pro-inflammatory response specifically in microglia, which switches into a more anti-inflammatory or subdued reaction upon prolonged HFD feeding.

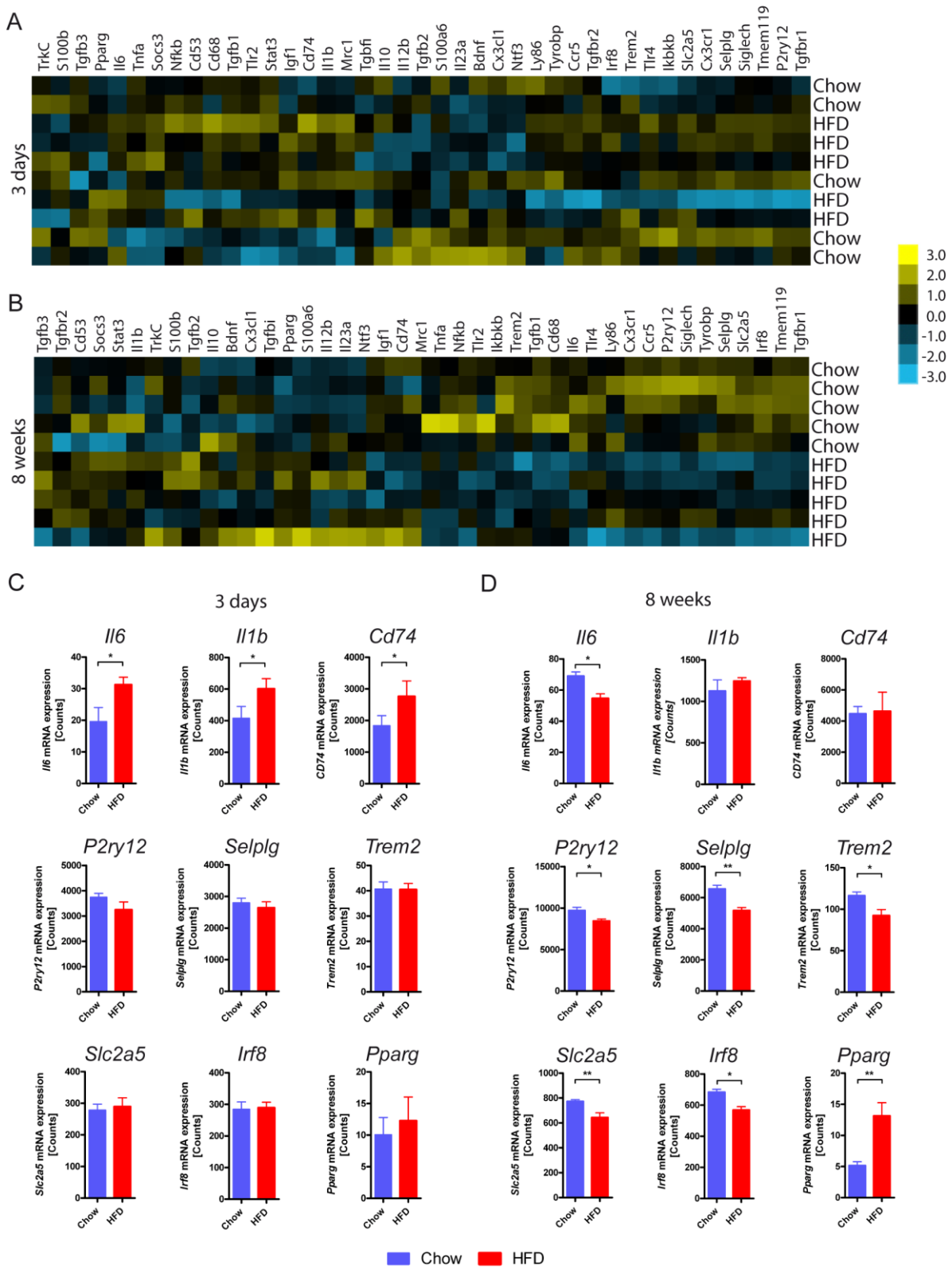

Figure 10: Quantitative gene expression analysis confirms anti-inflammatory response of isolated microglia to prolonged HFD. Heat map of normalized gene expression of microglia isolated from mice fed HFD or chow for (A) 3 days and (B) 8 weeks. mRNA counts of inflammatory and microglia-specific genes in isolated microglia from mice fed HFD or chow for (C) 3 days and (D) 8 weeks. n=5 per group. *p>0.05, **p>0.01 based on student's t-test. Data represents means +/- s.e.m.

5.1.6 Stimulation of primary adult microglia with serum derived from HFD-fed mice

High fat diet feeding leads to an increase in hormones (e.g. insulin and leptin) and cytokines in the blood. Blood components, such as leptin, are known to alter hypothalamic neuronal activity [20, 108]. To determine whether microglia reactivity in the hypothalamus of mice fed a high fat diet represents a primary glial reaction that may in turn lead to secondary neuronal effects or rather a secondary reaction to altered neuronal homeostasis, microglia from adult mice were isolated using CD11b+ magnetic beads, immediately cultured in a 24-well plate and on the next day stimulated with plasma of mice that were fed HFD or chow for 16 weeks (Figure 11). Cytokines in the microglia-conditioned medium were measured using the Meso Scale® V-PLEX Plus Proinflammatory Panel. This analysis revealed that there was no change in cytokine production in microglia that were stimulated with plasma of HFD-fed mice compared to chow plasma revealing that direct exposure to plasma components from HFD-fed mice does not induce acute pro-inflammatory microglia cytokine responses under these experimental conditions. On the contrary, IL-1β, IL-6, CXCL1 and TNFα were reduced by more than half in both plasma treated groups compared to cells without plasma stimulation (Figure 11 I, J), which suggests that isolated microglia display an altered phenotype that can be normalized by addition of the plasma.

Based on the results of this analysis it appears that microglia do not react substantially to factors derived from the blood of HFD-fed animals. Thus, it is possible that the microglial reaction towards diets high in fat is rather secondary to HFD-related changes in neurons.

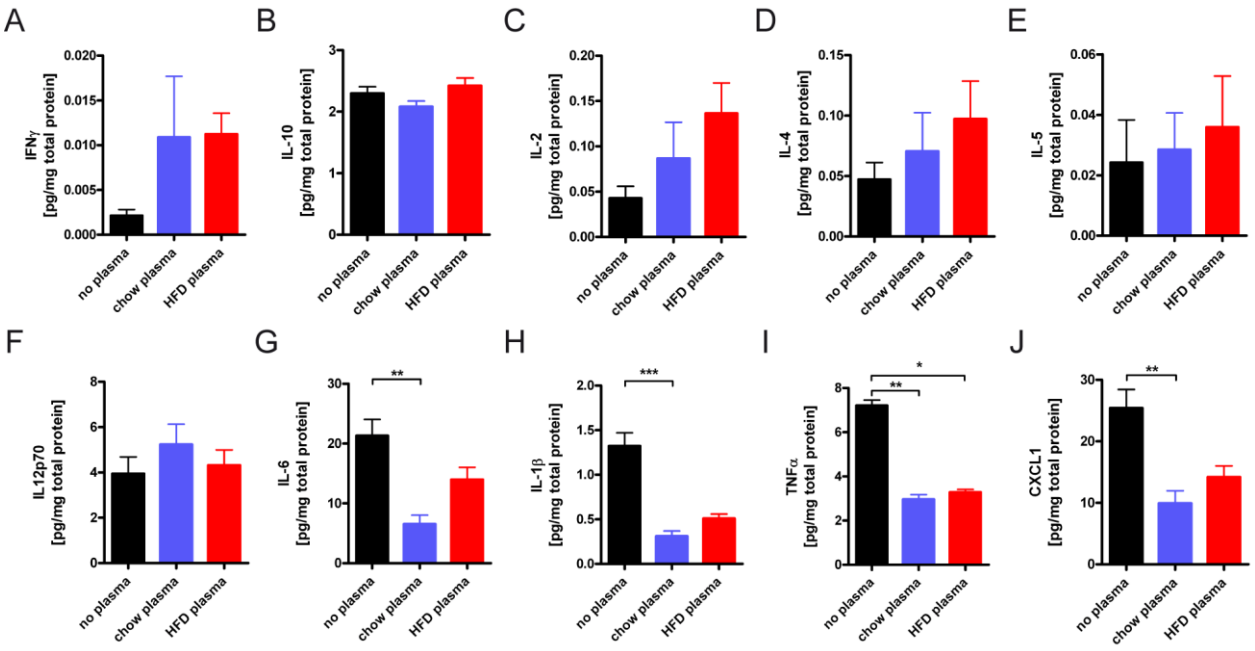

Figure 11: Plasma of HFD-fed mice does not induce cytokine production in isolated adult microglia. (A) IFNγ, (B) IL-10, (C) IL-2, (D) IL-4, (E) IL-5, (F) IL12p70, (G) IL-6, (H) IL-1β, (I) TNFα, and (J) CXCL1 protein levels in the supernatant of isolated microglia stimulated for 5 hours with 10 % plasma of mice fed HFD or chow for 16 weeks. n=3 independent experiments. *P<0.05, ***P<0.001, **P<0.01 based on One-Way ANOVA with Dunn's Multiple Comparison Post-Test. Data represents means +/- s.e.m. HFD, high fat diet.

5.1.7 LPS stimulation of microglia isolated from HFD-fed mice

Microglia priming is a phenomena known to occur in aging and neurodegenerative diseases [115, 116]. Microglia that are primed are more susceptible to a second inflammatory stimulus and react with an increased production of inflammatory cytokines. A common stimulus utilized to assess the microglia inflammatory reaction is lipopolysaccharide (LPS), which is a major component of the outer membrane of Gram-negative bacteria and a strong stimulus for innate immune cells. To determine whether chronic high fat diet primes microglia, cells were isolated from the hypothalamus of mice fed high fat diet or chow for 16 weeks using CD11b+ magnetic beads, immediately cultured in a 24-well plate and on the next day stimulated with LPS or PBS (Figure 12). The microglia-conditioned medium was collected before and after 14 h of LPS or PBS stimulation and analyzed for the cytokines TNFα, CXCL1, IL-6, IL12p70, IL-1β and IL-10 using the Meso Scale® V-PLEX Proinflammatory Panel.

Analysis of the basal cytokine production revealed no difference in cytokine expression between microglia of mice fed high fat diet compared to microglia from chow-fed mice, confirming previous findings (Figure 9 C, D). Furthermore, stimulation with PBS as control did not cause any changes in the cytokine expression of microglia derived from HFD- or chow-fed mice. On the other hand, LPS stimulation induced a significant increase in TNFα, CXCL1 and IL-6 in microglia independent of the diet they were exposed to previously (Figure 12 A-C). IL12p70, IL-1β and IL-10 production were not changed by LPS stimulation (Figure 12 D-F).

These results demonstrate that microglia are neither primed by high fat diet nor impaired in their reaction to strong stimuli like LPS.

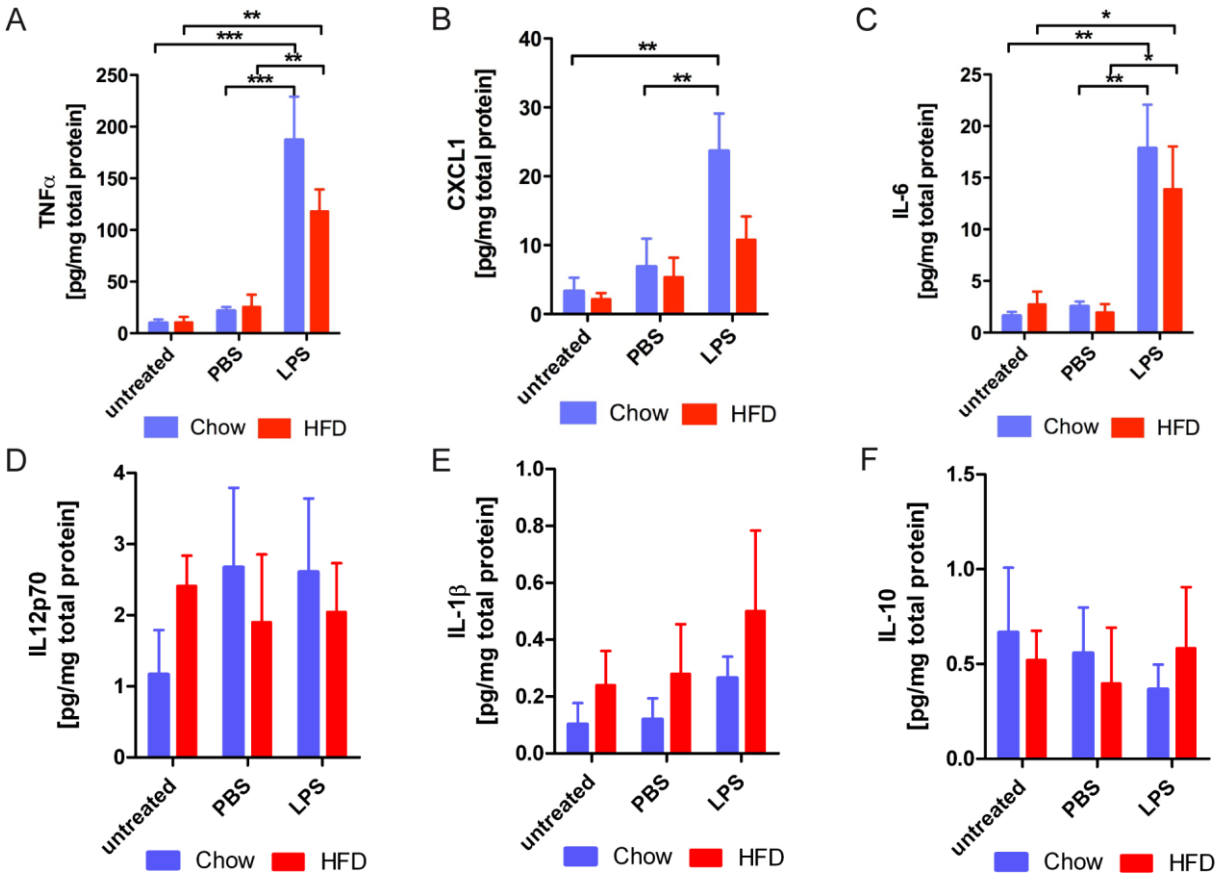

Figure 12: Microglia exposed to chronic high fat diet react normally to LPS stimulation. (A) TNFα, (B) CXCL1, (C) IL-6, (D) IL12p70, (E) IL-1β and (F) IL10 protein levels in the supernatant of untreated, PBS and LPS stimulated isolated adult hypothalamic microglia of mice fed HFD or chow for 16 weeks. n=3 independent experiments. *p<0.05, ***p<0.001, **p<0.01 based on Two-Way ANOVA with Bonferroni's multiple comparison post-test. Data represents means +/- s.e.m. LPS, lipopolysaccharide; HFD, high fat diet.

5.2 Physiological role of microglia in body weight homeostasis

Microglia are known to play an important role in brain development and normal brain homeostasis [77, 78, 117]. As described in the previous chapter, microglia react to diets high in fat, though this reaction is neither exclusively pro-inflammatory as it has been suggested by other studies [59, 89] nor does HFD exposure impair the cellular reaction to other stimuli. This differential response of microglia to HFD can be seen specifically in the hypothalamus, which suggests that they impart an important influence on the function of this brain region that controls food intake and energy expenditure. To assess the role of microglia in the regulation body weight homeostasis in the second part of this thesis, CD11b-HSVTK (from now on called CD11b-TK) mice were used, which allow for an inducible and specific depletion of microglia cells in the brain.

5.2.1 Metabolic phenotyping of transgenic CD11b-TK and wild-type mice

To set a baseline for the following experiments several parameters involved in body weight homeostasis were analyzed in untreated wild-type and CD11b-TK mice. This metabolic phenotyping included assessment of body weight, body composition, food intake, serum levels of the regulatory hormones insulin and leptin, as well as locomotor activity and energy expenditure using PhenoMaster cages (TSE Systems). Moreover, hypothalamic gene expression of genes important for the regulation of food intake and energy expenditure (*Npy*, *Pomc* and *Socs3*) were measured. Figure 13 A shows the correlation between body weight and age of wild-type and CD11b-TK mice. Linear regression analysis revealed a significant difference between the two groups. The regression line for CD11b-TK mice runs above the line for wild-type mice indicating that the transgenic mice had a higher body weight than age-matched mice negative for the transgene. This was due to a higher percentage of fat mass in CD11b-TK mice (19,4 ± 1,4 %) compared to wild-type mice (12,6 ± 0,7 %) as shown by the analysis of body composition (Figure 13 B). In addition, the percentage of lean mass was reduced in the transgenic mice (CD11b-TK: 71,5 ± 1,1 %, wild-type: 80,8 ± 0,6 %). However, there was no difference in food intake as measured in the metabolic cages between CD11b-TK and wild-type mice (Figure 13 C). Furthermore, no significant difference was detected in insulin and leptin levels in the serum of these mice (Figure 13 F). Similarly, locomotor

activity and energy expenditure were comparable in CD11b-TK and wild-type mice (Figure 13 D, E, G, H). Both parameters show the expected day and night pattern of mice: reduced locomotor activity and energy expenditure during the day and an increase during the night, when the mice are active. Lastly, no difference was detected in hypothalamic gene expression of the genes *Npy*, *Pomc* and *Socs3* (Figure 13 I). Taken together, there was no baseline difference between CD11b-TK and wild-type mice in the measured parameter, namely food intake, serum insulin and leptin level, hypothalamic gene expression as well as locomotor activity and energy expenditure. However the elevated body weight of the CD11b-TK mice should be considered for the further analyses.

5.2.2 Microglia depletion and myeloid cell repopulation in the hypothalamus of CD11b-TK mice

As described in chapter 3.8, depletion of microglia in CD11b-TK mice leads to repopulation of the whole brain with peripherally-derived myeloid cells [102]. This offers the opportunity to study whether these cells are able to functionally replace endogenous microglia in a specific context. For this reason, the time points for the analyses in the following experiment were chosen in a way that the effect of microglia depletion (10 days ganciclovir (GCV), ‘Depletion’ paradigm) as well as the effect of short-term (28 days GCV, ‘Short-term repopulation’ paradigm) and long-term (4 weeks GCV and 4 weeks without GCV treatment (8-weeks time point), ‘Long-term repopulation’ paradigm) repopulation with peripherally-derived myeloid cells was analyzed (Figure 14 A, D, G). Furthermore, the following analyses were focused on the hypothalamus - the central brain region responsible for the regulation of food intake and energy expenditure (see chapter 3.2 of the introduction).

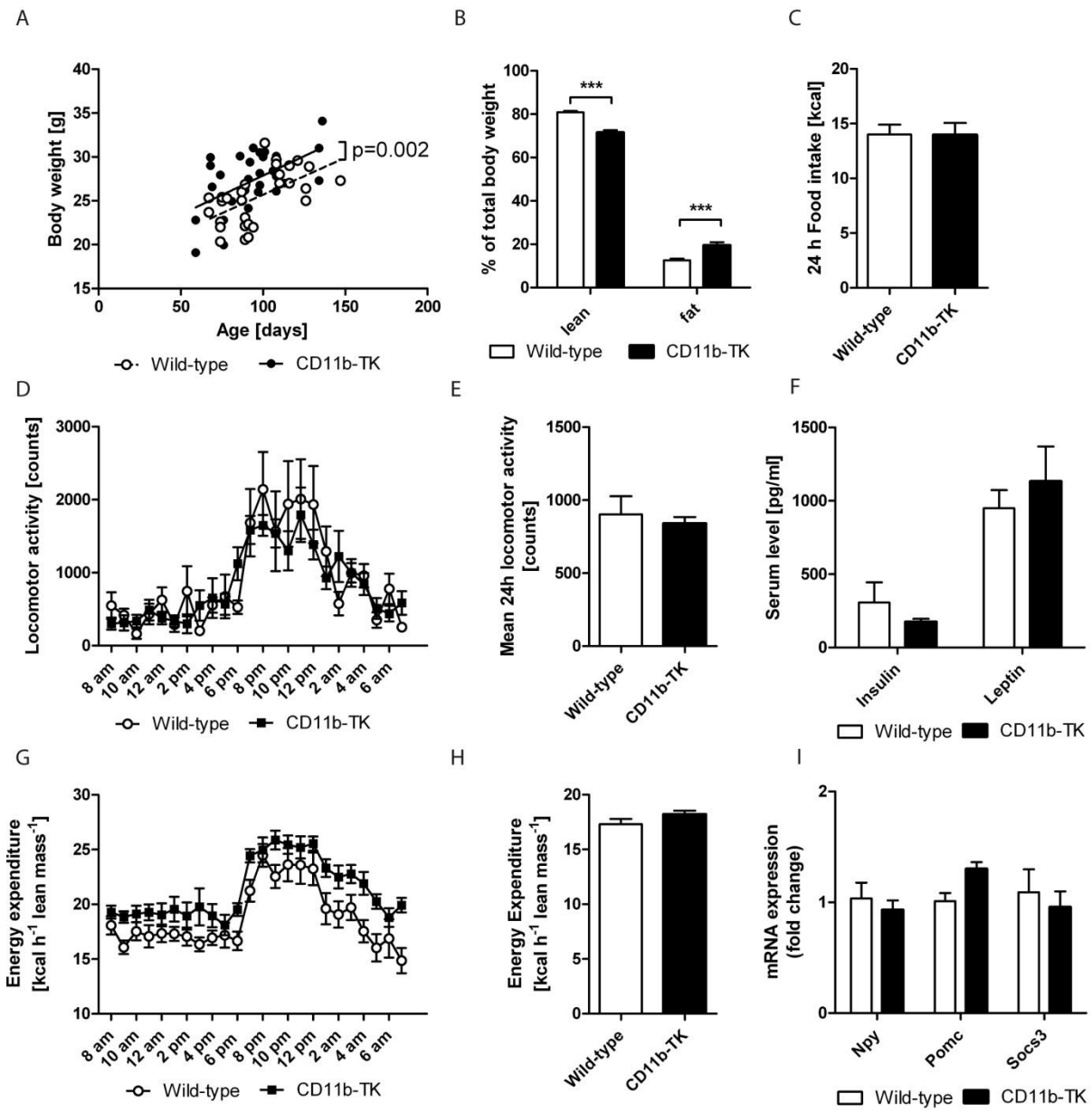

Figure 13: Metabolic phenotyping of CD11b-TK-transgenic versus wild-type mice. (A) Correlation of age and body weight of TK-transgenic mice and negative littermates (wild-type). (B) Body composition of 100-120 days old CD11b-TK and wild-type mice. (C) Food intake of 100-120 days old CD11b-TK and wild-type mice in metabolic cages over 24 h. (D) 24 h and (E) mean locomotor activity of 100-120 days old CD11b-TK and wild-type mice in metabolic cages. (F) Insulin and leptin levels in the serum of 100-120 days old CD11b-TK and wild-type mice. (G) 24 h and (H) mean energy expenditure of 100-120 days old CD11b-TK and wild-type mice in metabolic cages. (I) *Npy*, *Pomc* and *Socs3* mRNA expression in the hypothalamus of 100-120 days old CD11b-TK and wild-type mice. n=10 per group. ***p<0.001 based on Two-Way ANOVA with Bonferroni's multiple comparison post-test. Data represents means +/- s.e.m.

To first assess the extent of microglia depletion and myeloid cell repopulation, the hypothalamus of mice treated along the three different treatment paradigms was analyzed histologically using the microglia/myeloid cell marker Iba1. 10 days ganciclovir treatment led to an 87 % percent reduction of Iba1-positive cells in the hypothalamic area (Figure 14 C) which is also evident in the histological images (Figure 14 B). Although ganciclovir was applied continuously, at 28 days after the start of GCV treatment, the hypothalamus was already repopulated with Iba1+ cells that have been proven to be peripherally-derived [102] and can also indirectly be distinguished from resident microglia histologically by their elongated cell bodies and shorter and less ramified processes (Figure 14 E, right insert). Quantification of Iba1-positive cell number in the hypothalamus of mice with this short-term myeloid cell repopulation revealed an increase of 112 % in the total number of Iba1+ cells in comparison to wild-type mice still harboring endogenous microglia (Figure 14 F). Likewise, after long-term repopulation with peripherally-derived myeloid cells the number of Iba1-positive cells the hypothalamus of CD11b-TK mice was comparable to what was detected upon short-term repopulation (Figure 14 H, I).

The histological analysis revealed that microglia were effectively depleted from the hypothalamus, the region that is responsible for the regulation of body weight homeostasis, followed by a rapid and successful replacement by peripherally-derived myeloid cells. These peripheral cells were more numerous and displayed a distinct morphology, which does not change to a great extent over the time course analyzed in this study.

5.2.3 Body weight, body composition and food intake of GCV-treated CD11b-TK and wild-type mice

Next, to get a first impression of the effect of microglia depletion and myeloid cell repopulation in the brains of CD11b-TK mice on general body weight homeostasis, body weight, body composition and food intake of these mice were assessed and compared to wild-type mice, which still harbor endogenous microglia. Body weight of CD11b-TK and wild-type mice treated with GCV for the described time points (Figure 14) was assessed before and at the end point of the treatment.

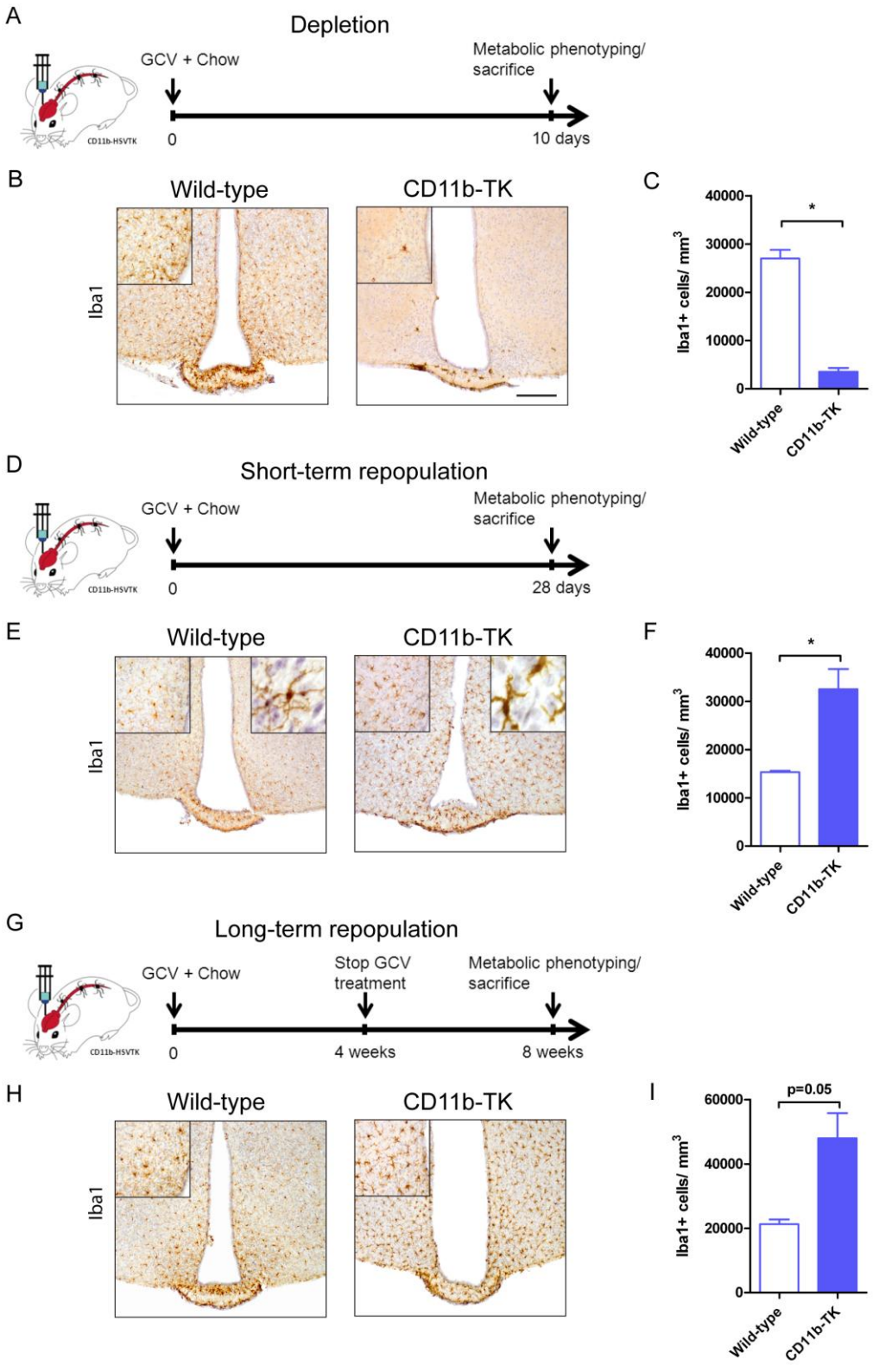

Figure 14: Microglia depletion and peripherally-derived myeloid cell repopulation in CD11b-TK and wild-type mice treated with ganciclovir (GCV) for 10 days, 28 days and 4 weeks followed by an additional 4 weeks without GCV treatment. (A) Experimental time course of the 10 days paradigm of GCV delivery to deplete resident microglia (Depletion). (B) Iba1-immunoreactivity in CD11b-TK and wild-type mice treated with GCV for 10 days allowing stereological assessment of the amount of microglial

numbers. (C) Quantification of Iba1+ cells in the hypothalamus of CD11b-TK and wild-type mice treated with GCV for 10 days. n=4 per group. (D) Experimental time course of 28 day paradigm of GCV delivery (Short-term repopulation). (E) Iba1-immunoreactivity in wild-type and CD11b-TK mice treated with GCV for 28 days allowing stereological assessment of the amount of microglial numbers. (F) Quantification of Iba1+ cells in the hypothalamus of CD11b-TK and wild-type mice treated with GCV for 28 days. n=5 per group. (G) Experimental time course of the 8 weeks paradigm of GCV delivery (Long-term repopulation). (H) Iba1-immunoreactivity in CD11b-TK and wild-type mice treated along the 8 weeks paradigm allowing stereological assessment of the amount of microglial numbers. (I) Quantification of Iba1+ cells in the hypothalamus of CD11b-TK and wild-type mice treated along the 8 weeks paradigm. Scale bar, 200 µm. n=4 per group. *p<0.05 based on student's t-test. Data represents means +/- s.e.m. GCV: ganciclovir.

Figure 15 A displays the body weight change compared to the initial body weight in percent. This analysis revealed that wild-type mice lost 2 % of their initial body weight (Figure 15 A, 'Depletion' time point). Similarly, microglia-depleted CD11b-TK mice lost 2 %, which suggests that this is an effect of the surgical procedure. In line with this, wild-type mice recovered from the operation and had gained 10 % body weight 28 days after the operation ('Short-term repopulation' time point), possibly due to age-related body weight gain. In contrast, short-term repopulated CD11b-TK mice displayed a significant 10 % reduction of their initial body weight. Interestingly, with long-term repopulation CD11b-TK mice gained weight again, which was then almost equal to their initial body weight and to the body weight of wild-type mice (Figure 15 A, 'Long-term repopulation' time point).

Analysis of body composition supports these findings (Figure 15 B, C). In wild-type mice, fat mass gradually increases and was significantly increased after 8 weeks (Figure 15 B, 'Long-term repopulation' time point). Concomitant with the increase in fat mass, a significant decrease of was measured in lean mass (Figure 15 C). In CD11b-TK mice a reduction of 6 % in fat mass was detected with short-term repopulation, in line with the reduction in body weight seen at that time point (Figure 15 A). Then, fat mass increases again with long-term repopulation, similar to the body weight gain of these mice see in (A). As was observed in wild-type mice, the increase in fat mass went along with a significant decrease in lean mass of CD11b-TK mice with long-term repopulation (Figure 15 C).

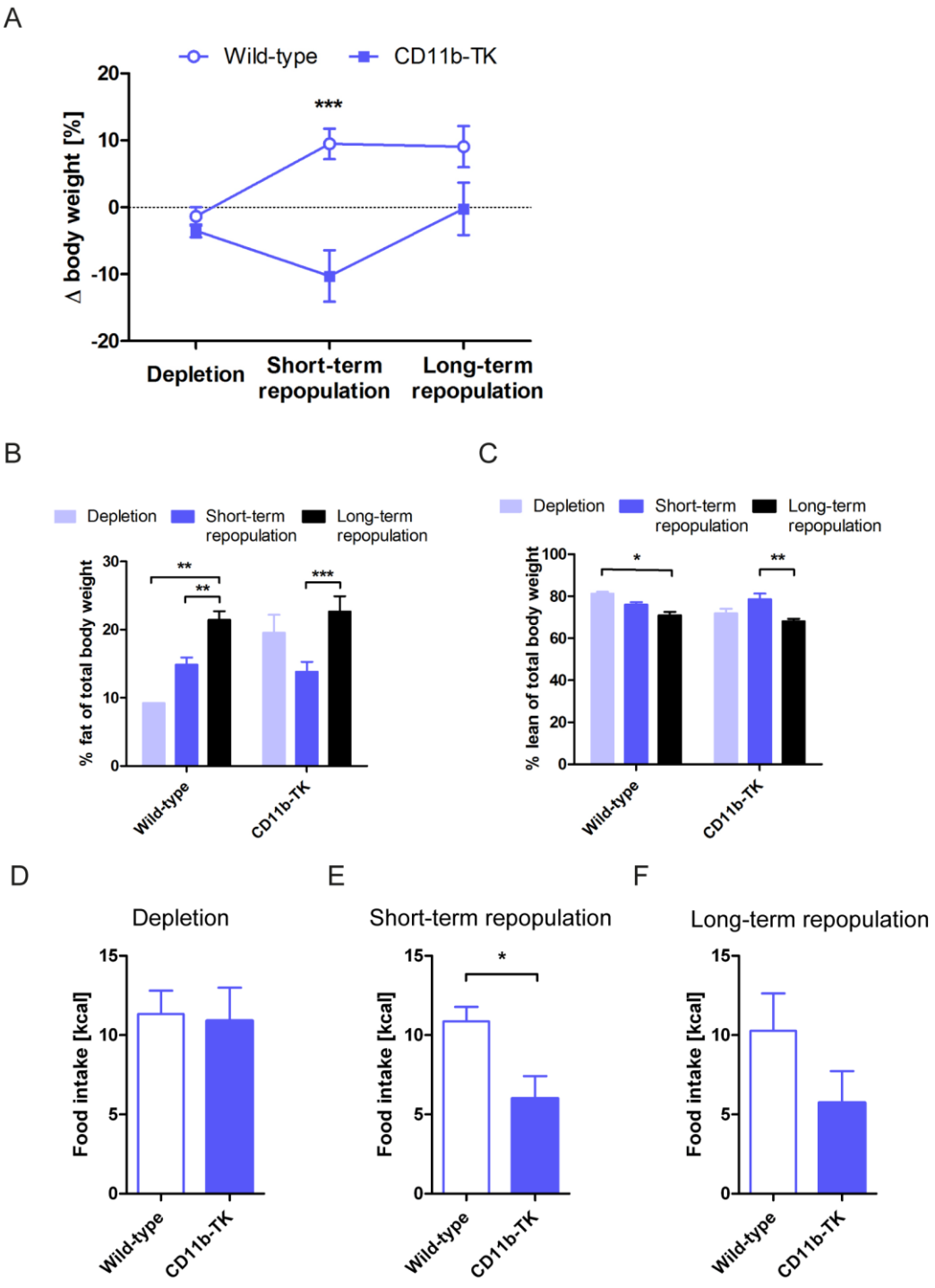

Figure 15: Body weight, body composition and food intake of GCV-treated CD11b-TK and wild-type mice. (A) Body weight change in % at the end of the three treatment paradigms. (B) Percent fat mass of total body weight and (C) percent lean mass of total body weight of CD11b-TK and wild-type mice at the end of the three treatment paradigms. Food intake of CD11b-TK and wild-type mice in metabolic cages over 24 h after (D) 10 days, (E) 28 days and (F) 8 weeks. 10 d: n=7 CD11b-TK, n=9 wild-type, 28 d: n=10 both groups, 8 w: n=6 CD11b-K, n=8 wild-type. *p<0.05, **p<0.01, ***p<0.001 based on student's t-test or Two-Way ANOVA with Bonferroni's multiple comparison post-test. Data represents means +/- s.e.m.

Food intake in the metabolic cages was not different between wild-type and CD11b-TK mice at the ‘Depletion’ time point (Figure 15 D) matching the unchanged body weight. However, CD11b-TK mice with short-term repopulation, which exhibited a reduced body weight, also displayed a significant reduction in food intake (Figure 15 E), which was no longer detectable with long-term repopulation (Figure 15 F).

Taken together, these results indicate an effect of microglia depletion and short-term myeloid cell repopulation on body weight in CD11b-TK mice. The observed reduction in body weight and fat mass due to microglia depletion and short-term repopulation can be rescued by long-term repopulation of the brain with peripherally-derived myeloid cells.

5.2.4 Locomotor activity and energy expenditure of GCV-treated CD11b-TK and wild-type mice

Apart from the change in food intake, which was significantly reduced in CD11b-TK mice repopulated with peripherally-derived myeloid cells compared to wild-type mice harboring endogenous microglia, an increase in locomotor activity or energy expenditure could, in principle, also explain the decrease in body weight in CD11b-TK mice. For this reason these parameters were analyzed in CD11b-TK and wild-type mice treated along the described three treatment paradigms.

Microglia-depleted CD11b-TK mice appeared to move less during the night (Figure 16 A). However, this reduction was not significant and moreover, the mean locomotor activity over 24 h was not significantly different between groups (Figure 16 B). Furthermore, no change in energy expenditure was measured in microglia-depleted CD11b-TK (Figure 16 C, D).

The locomotor activity of short-term repopulated CD11b-TK mice showed high variations over the 24 h measurement period (Figure 16 E). However, there was no significant difference in the mean of the 24 h measurement (Figure 16 F). In addition, energy expenditure was not changed between CD11b-TK and wild-type mice at that time point. Similarly, long-term repopulation of the brains of CD11b-TK mice did not induce differences in locomotor activity or energy expenditure (Figure 16 I-L).

These results show that neither locomotor activity nor energy expenditure are changed upon microglia depletion or myeloid cell repopulation in CD11b-TK mice and thus cannot explain the reduction in body weight.

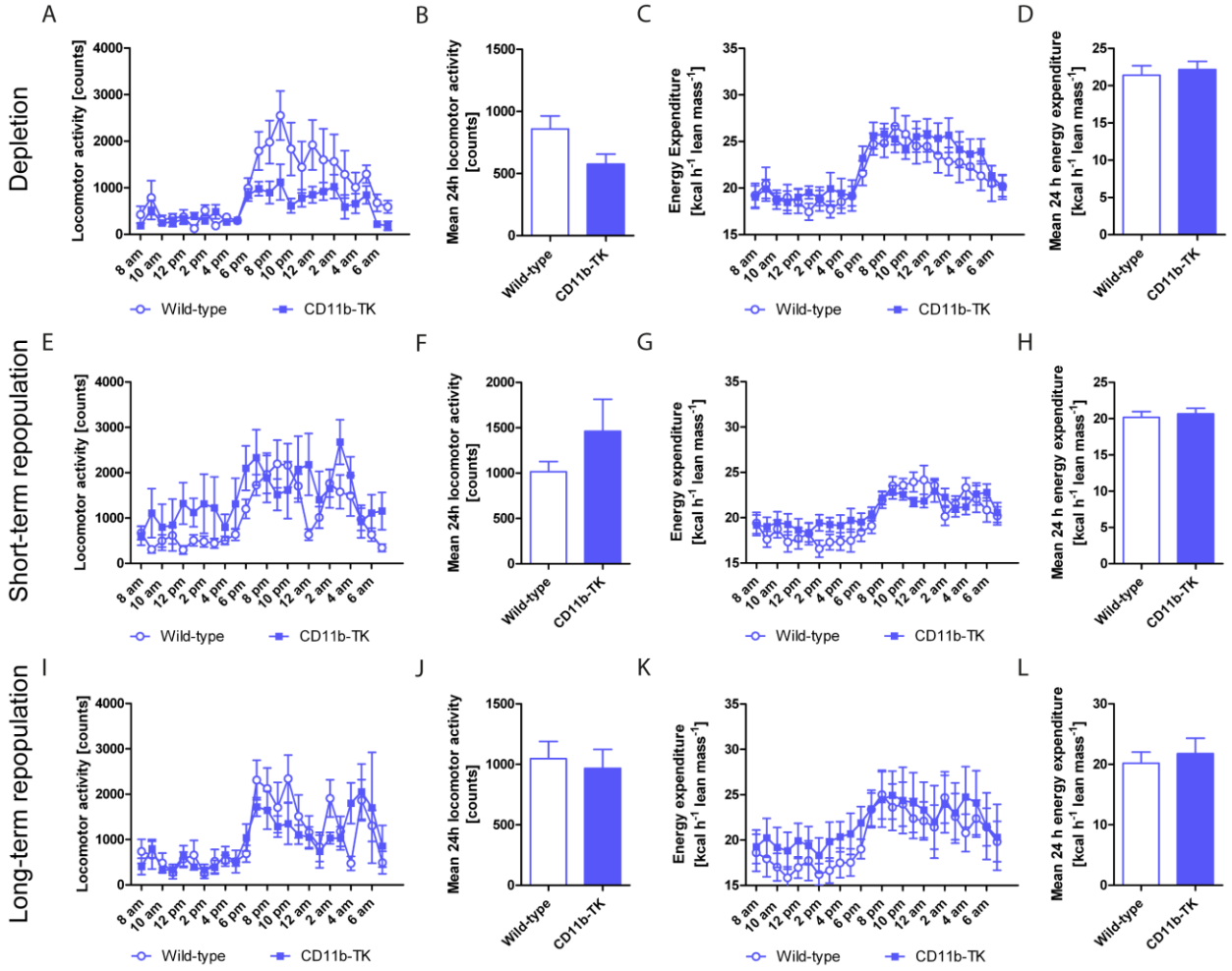

Figure 16: Locomotor activity and energy expenditure of GCV-treated CD11b-TK and wild-type mice. (A) 24 h locomotor activity, (B) Mean 24 h locomotor activity, (C) 24 h energy expenditure, (D) Mean 24 h energy expenditure of CD11b-TK and wild-type mice treated with GCV for 10 days. n=7 CD11b-TK, n=9 wild-type. (E) 24 h locomotor activity, (F) Mean 24 h locomotor activity, (G) 24 h energy expenditure, (H) Mean 24 h energy expenditure of CD11b-TK and wild-type mice treated with GCV for 28 days. n=10 per group. (I) 24 h locomotor activity, (J) Mean 24 h locomotor activity, (K) 24 h energy expenditure, (L) Mean 24 h energy expenditure of CD11b-TK and wild-type mice treated along the 8-weeks paradigm. n=6 CD11b-TK, n=8 wild-type. Data represents means +/- s.e.m.

5.2.5 Well-being of GCV-treated CD11b-TK and wild-type mice

To rule out the possibility of sickness behavior as a cause for the decrease in body weight observed in the previous experiment, which was most pronounced in CD11b-TK with short-term myeloid cell repopulation, blood serum of CD11b-TK and wild-type mice treated with GCV for 28 days was analyzed for C-reactive protein (CRP), IL-6,

corticosterone, alanine transaminase (ALT) and aspartate transaminase (AST) (Figure 17). All of these factors are expected to be increased in case of general sickness. However, no significant increase was detected in all investigated parameters in CD11b-TK compared to wild-type mice (Figure 17 A-D).

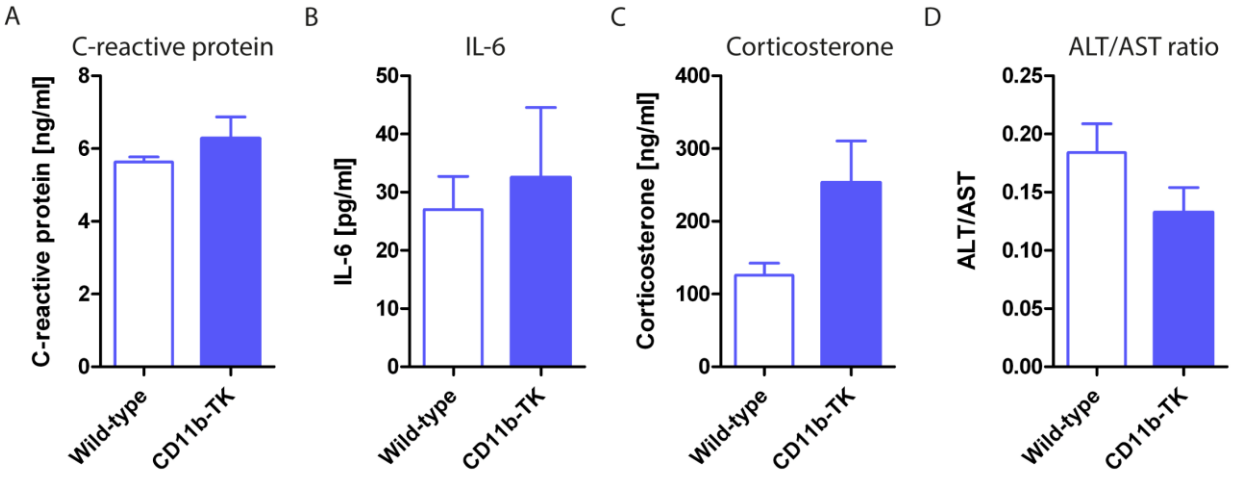

Figure 17: Serum parameters measured to exclude sickness behavior of CD11b-TK and wild-type mice treated with GCV for 28 days. (A) C-reactive protein, (B) IL-6 and (C) corticosterone level in the serum of CD11b-TK and wild-type mice treated with GCV for 28 days. (D) Ratio of alanine transaminase (ALT) and aspartate transaminase (AST) serum level of CD11b-TK and wild-type mice treated with GCV for 28 days. n=10 per group. Data represents means +/- s.e.m.

5.2.6 Insulin and leptin levels of GCV-treated CD11b-TK and wild-type mice

To further assess the impact of central microglia depletion and myeloid cell repopulation on peripheral metabolic parameters, the hormones insulin and leptin were analyzed in the serum of CD11b-TK and wild-type mice at the end of the three treatment paradigms (Figure 14) using the Mouse Metabolic Kit from Meso Scale®. 10 days GCV treatment, which led to microglia depletion in CD11b-TK mice, did not induce changes in either hormone (Figure 18 A). Short-term repopulation in CD11b-TK led to a slight reduction in leptin levels, though this difference was not significant (Figure 18 B). Finally, also with long-term repopulation, insulin and leptin levels were not changed in CD11b-TK mice (Figure 18 C). Therefore, the reduction in body weight of CD11b-TK mice can probably also not be attributed to changes in insulin or leptin levels.

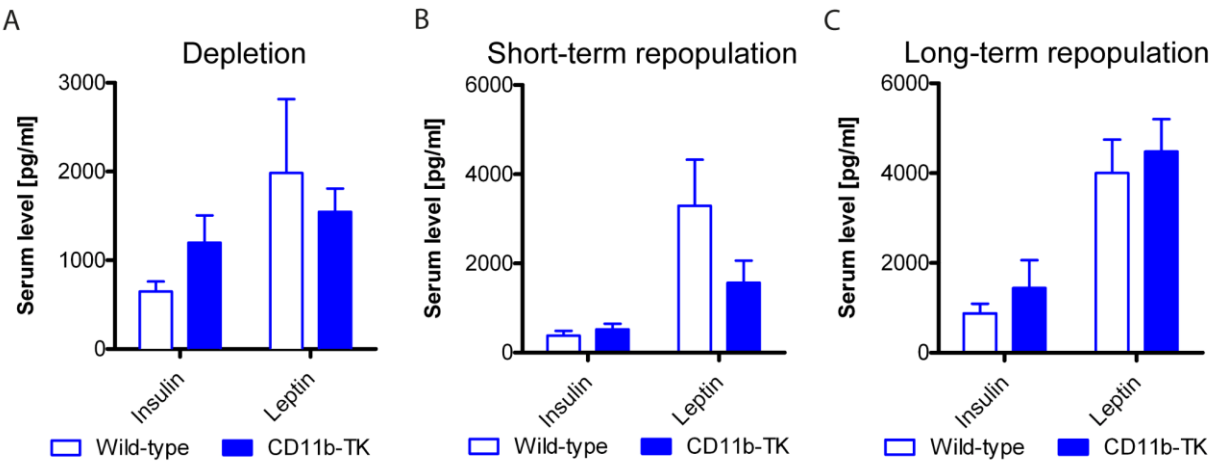

Figure 18: Insulin and leptin serum levels of GCV-treated CD11b-TK and wild-type mice. (A) Insulin and leptin levels in the serum of CD11b-TK and wild-type mice treated with GCV for 10 days. n=7 CD11b-TK, n=10 wild-type. (B) Insulin and leptin levels in the serum of CD11b-TK and wild-type mice treated with GCV for 28 days. n=10 per group. (C) Insulin and leptin levels in the serum of CD11b-TK and wild-type mice treated with along the 8-weeks paradigm. n=6 CD11b-TK, n=8 wild-type. Data represents means +/- s.e.m.

5.2.7 Hypothalamic gene expression of GCV-treated CD11b-TK and wild-type mice

POMC and NPY neurons in the hypothalamus play a key role in regulating body weight homeostasis. POMC+-neurons act to increase energy expenditure and decrease food intake, while NPY+-neurons, mediate the opposing responses leading to a decrease in energy expenditure and an increase in food intake. To address the effects of microglia depletion and/or repopulation with peripherally-derived myeloid cells on hypothalamic neurons, *Pomc* and *Npy* gene expression were analyzed in hypothalamic tissue of CD11b-TK and wild-type mice treated with GCV for 10 days (‘Depletion’ paradigm), 28 days (‘Short-term repopulation’ paradigm) and 4 weeks followed by 4 weeks without GCV treatment (‘Long-term repopulation’ paradigm) (Figure 19). Apart from *Pomc* and *Npy*, *Socs3* gene expression was also assessed, as it is involved in the development of leptin resistance [118] as was also described in chapter 3.2 of the introduction.

Microglia depletion did not induce changes in *Pomc* and *Npy* gene expression. However, *Socs3* expression was significantly increased by 3-fold at that time point (Figure 19 A). Short-term repopulation in CD11b-TK mice induced a 3-fold increase in *Npy* expression, which was significant compared to *Npy* expression in wild-type mice

(Figure 19 B), while there was no significant difference in *Pomc* and *Socs3* gene expression. In CD11b-TK mice with long-term repopulation, *Npy* expression was still significantly increased by 2.5-fold, as was *Socs3* expression, while *Pomc* gene expression remained unchanged (Figure 19 C).

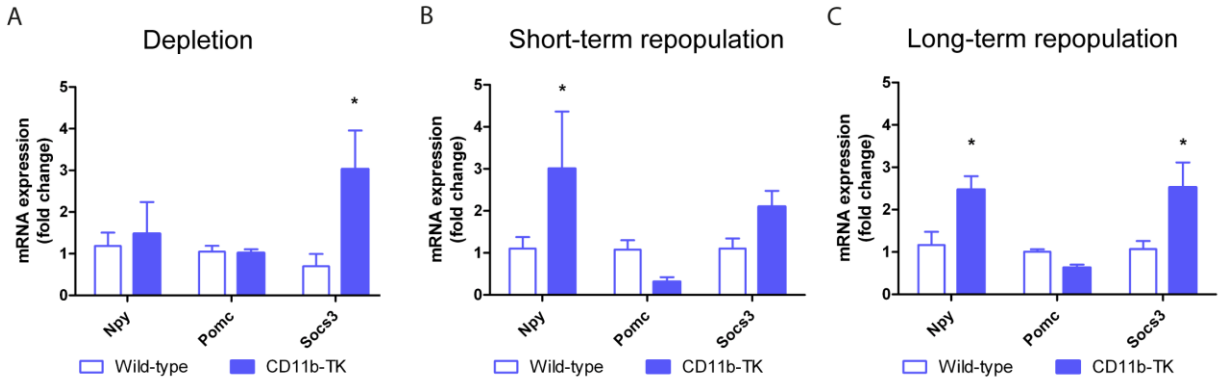

Figure 19: mRNA expression of genes involved in energy regulation in the hypothalamus of GCV-treated CD11b-TK and wild-type mice. *Npy*, *Pomc* and *Socs3* mRNA expression in the hypothalamus of CD11b-TK and wild-type mice treated with GCV for (A) 10 days. n=5 per group (B) 28 days. n=4 per group (C) 4 weeks with an additional 4 weeks without GCV treatment. n=5 CD11b-TK, n=4 wild-type. *p<0.05 based on Two-Way ANOVA with Bonferroni's multiple comparison post-test. Data represents means +/- s.e.m.

Even though a general sickness of the mice was previously excluded (Figure 17), inflammation in the hypothalamus due to the exchange of resident microglia with peripherally-derived myeloid cells could impact body weight homeostasis. Therefore, inflammatory genes were analyzed in the hypothalamus of CD11b-TK and wild-type mice (Figure 20). This analysis revealed a 3.9-fold increase in *Il1b* in microglia-depleted mice, which was significant compared to wild-type mice, whereas *Tnfa*, *Nfkb* and *Ikkb* were not changed by microglia depletion (Figure 20 A). When the hypothalamus of CD11b-TK mice was repopulated for a short period of time, there was a trend towards increased *Il1b* and *Tnfa* gene expression (Figure 20 B). After long-term repopulation in CD11b-TK mice, *Tnfa* was significantly increased by 6-fold and there was still a trend towards increased *Il1b* (Figure 20 C). *Nfkb* and *Ikkb* gene expression remained unchanged with short- and long-term repopulation.

To conclude, increased hypothalamic *Npy* expression in repopulated CD11b-TK mice may occur in response to the reduced body weight, since it should induce genes to decrease energy expenditure and increase food intake. *Socs3* upregulation may

indicate an early leptin resistance in CD11b-TK mice, though this would not explain the decrease in body weight. The increase in pro-inflammatory genes is possibly due to the repopulation by infiltrating peripherally derived myeloid cells.

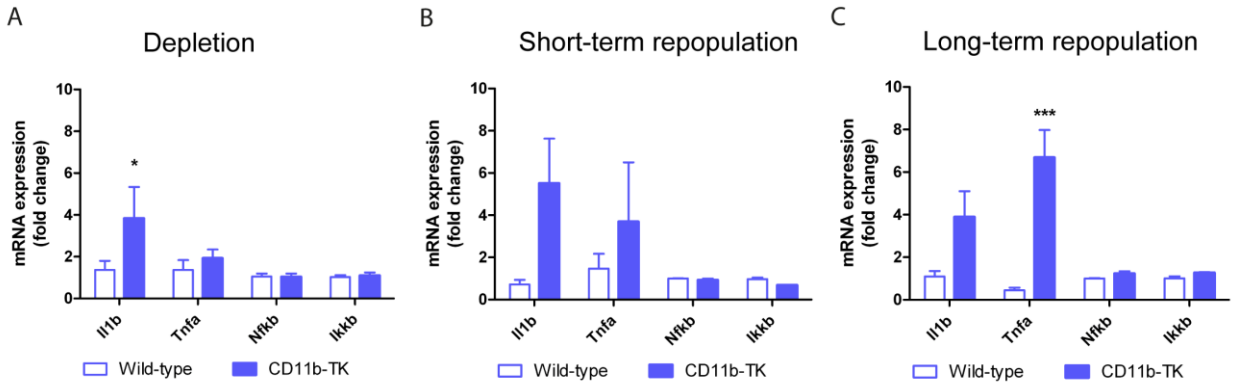

Figure 20: mRNA expression of inflammatory genes in the hypothalamus of GCV-treated CD11b-TK and wild-type mice. *Il1b*, *Tnfa, Nfkb* and *Ikkb* mRNA expression in the hypothalamus of CD11b-TK and wild-type mice treated with GCV for (A) 10 days. n=5 per group (B) 28 days. n=4 per group (C) 4 weeks with an additional 4 weeks without GCV treatment. n=5 CD11b-TK, n=4 wild-type. *p<0.05, ***p<0.001 based Two-Way ANOVA with Bonferroni's multiple comparison post-test. Data represents means +/- s.e.m.

5.2.8 Gene expression in brown and white adipose tissue of GCV-treated CD11b-TK and wild-type mice

Peripheral signals about the nutrient status of the body are integrated in the hypothalamus and from there energy homeostasis is adjusted accordingly. The brown and the white adipose tissue are amongst the peripheral organs that receive signals from the brain, which can change their expression of genes related to energy metabolism. Prominent amongst those genes is uncoupling protein 1 *(Ucp1),* which is important for heat production, called thermogenesis, in brown adipose tissue. Furthermore, it can be upregulated in white adipose tissue and initiate a process called 'browning'. This browning of the white adipose tissue can lead to increased thermogenesis and thus induce slimming. *Ucp1* expression is driven by the transcription factor peroxisome proliferator-activated receptor-γ coactivator 1 alpha (*Ppargc1a*). Independently of *Ucp1*, *Ppargc1a* regulates fatty acid oxidation and mitochondrial gene expression. To assess whether microglia depletion and myeloid cell repopulation in the

hypothalamus lead to changes in gene expression in peripheral organs, which might explain the weight reduction seen in short-term repopulated CD11b-TK mice (Figure 15 A), *Ucp1* and *Ppargc1a* gene expression were analyzed in CD11b-TK and wild-type mice treated with GCV for 10 days ('Depletion' paradigm), 28 days ('Short-term repopulation' paradigm) and 4 weeks followed by 4 weeks without GCV treatment ('Long-term repopulation' paradigm) (Figure 21).

Overall no significant changes in *Ucp1* and *Ppargc1a* gene expression were detected in brown adipose tissue of CD11b-TK mice at any time point (Figure 21 A-C). Similarly, in white adipose tissue, *Ucp1* and *Ppargc1a* gene expression were unchanged in microglia-depleted and short-term repopulated CD11b-TK mice. However, in white adipose tissue of CD11b-TK with long-term repopulation, *Ppargc1a* was significantly upregulated by 4-fold.

The upregulation of *Ppargc1a* in white adipose tissue of CD11b-TK mice with long-term repopulation may be a sign of increased fatty acid oxidation in white adipose tissue. This in turn may have an effect on body weight of CD11b-TK mice. Even though at the time point this increase was measured the body weight was normal again, the effect on gene expression in the periphery could still be measurable and might decrease later.

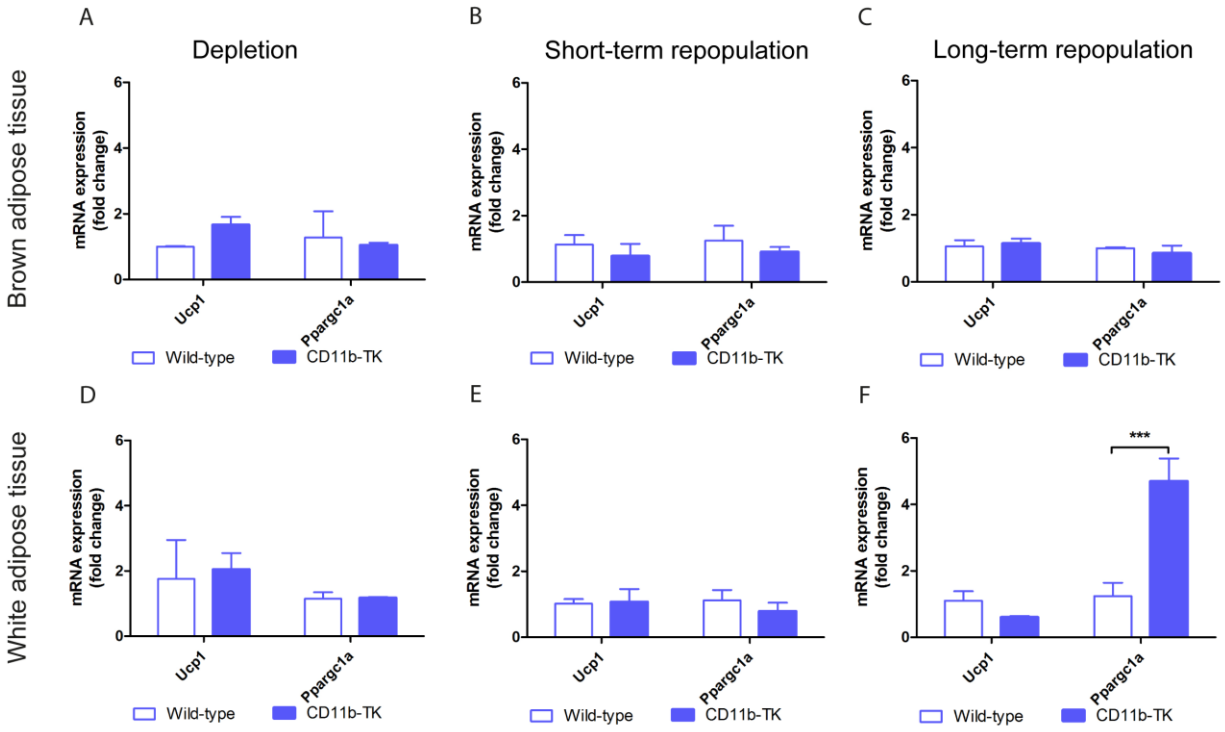

Figure 21: *Ucp1* and *Ppargc1a* gene expression in brown and white adipose tissue of GCV-treated CD11b-TK and wild-type mice. *Ucp1 and Ppargc1a* gene expression in brown adipose tissue of mice

treated with GCV for (A) 10 days (n=3 per group), (B) 28 days (n=4 per group) and (C) 4 weeks with an additional 4 weeks without GCV treatment (n=4 per group). *Ucp1* and *Ppargc1a* gene expression in white adipose tissue of mice treated with GCV for (D) 10 days (n=3 per group), (E) 28 days (n=4 per group) and (F) 4 weeks with an additional 4 weeks without GCV treatment (n=4 per group). ***p<0.001 based on Two-Way ANOVA with Bonferroni's multiple comparison post-test Data represents means +/- s.e.m.

5.3 Role of microglia in body weight homeostasis in the context of high fat diet (HFD)

The previous experiments were intended to gain insights into the role of microglia in body weight homeostasis under physiological conditions. At baseline, there was no difference between wild-type and CD11b-TK mice in terms of metabolic parameters, even though CD11b-TK mice display higher body weight and fat mass compared to age-matched transgene-negative littermates. Depletion of microglia reduces body weight of CD11b-TK mice, which is regained when peripherally-derived myeloid cells infiltrate the brain. In light of the body weight phenotype observed in microglia-depleted CD11b-HSVTK mice, this raises the question of how these animals would respond to diet-induced obesity. For the purpose of these experiments, CD11b-TK and wild-type mice were fed with a high fat diet comprised of 60 % of calories from fat.

5.3.1 Microglia depletion and myeloid cell repopulation in the hypothalamus of CD11b-TK mice fed HFD

To analyze the effect of diet-induced obesity on mice depleted of endogenous microglia or repopulated with peripherally-derived myeloid cells, the same time points were used that were described in chapter 5.2.2: GCV for 10 days (‘Depletion’ paradigm), 28 days (‘Short-term repopulation’ paradigm) and 4 weeks followed by 4 weeks without GCV treatment (8-weeks time point; ‘Long-term repopulation’ paradigm). In combination with a diet high in fat these time courses allow not only to study depletion and repopulation but also to assess different degrees of diet-induced obesity. 10 days of high fat diet are not expected to have a significant impact on body weight and hormone level. However, this time point includes the very early effects of HFD on hypothalamic pro-inflammatory cytokine expression, which was found to be increased 3 to 7 days after the start of HFD feeding (Figure 9 A). At 28 days, already a mild effect of diet-induced obesity on body

weight, insulin and leptin serum levels can be expected. Even more, 8 weeks of HFD should increase body weight as well as insulin and leptin serum levels, which are a sign of a developing insulin and leptin resistance.

As described in chapter 5.2.2 for CD11b-TK mice fed chow diet, at first microglia depletion and myeloid cell repopulation were analyzed histologically using the marker Iba1 to qualitatively and quantitatively assess the effect of ganciclovir (GCV) treatment in combination with HFD on microglia/myeloid cells in the hypothalamus of CD11b-TK and wild-type mice. Figure 22 depicts the different treatment paradigms as well as the Iba1-positive cells at the respective time points. Similar to the effects seen with chow diet, after 10 days of GCV treatment under HFD conditions 76 % of Iba1-positive cells were depleted in the hypothalamus (Figure 22 C), which is also evident in the histological images (Figure 22 B). After 28 days GCV treatment and HFD feeding, the hypothalamus was repopulated with peripherally-derived myeloid cells (Figure 22 E, F). Similar to the previous experiment (Figure 14), the short-term repopulated hypothalamus harbored an increased number of Iba1-positive cells compared to the number of endogenous microglia in wild-type mice. As described in chapter 5.1.1 (Figure 6 A, B), high fat diet leads to an increase in microglia number in the hypothalamus of wild-type mice. Probably due to this increase in wild-type mice, short-term repopulated CD11b-TK animals harbored only 76 % more Iba1-positive cells than wild-type mice fed HFD compared to 112 % seen under conditions of chow feeding. This effect was even more pronounced at the 8-weeks time point when gliosis was visible in the representative images of HFD-fed wild-type mice (Figure 22 H) and the amount of Iba1-positive cells in CD11b-TK mice with long-term repopulation was increased only 41 % (Figure 22 I). Interestingly, in repopulated CD11b-TK mice, some Iba1-positive cells close to the ventricle in the arcuate nucleus region appeared morphologically more altered with a ‘bushy’ appearance (Figure 22 H, insert) indicating that these cells may react similarly to the diet as endogenous microglia.

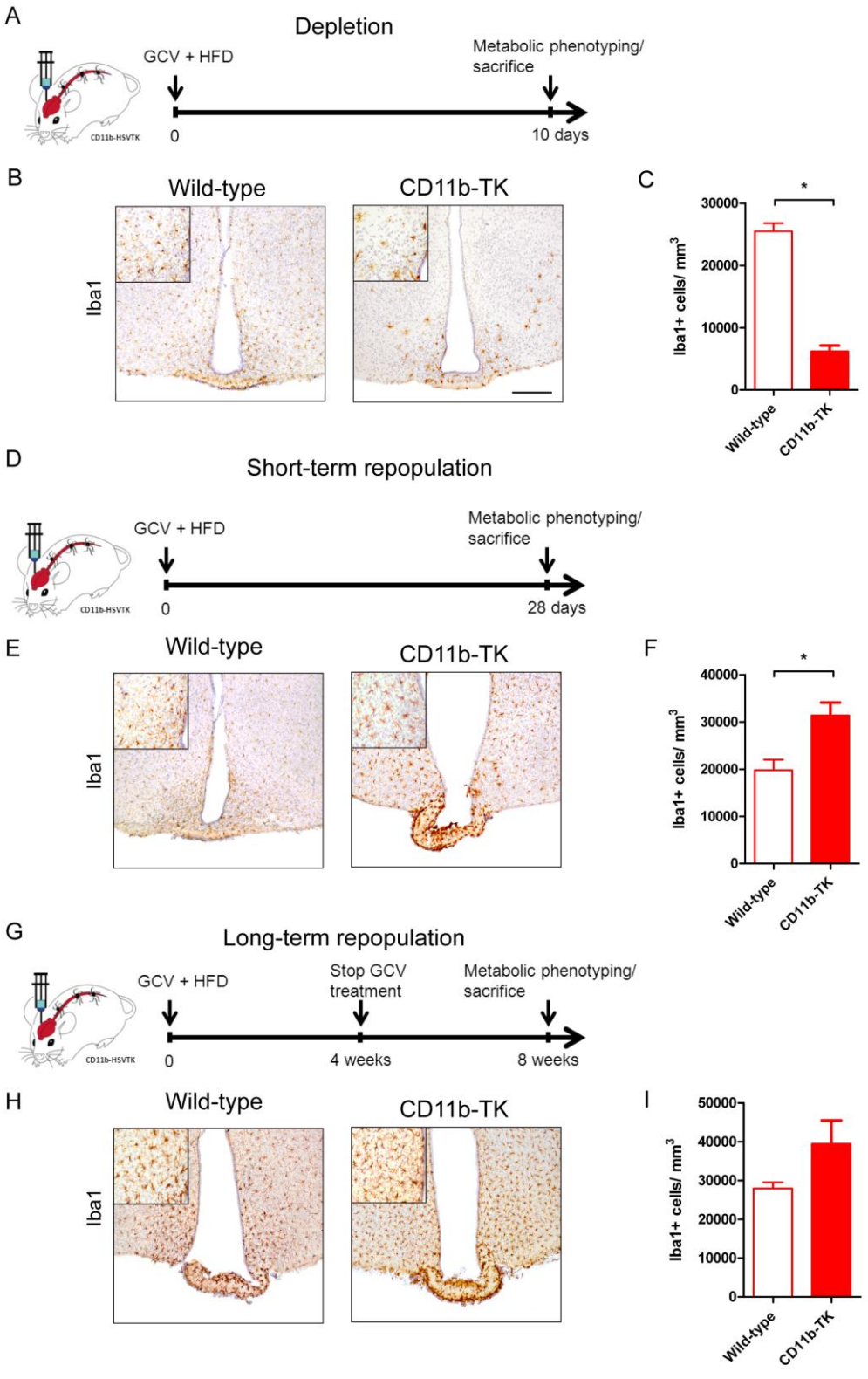

Figure 22: Microglia depletion and myeloid cell repopulation in CD11b-TK and wild-type mice treated with ganciclovir (GCV) and fed HFD for 10 days, 28 days and 8 weeks. (A) Experimental time course of the 10 days paradigm of GCV delivery to deplete resident microglia under HFD conditions (Depletion). (B) Iba1-immunoreactivity in CD11b-TK and wild-type mice treated with GCV for 10 days and fed HFD at the same time allowing stereological assessment of the amount of microglial numbers. (C)

Quantification of Iba1+ cells in the hypothalamus of CD11b-TK and wild-type mice treated with GCV for 10 days and fed HFD at the same time. n=4 per group. (D) Experimental time course of the 28 day paradigm of GCV delivery (Short-term repopulation). (E) Iba1-immunoreactivity in CD11b-TK and wild-type mice treated with GCV for 28 days and fed HFD at the same time allowing stereological assessment of the amount of microglial numbers. (F) Quantification of Iba1+ cells in the hypothalamus of CD11b-TK and wild-type mice treated with GCV for 28 days and fed HFD at the same time. n=5 per group. (G) Experimental time course of the 8 week paradigm of GCV delivery (Long-term repopulation). (H) Iba1-immunoreactivity in CD11b-TK and wild-type mice treated with GCV for 4 weeks with an additional 4 weeks without GCV treatment and HFD feeding throughout the 8 weeks allowing stereological assessment of the amount of microglial numbers. (I) Quantification of Iba1+ cells in the hypothalamus of CD11b-TK and wild-type mice treated along the 8 weeks paradigm. Scale bar, 200 µm. n=4 per group. *p<0.05 based on student's t-test. Data represents means +/- s.e.m.

5.3.2 Body weight, body composition and food intake of GCV-treated CD11b-TK and wild-type mice fed HFD

In order to assess the impact of HFD-feeding in general, body weight and body composition were measured at the beginning and the end of each of the three treatment paradigms: GCV for 10 days ('Depletion' paradigm), 28 days ('Short-term repopulation' paradigm) and 4 weeks followed by 4 weeks without GCV treatment (8-weeks time point; 'Long-term repopulation' paradigm)) (Figure 23).

Wild-type mice fed HFD for 10 days displayed a 4 % increase in body weight in comparison to their initial body weight. With longer duration of the HFD feeding, they gained up to 40 % of body weight (Figure 23 A, 'Long-term repopulation' time point).

In contrast, microglia-depleted and short-term repopulated CD11b-TK mice fed HFD did not gain weight. This was similar to chow-fed CD11b-TK mice that even had initially lost body weight (Figure 15 A). At the short-term repopulation time point body weight of CD11b-TK mice was significantly lower than that of wild-type mice. However, with long-term repopulation CD11b-TK gained about 30 % body weight similar to wild-type mice at this time point.

The analysis of body composition revealed that prolonged HFD induced a continuous significant increase in fat mass in wild-type mice (Figure 23 B). Along with this increase in fat mass, lean mass was significantly decreased (Figure 23 C).

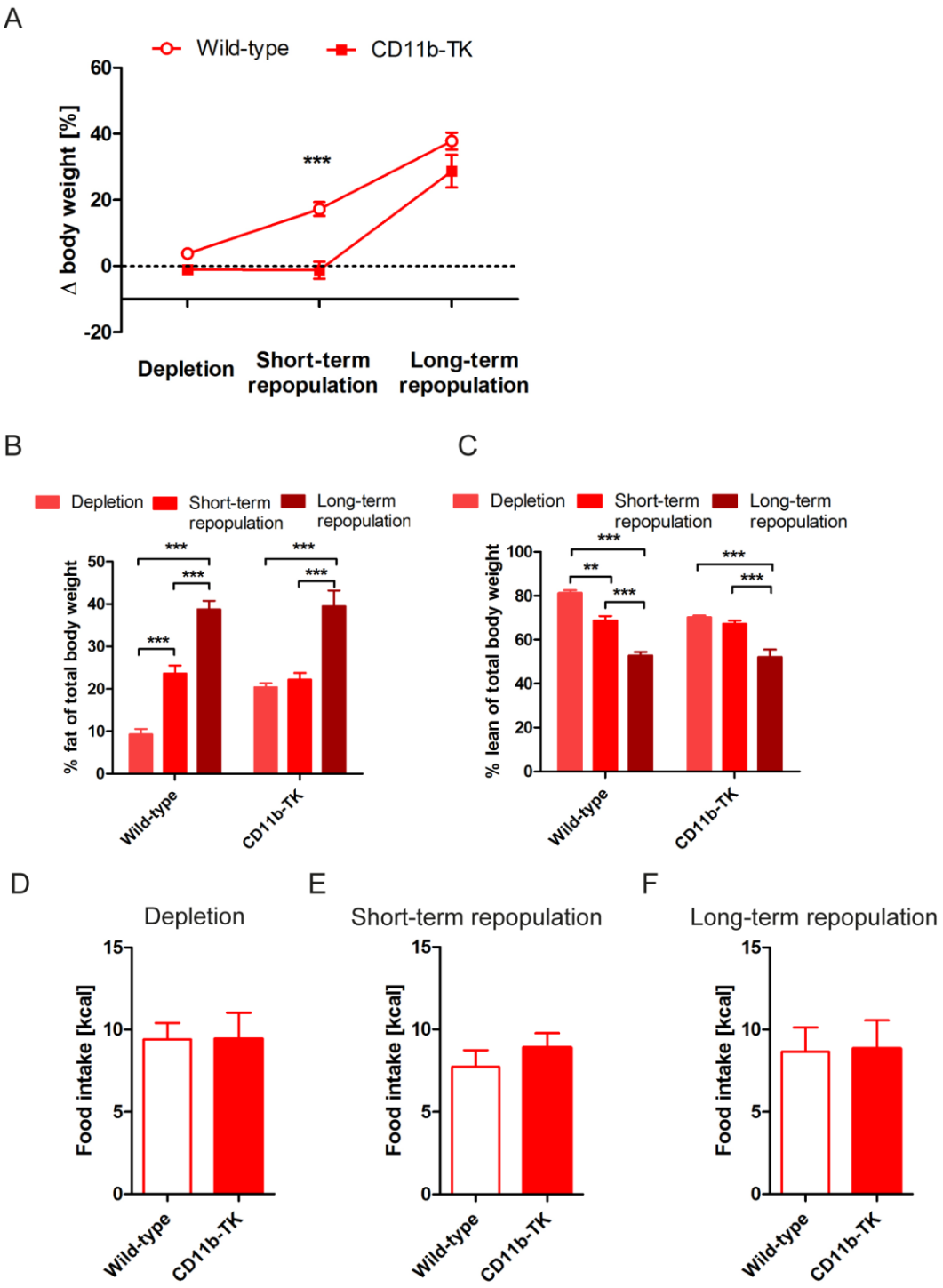

Figure 23: Body weight, body composition and food intake of GCV-treated CD11b-TK and wild-type mice fed HFD. (A) Body weight change in % at the end of the three treatment paradigms. (B) Percent fat mass of total body weight and (C) percent lean mass of total body weight of CD11b-TK and wild-type mice at the end of the three treatment paradigms. Food intake of CD11b-TK and wild-type mice in metabolic cages over 24 h after (D) 10 days, (E) 28 days and (F) 8 weeks. 10d: n=7 CD11b-TK, n=9 wild-type; 28 d: n=10 both groups; 8 w: n=6 CD11b-TK, n=8 wild-type. *p<0.05, **p<0.01, ***p<0.001 based on Two-Way ANOVA with Bonferroni's multiple comparison post-test. Data represents means +/- s.e.m.

In CD11b-TK mice this continuous change in lean and fat mass was not seen as both parameters remained unchanged in microglia-depleted and short-term repopulated CD11b-TK mice fed HFD matching the body weight phenotype seen in (A). Only under conditions of long-term repopulation and HFD feeding, fat mass of CD11b-TK mice was significantly increased while lean mass decreased (Figure 23 B, C). Similar to body weight (Figure 23 A), CD11b-TK and wild-type mice displayed the same percentage of fat and lean mass at the long-term repopulation time point.

The 24 h food intake in the metabolic cages was not changed in CD11b-TK mice at any of the analyzed time points (Figure 23 D-F). This was in contrast to CD11b-TK mice fed chow, which displayed a significantly reduction in food intake upon short-term depletion (Figure 15 E).

Taken together, CD11b-TK mice initially did not gain body weight under HFD conditions, associated with an unchanged fat mass. However, with long-term repopulation and HFD feeding their body weight was elevated to wild-type level. At this time point also the percentage in fat mass was similar in both groups. These results indicate an effect of microglia depletion and myeloid cell repopulation on body weight in CD11b-TK mice similar to what was observed in chow-fed CD11b-TK mice previously (Figure 15).

5.3.3 Locomotor activity and energy expenditure of GCV-treated CD11b-TK and wild-type mice fed HFD

As described in chapter 5.2.3, locomotor activity and energy expenditure were assessed in CD11b-TK and wild-type mice under the three treatment paradigms (Figure 22) using metabolic cages from Labmaster® (Figure 24). Overall, the activity pattern of wild-type and CD11b-TK mice exposed to GCV treatment and HFD feeding revealed no difference over 24 hours (Figure 24 A, E, I). As expected, mice moved less during the day (8 a.m. to 6 p.m.) and increased locomotion during their active phase (6 p.m. to 8 a.m.). Additionally, there was no difference in mean locomotor activity between the two groups at the different time points (Figure 24 B, F, J). However, upon prolonged HFD-feeding, the mean activity counts decreased from 1000 to ca. 800, probably due to higher body weight and concomitant decreased motivation to move. Whereas food intake and locomotor activity were not changed in microglia-depleted and/or myeloid

cell-repopulated CD11b-TK mice, energy expenditure was significantly increased at all analyzed time points. This could be appreciated already over the 24-h time course (Figure 24 C, G, K), but was even more obvious when assessing the mean energy expenditure (Figure 24 D, H, L).

An increase in energy expenditure would lead to a greater demand of 'fuel', thus explaining the decrease in body weight of GCV-treated CD11b-TK mice through a decrease in fat mass. However such increase in energy expenditure was not detected in chow-fed CD11b-TK mice - even though the latter mice lost body weight and fat mass similar to HFD-fed CD11b-TK mice. Therefore the increase in energy expenditure alone does not suffice to explain the reduction in body weight of microglia-depleted and myeloid cell-repopulated CD11b-TK mice.

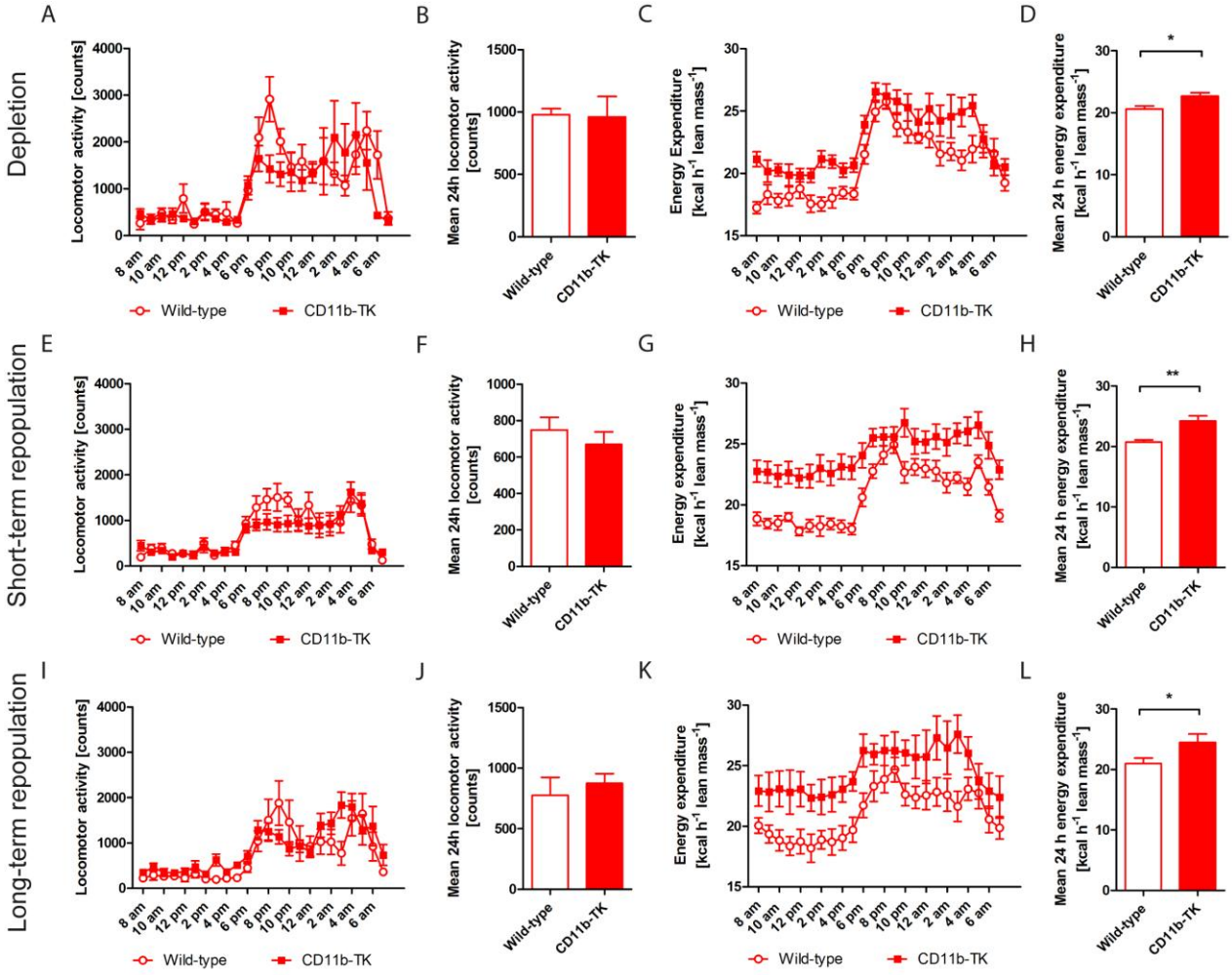

Figure 24: Locomotor activity and energy expenditure of GCV-treated CD11b-TK and wild-type mice fed HFD. (A) 24 h locomotor activity, (B) Mean 24 h locomotor activity, (C) 24 h energy expenditure, (D) Mean 24 h energy expenditure of CD11b-TK and wild-type mice treated with GCV and fed HFD for 10 days. n=9 (wild-type), 7 (CD11b-TK) (E) 24 h locomotor activity, (F) Mean 24 h locomotor activity, (G) 24

h energy expenditure, (H) Mean 24 h energy expenditure of CD11b-TK and wild-type mice treated with GCV and fed HFD for 28 days. n=10 per group (I) 24 h locomotor activity, (J) Mean 24 h locomotor activity, (K) 24 h energy expenditure, (L) Mean 24 h energy expenditure of CD11b-TK and wild-type mice treated with GCV for 4 weeks with an additional 4 weeks without GCV treatment and HFD feeding throughout the 8 weeks. n=6 CD11b-TK, n=8 wild-type. *p<0.05, **p<0.01 based on student's t-test or Two-Way ANOVA with Bonferroni's multiple comparison post-test. Data represents means +/- s.e.m.

5.3.4 Well-being of GCV-treated CD11b-TK and wild-type mice fed HFD

Due to the increase in energy expenditure in HFD-fed CD11b-HSVTK mice, again the sickness behavior was analyzed. Since the elevated energy expenditure may arise e.g. from fever, in addition to the serum parameters, namely C-reactive protein, IL-6, corticosterone, AST and ALT, body surface temperature of CD11b-TK and wild-type mice treated with GCV and fed HFD for 28 days was measured weekly (Figure 25). Alike in chow-fed CD11b-HSVTK mice, no significant differences were detected between HFD-fed CD11b-TK and wild-type mice with respect to CRP, IL-6, corticosterone levels or the ratio of the liver enzymes ALT and AST (Figure 25 A-D). Similarly, body surface temperature was not different between the two groups (Figure 25 E).

These results show that there is no general sickness behavior in CD11b-TK mice despite the reduction in body weight and the increase in energy expenditure. However, it has to be noted that only the surface body temperature was analyzed and body core temperature in principle, may still be altered in CD11b-TK.

5.3.5 Insulin and leptin levels of GCV-treated CD11b-TK and wild-type mice fed HFD

Other parameters allowing for the assessment of changes in body weight homeostasis are the serum levels of the hormones insulin and leptin, which are important for its regulation. As in chow-fed mice (5.2.6) they were analyzed in the serum of CD11b-TK and wild-type mice at the end of the three treatment paradigms using the Mouse Metabolic Kit from Meso Scale®. There was no difference detectable between microglia-depleted and myeloid cell-repopulated CD11b-TK and equally treated wild-type mice in either insulin or leptin (Figure 26). However, leptin levels increased with the

duration of HFD feeding in both CD11b-TK and wild-type mice from around 3000 pg/ml at 10 days (labeled ‘Depletion’) to 7000 pg/ml after 28 day (labeled ‘Short-term repopulation) and around 20,000 pg/ml after 8 weeks (labeled ‘Long-term repopulation) of HFD-feeding, which is a sign of a developing leptin resistance.

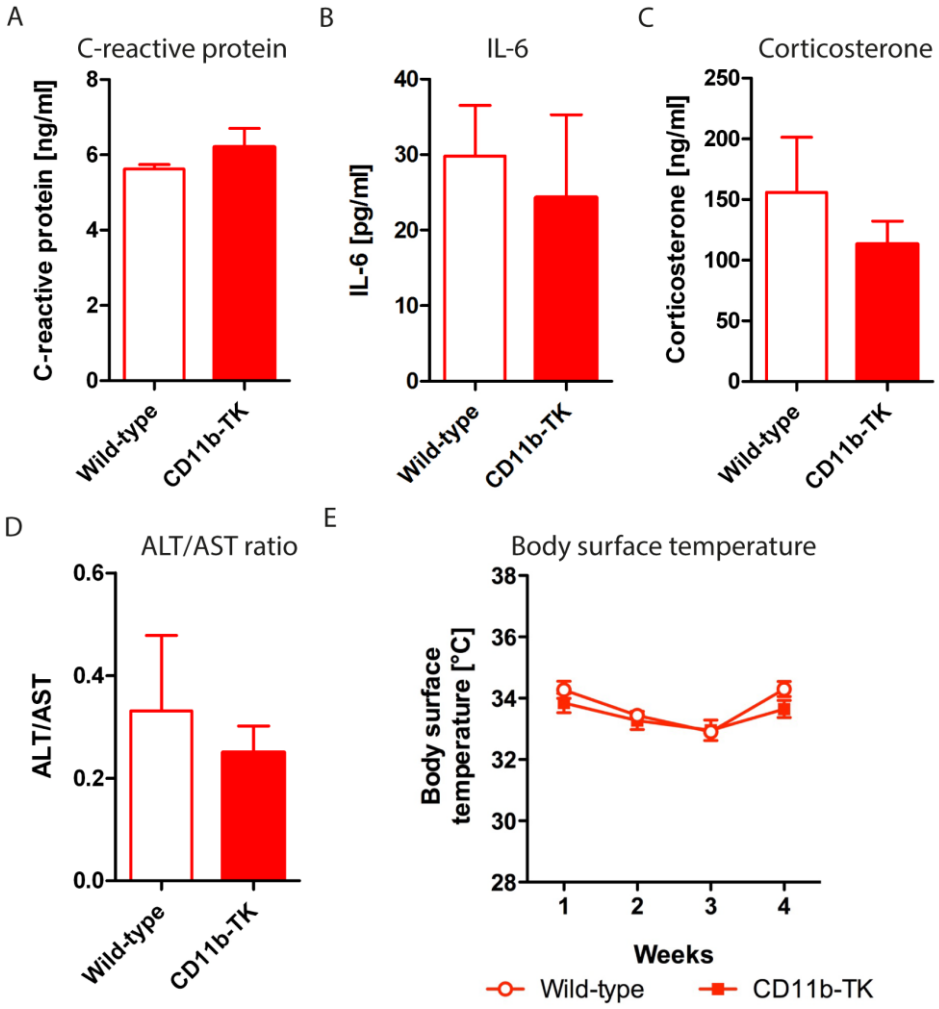

Figure 25: Serum parameters and body surface temperature measured to exclude sickness behavior of GCV-treated CD11b-TK and wild-type mice fed HFD. (A) C-reactive protein, (B) IL-6 and (C) Corticosterone, (D) ratio of ALT and AST level in the serum of CD11b-TK and wild-type mice treated with GCV for 28 days. (E) Body surface temperature of CD11b-TK and wild-type mice treated with GCV for 28 days. n=10 per group. Data represents means +/- s.e.m.

5.3.6 Hypothalamic gene expression of GCV treated CD11b-TK and wild-type mice fed HFD

As described in chapter 3.2, *Npy* and *Pomc* are important for the regulation of body weight homeostasis. Whereas *Pomc* decreases food intake and increases energy expenditure, *Npy* counteracts *Pomc* action. Analysis of the expression of *Npy* and *Pomc* in the hypothalamus of microglia-depleted or myeloid cell-repopulated CD11b-TK mice revealed no difference to wild-type mice at any of the analyzed time points (Figure 27). However, *Socs3*, which is involved in hypothalamic leptin resistance, was significantly upregulated in microglia-depleted and short-term repopulated CD11b-TK mice (Figure 27 A, B) and normalized again with long-term repopulation (Figure 27 C).

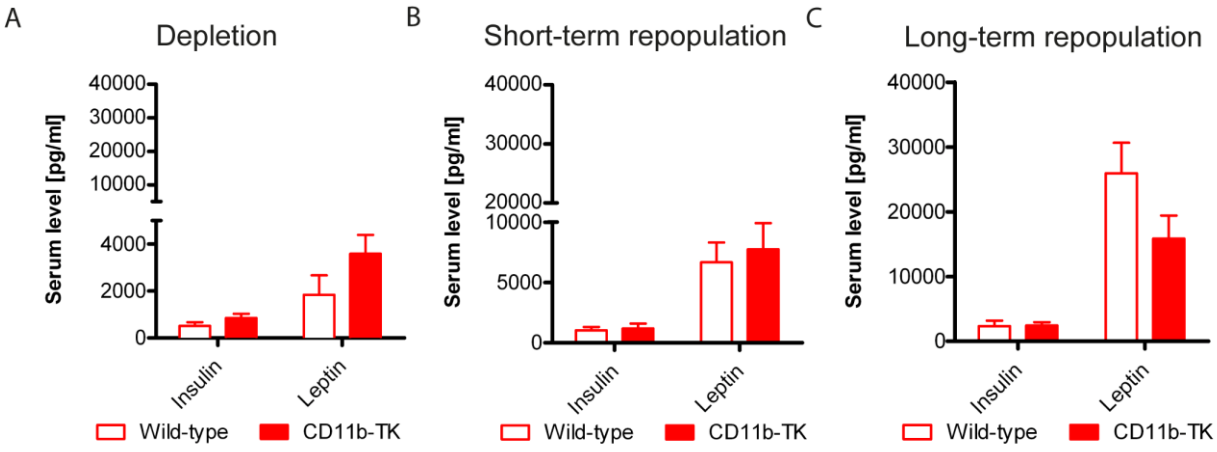

Figure 26: Insulin and leptin serum levels of GCV-treated CD11b-TK and wild-type mice fed HFD.

(A) Insulin and leptin levels in the serum of CD11b-TK and wild-type mice treated with GCV for 10 days. n=7 CD11b-TK, n=10 wild-type. (B) Insulin and leptin levels in the serum of CD11b-TK and wild-type mice treated with GCV for 28 days. n=10 per group. (C) Insulin and leptin levels in the serum of CD11b-TK and wild-type mice treated along the 8 weeks paradigm. n=6 CD11b-TK, n=8 wild-type. Data represents means +/- s.e.m.

Furthermore, as described previously (5.2.7) expression of genes involved in inflammation was analyzed. No difference in pro-inflammatory gene expression in the hypothalamus was detectable between microglia-depleted CD11b-TK and wild-type mice (Figure 28 A). Short-term repopulation in CD11b-TK mice upon HFD conditions led to a significant 15-fold increase in *Tnfa* gene expression. In addition, a trend towards increased *Il1b* was also detected in those mice (Figure 28 B). The same was true for

CD11b-TK mice with long-term repopulation, where *Tnfa* gene expression was still significantly increased 11-fold and *Il1b* was slightly elevated, though this difference was not significant (Figure 28 C).

Taken together, similar to the situation in chow-fed CD11b-TK mice, hypothalamic *Socs3* gene expression was increased in HFD-fed microglia-depleted and short-term repopulated CD11b-TK mice, which suggests an early induction of leptin resistance. However, this increase disappeared in CD11b-TK mice with long-term repopulation. Furthermore, the increase in pro-inflammatory markers in HFD-fed CD11b-TK mice is comparable to that in chow-fed CD11b-TK mice and probably also represents the reaction of infiltrating peripherally-derived myeloid cells.

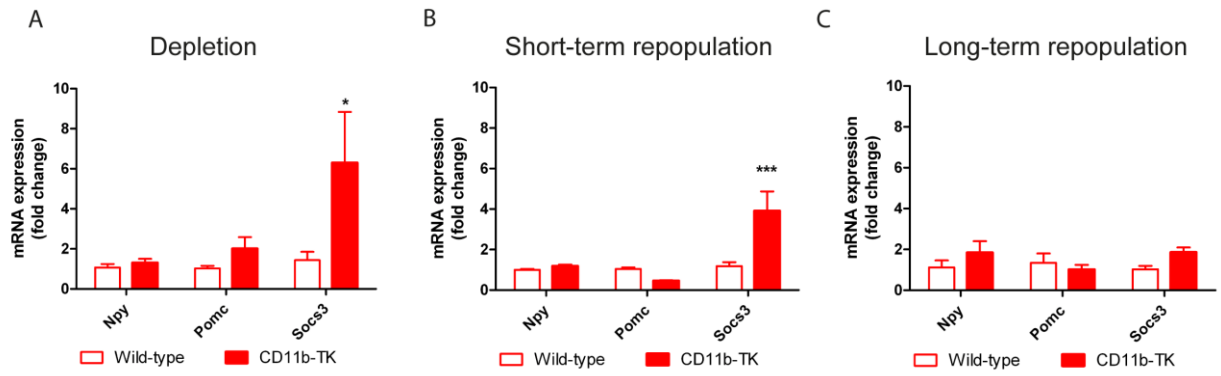

Figure 27: mRNA expression of genes involved in energy regulation in the hypothalamus of GCV-treated CD11b-TK and wild-type mice fed HFD. *Npy*, *Pomc* and *Socs3* mRNA expression in the hypothalamus of CD11b-TK and wild-type mice treated with GCV for (A) 10 days. n=5 per group (B) 28 days. n=4 per group (C) 28 days with an additional 4 weeks without treatment. n=5 CD11b-TK, n=4 wild-type. *p<0.05 based on Two-Way ANOVA with Bonferroni's multiple comparison post-test. Data represents means +/- s.e.m.

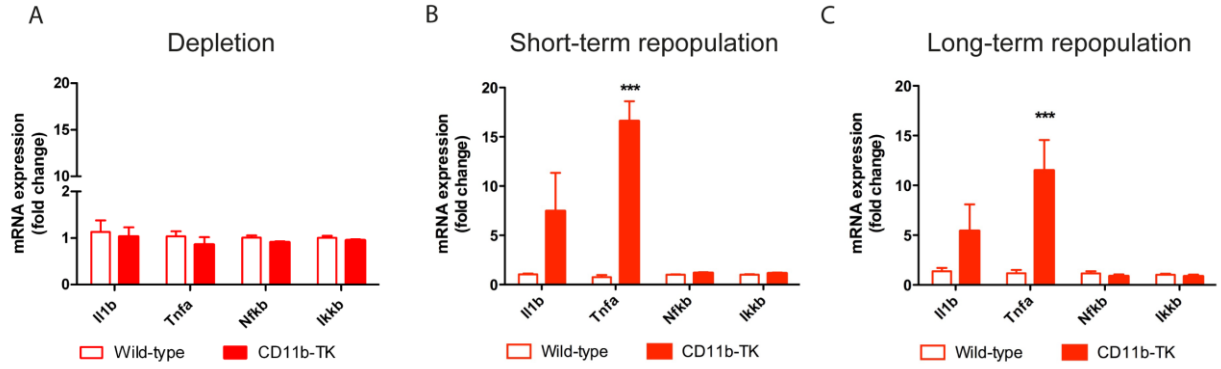

Figure 28: mRNA expression of inflammatory genes in the hypothalamus of GCV-treated CD11b-TK and wild-type mice fed HFD. *Il1b*, *Tnfa, Nfkb* and *Ikkb* mRNA expression in the hypothalamus of

CD11b-TK and wild-type mice treated with GCV for (A) 10 days. n=5 per group, (B) 28 days. n=4 per group, and (C) 4 weeks with an additional 4 weeks without treatment. n=5 CD11b-TK, n=4 wild-type. *p<0.05, ***p<0.001 based Two-Way ANOVA with Bonferroni's multiple comparison post-test. Data represents means +/- s.e.m.

5.3.7 Gene expression in brown and white adipose tissue of GCV-treated CD11b-TK and wild-type mice fed HFD

As described in chapter 5.2.8, *Ucp1* and *Ppargc1a* are key genes for regulation and induction of heat production especially in brown, but in particular conditions also in white adipose tissue. To assess whether HFD induces changes of these peripheral factors in CD11b-TK and wild-type mice treated centrally with GCV under the three different treatment paradigms, brown and white adipose tissues were collected, RNA isolated and gene expression of *Ucp1* and *Ppargc1a* was analyzed using qRT-PCR.

In brown adipose tissue, *Ppargc1a* expression was significantly upregulated by 2-fold in microglia-depleted CD11b-TK mice (Figure 29 A). However, no changes were detected in *Ucp1* expression at this time point. Short-term repopulation under HFD feeding conditions induced a significant upregulation of 2.8-fold of *Ucp1* gene expression, while *Ppargc1a* expression was not elevated at that time point any longer (Figure 29 B). Under conditions of long-term repopulation, the expression of both genes was normalized (Figure 29 C).

In white adipose tissue, no change in *Ucp1* or *Ppargc1a* expression was measurable in microglia-depleted mice (Figure 29 D). However, *Ppargc1a* expression was significantly increased by 3-fold in white adipose tissue of short-term repopulated CD11b-TK mice, whereas *Ucp1* expression was not changed at this time point (Figure 29 E). Similarly, long-term repopulation did not change *Ucp1* or *Ppargc1a* gene expression in CD11b-TK mice (Figure 29 F).

Taken together, increased expression of *Ucp1* in brown adipose tissue of CD11b-TK mice probably reflects an exaggerated response of these mice to HFD, which may also explain the increase in *Socs3* expression in the hypothalamus. Furthermore, *Ppargc1a* was increased in white adipose tissue of repopulated CD11b-TK mice fed HFD, similar to the observed changes in chow-fed repopulated CD11b-TK mice, which may present a possible explanation for the reduction in fat mass in these animals.

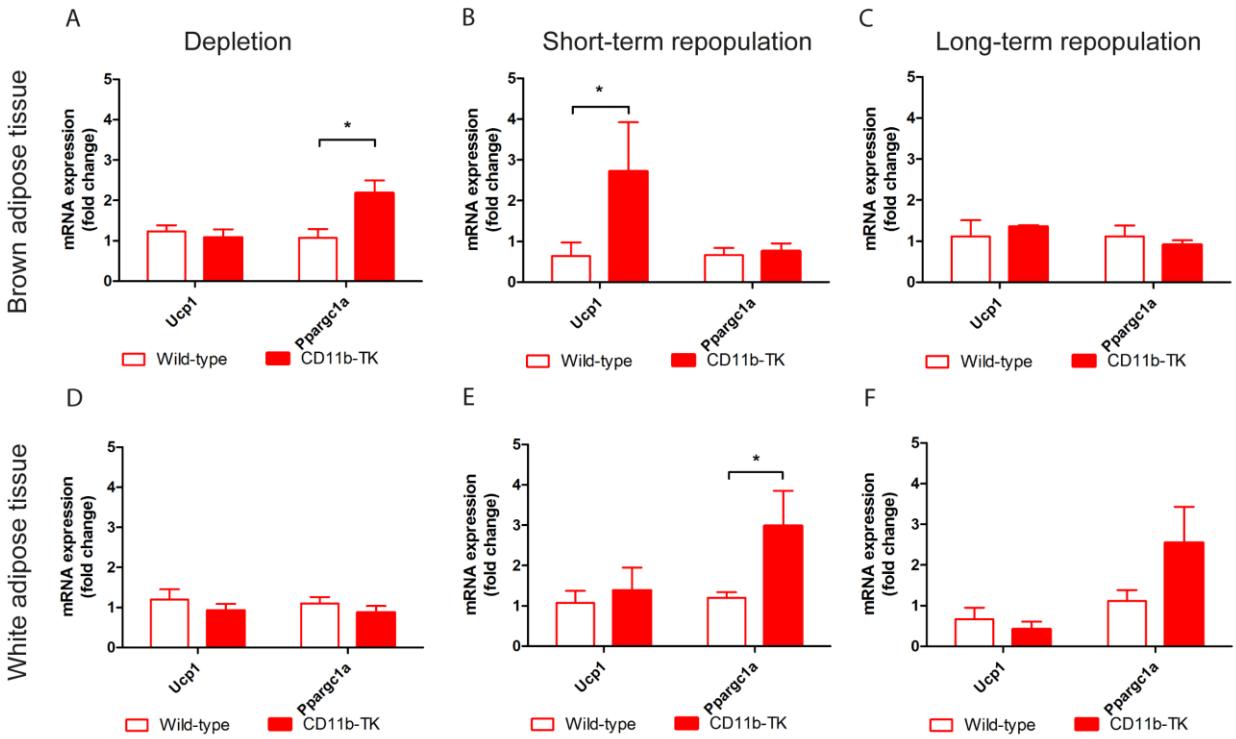

Figure 29: *Ucp1* and *Ppargc1a* gene expression in brown and white adipose tissue of GCV-treated CD11b-TK and wild-type mice. *Ucp1 and Ppargc1a* gene expression in brown adipose tissue of mice treated with GCV for (A) 10 days (n=8 per group), (B) 28 days (n=7 per group) and (C) 4 weeks with an additional 4 weeks without GCV treatment (n=3 per group). *Ucp1 and Ppargc1a* gene expression in white adipose tissue of mice treated with GCV for (D) 10 days (n=8 CD11b-TK, n=6 wild-type), (E) 28 days (n=5 per group) and (F) 4 weeks with an additional 4 weeks without GCV treatment (n=3 per group). ***p<0.001 based on Two-Way ANOVA with Bonferroni's multiple comparison post-test Data represents means +/- s.e.m.

5.3.8 Metabolic phenotyping of CD11b-TK and wild-type mice treated with artificial cerebrospinal fluid (aCSF) and fed HFD for 28 days

Depletion of microglia led to a decrease in body weight in CD11b-TK mice fed chow or HFD. The presented analyses aimed at elucidating the reason for this decrease. In light of a reduced fat mass (determined by means of body composition NMR) as well as an increase in *Ppargc1a* expression in white adipose tissue, an upregulation of fatty acid oxidation leading to a reduction in fat mass might – at least in part - serve as an explanation. Interestingly, HFD-fed CD11b-TK mice displayed an increase in energy expenditure that was not observed in chow-fed CD11b-TK mice and thus cannot be the sole reason for the body weight loss. However, to test the possibility that endogenous

microglia play a specific role in the regulation of energy expenditure in the context of HFD, a group of CD11b-TK and wild-type mice was treated with aCSF for 28 days (which will not induce microglia depletion). Mice were then analyzed for body weight, body composition, food intake, locomotor activity, energy expenditure, serum insulin and leptin levels as well as hypothalamic gene expression.

Body weight of aCSF-treated CD11b-TK mice developed normally and was even increased by 16 % compared to wild-type mice similarly treated with aCSF after 28 days of HFD (Figure 30 A). The analysis of body composition confirms this increase in body weight (Figure 30 B), which is in contrast to the decrease in body weight observed in CD11b-TK mice treated with GCV thus lacking resident microglia (Figure 15 and 23). The metabolic phenotyping revealed no change in food intake or locomotor activity in aCSF-treated CD11b-TK (Figure 30 C, D, E). Furthermore, serum insulin and leptin levels were not different between the two groups (Figure 30 H). However, energy expenditure was significantly higher in CD11b-TK mice treated with aCSF and fed HFD for 28 days (Figure 30 F, G). In addition, hypothalamic *Socs3* expression was significantly increased in CD11b-TK mice treated with aCSF (Figure 30 I), similar to the situation in CD11b-TK mice treated with GCV (Figure 19 and 27).

These results indicate that the observed increase in energy expenditure is not due to microglia depletion, but rather an intrinsic, so far unknown phenomenon of CD11b-TK transgenic mice when fed with HFD.

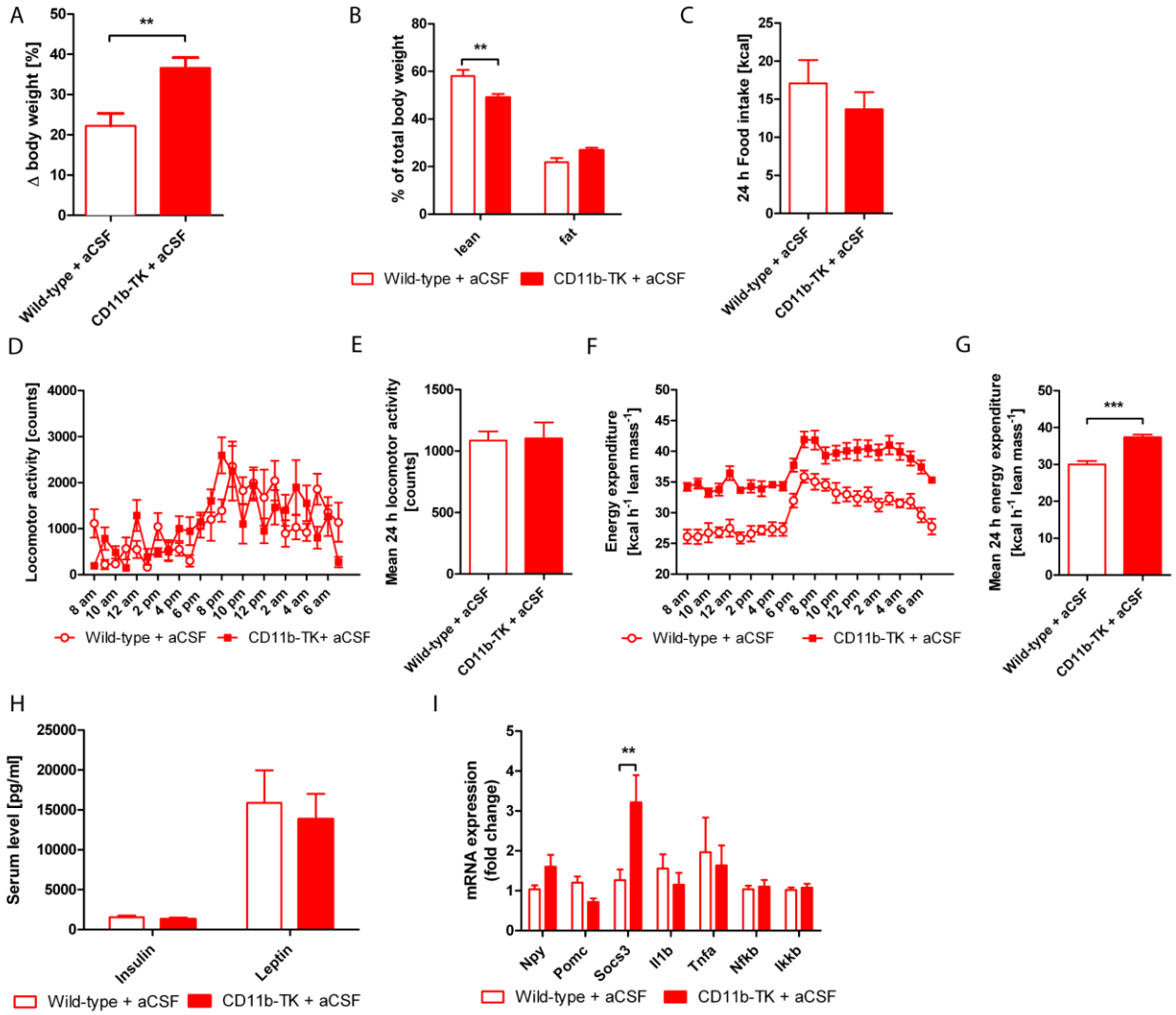

Figure 30: Metabolic phenotyping of CD11b-TK and wild-type mice treated with aCSF and fed HFD for 28 days. (A) Percental change in body weight, (B) Body composition, (C) Food intake, (D) 24 h locomotor activity, (E) Mean 24 h locomotor activity, (F) 24 h energy expenditure, (G) Mean 24 h energy expenditure, (H) Insulin and leptin serum level, (I) hypothalamic gene expression of CD11b-TK and wild-type mice treated with aCSF and fed HFD for 28 days. n=9 CD11b-TK, n=8 wild-type. ***p<0.001 based on student's t-test, **p<0.01 based on Two-Way ANOVA with Bonferroni's multiple comparison post-test Data represents means +/- s.e.m.

6 Discussion

The aim of the presented thesis was to characterize the glial response to HFD and to determine whether microglia play a role in physiological body weight homeostasis or in the context of HFD. Obesity research has focused on the effect of high fat diet on peripheral organs for many years, but the CNS only came into the focus recently. It has been suggested that diets high in fat cause detrimental inflammation in the brain and that microglia, the brain's innate immune cells, are the mediators of this inflammation. To gain a better insight into the type of response of microglia to different lengths of high fat diet exposure, histological, gene and protein expression analyses were conducted. Furthermore, to assess whether human brain glia cells react to HFD in a similar manner as seen in mice, the glial response in the hypothalamus of human autopsy cases was analyzed histologically. Since microglia have been shown to be responsible for brain homeostasis, and the initial microglia reaction to HFDs takes place in the hypothalamus - the brain region that is central for the regulation of food intake and energy expenditure - it is possible that these cells play an important role in the homeostasis of this brain region as well as in its response to nutrient excess. For this reason, CD11b-TK mice, which allow for an inducible and specific depletion of microglia, thus offering the possibility to study metabolic parameters in the absence of these cells, were used in the second part of this thesis. The effect of microglia depletion on body weight homeostasis was assessed under physiological conditions in mice fed chow food and in the context of HFD, where mice received food with 60 % calories from fat.

6.1 Characterization of the glial response to high fat diet in the hypothalamus of mice and humans

6.1.1 Glial and inflammatory response to high fat diet in the hypothalamus

Recent studies have reported increased cytokine gene expression in the hypothalamus upon HFD that is accompanied by an increase in the expression of microglia markers [59, 89], implying a potentially detrimental microglia response to HFD and obesity. In line with these studies, an inflammatory response consisting of increased *Il1b* and *Tnfa* expression in the hypothalamus was detected only 3 days after initiating HFD in the herein presented experiments. Importantly however, this response appears to represent

an acute reaction to diet in this experimental setting as an elevation in pro-inflammatory cytokine expression was not evident after 4 or 8 weeks of HFD feeding. Notably, significant increases in microglia numbers and astrocyte reactivity were detected after 8 weeks of HFD, suggesting a specific glial cell response to diet. While immunohistochemical stainings revealed morphologically changed glial cells characterized by enlarged cell bodies and shortened, deramified processes, the gene expression at this time point does not speak in favor of a pro-inflammatory phenotype. These findings are consistent with those of another study using the same HFD formulation in which the authors also failed to observe a pro-inflammatory reaction on either the mRNA or protein level after 8 weeks of feeding [119].

In contrast to the expected pro-inflammatory reaction, an increase in anti-inflammatory molecules was detected in the hypothalamus of mice fed HFD for 8 weeks, suggesting that at this time point, microglia switched from a rather pro-inflammatory to an anti-inflammatory phenotype. This type of temporal microglia reaction to stimuli has been reported in other settings such that while acute stimulation with LPS induced a pro-inflammatory response, chronic LPS stimulation resulted in an increase in anti-inflammatory markers [120, 121]. However, analysis of protein levels in whole hypothalamus tissue preparations did not confirm the changes in gene expression. The reason for this could be that the changes in gene expression were not high enough to translate into protein level and/or the changes on protein level were too small to be detected. Furthermore, the time point of the analysis could be inaccurate as changes in gene expression might not yet have translated to protein levels.

Radiologic evidence of gliosis in the hypothalamus of obese individuals provided the first hints of the effects of BMI on the CNS [59]. This thesis now presents the first histological evidence confirming this suspected hypothalamic gliosis in overweight patients, which is more pronounced in microglia cells, than in the astrocyte population. Further molecular analyses are required to reveal whether these alerted, somewhat altered microglia show a similar anti-inflammatory and subdued phenotype as seen in the mouse model, thus providing important clues for potential new strategies to modulate metabolic disease.

6.1.2 Contribution of peripheral monocytes to the hypothalamic response to high fat diet

Obesity is associated with an infiltration of the adipose tissue with inflammatory macrophages [37]. Likewise, inflammatory brain diseases, such as experimental autoimmune encephalomyelitis (EAE) or stroke, are accompanied by an infiltration of peripherally-derived myeloid cells into the brain [69, 122]. When addressing whether similar cellular processes occur in the context of obesity, no significant influx of peripheral macrophages into the hypothalamus of GFP+-harboring bone marrow chimeras was found after 20 weeks of HFD, in contrast to an earlier report [123]. This difference may be due to slightly differing experimental time courses or to the fact that the previously published study used FACS analysis to quantify infiltrating cells, which may have resulted in the inclusion of different myeloid subsets (besides resident microglia) such as meningeal or perivascular macrophages. Another point that has to be considered when conducting experiments with bone marrow chimeras is that the irradiation can cause damage of the blood-brain barrier, thus allowing an increased influx of peripheral cells [124]. This effect can be minimized by shielding the head of the animal from the irradiation [124]. However, since no significant influx of peripheral cells was detected in the experiment presented in this thesis, this additional precaution was not essential. The finding of this thesis of a lack of a substantial CNS recruitment of peripheral myeloid cells in HFD-fed mice is further supported by the fact that no elevation in levels of the major macrophage-attracting chemokine CCL2 in the hypothalamus could be detected (data not shown), which typically is present in situations of myeloid cell recruitment to the CNS [101, 125]. Based on the increase in Iba1- and BrdU-double positive cells, it can be concluded that proliferation of endogenous microglia accounts for the increased myeloid cell numbers in the hypothalamus of HFD-fed mice.

6.1.3 Microglia-specific response to high fat diet

As the results of this thesis suggest there is no substantial contribution of peripheral monocytes to the hypothalamic response to high fat diet. Furthermore, the effects of HFD on hypothalamic cytokine expression discussed in the previous section (6.1.1)

have only been assessed in whole hypothalamic tissue. Therefore, to get an insight into the microglia-specific response to HFD the genetic profile of hypothalamic microglia acutely isolated from mice fed HFD or chow was analyzed. The results confirm that microglia indeed produce pro-inflammatory factors after short-term exposure to HFD, but adopt a rather anti-inflammatory phenotype in response to prolonged HFD feeding. The chosen genes were previously identified as factors that are important for microglial sensing of endogenous and exogenous signals, such as *P2ry12*, *Selplg*, *Slc2a5* and *Trem2* [114]. These factors were shown to decrease with aging, to presumably 'tone down' the otherwise detrimental microglia reaction and prevent a constant reaction. The analysis performed in this thesis also revealed a downregulation of *P2ry12*, *Selplg*, *Slc2a5*, and *Trem2* that suggests a similar reaction of microglia to prolonged HFD. These findings raise the possibility that neuronal stress and apoptosis occurring in response to HFD [58, 59] are not necessarily due to a neurotoxic, pro-inflammatory microglia response. Conversely, this subdued microglia phenotype may serve as a protective mechanism in response to an insult that is aimed at preserving neuronal homeostasis. These data are in line with recent findings of elevated anti-inflammatory gene expression in human adipose tissue [126], suggesting analogous responses in the CNS and in peripheral organs.

Moreover, analysis of cytokine expression of isolated adult microglia directly stimulated with the plasma of HFD-fed mice indicates that there is no excessive reaction of microglia cells to factors present in the plasma of HFD-consuming, overweight animals. This finding is in contrast to previous studies that have hinted at the possibility that blood-borne factors from HFD-fed mice influence the microglia reaction [85, 89]. However, in contrast to the herein presented study, the published data is based on cultured neonatal microglia, which have been shown to be genetically and functionally distinct from adult microglia [72] and therefore are likely to elicit a differential response to stimuli.

Different studies suggest that microglia are primed by exposure to high fat diet. Erion et al. demonstrated that forebrain microglia of leptin-receptor deficient *db/db* mice produce increased amounts of IL-1β [127], while another study observed priming of hippocampal microglia through stress-induced glucocorticoids [70]. However, no other study has analyzed priming specifically of hypothalamic microglia cells in the context of diet-

induced obesity. The experiments presented herein demonstrate that HFD for 16 weeks did not prime microglia nor did it impair their response to LPS stimulation. Therefore, it can be concluded that prolonged HFD does not lead to microglia priming or results in impaired cellular function in this experimental setting.

Taken together, these results demonstrate that endogenous microglia in the hypothalamus specifically react to high fat diet and that this reaction is not exclusively pro-inflammatory. Prolonged exposure to HFD resulted in an alternate microglia profile represented by a downregulation of microglia-specific genes involved in sensing microenvironmental changes, likely serving to counterbalance earlier pro-inflammatory changes. This response is characteristic of microglia reactions to chronic diseases or insults and implies that diets high in fat represent a chronic challenge to CNS and microglia homeostasis. In line with the findings in mice, gliosis was detected in the hypothalamus of obese individuals, thus emphasizing the need to study the glial reaction to diet in more detail in order to determine how it might influence neuronal activity and overall metabolic health.

6.2 Physiological role of microglia in body weight homeostasis

In the second part of this thesis the effect of microglia depletion on body weight homeostasis was analyzed. To determine a baseline for the parameters used in this study, an initial metabolic phenotyping of untreated CD11b-TK and transgene-negative littermate controls was conducted. A correlation analysis of age and body weight as well as the body composition analysis revealed that transgene-positive CD11b-TK mice display a slightly elevated body weight and fat mass compared to age-matched transgene-negative animals. Nevertheless, except for the higher body weight of CD11b-TK mice, there was no difference in food intake, serum insulin and leptin levels, hypothalamic gene expression, locomotor activity and energy expenditure between transgene-positive and -negative mice.

6.2.1 Effect of microglia depletion and myeloid cell repopulation on metabolic phenotyping parameters

Subsequently to the baseline characterization, CD11b-TK mice and wild-type mice were treated with ganciclovir (GCV) and fed a normal chow diet to study the effect of microglia depletion, short-term and long-term repopulation with peripherally-derived myeloid cells (termed ‘short-term repopulation’ and ‘long-term repopulation’) on body weight homeostasis under physiological conditions.
10 days GCV treatment of CD11b-TK mice lead to an almost complete ablation of microglia as reported previously [101, 103]. As was seen in other published studies, shortly after microglia depletion the brain was repopulated with peripherally-derived myeloid cells. It was reported that due to their shorter processes, invading myeloid cells cover less area and are thus more numerous than endogenous microglia cells [101, 102]. In line with this, an increased number of Iba1-positive cells was observed in the hypothalamus of CD11b-TK mice.

When microglia were depleted in CD11b-TK mice a reduction in body weight was observed. However, this was also the case in wild-type mice and therefore very likely a result of the stress due to the surgical procedures required for the implantation of the mini-osmotic pump delivering the drug ganciclovir, which was required to induce microglia depletion. Interestingly, CD11b-TK mice continued to loose body weight, which was not seen in wild-type mice. However, 8 weeks after surgery (i.e. 8 weeks after initiation of microglia depletion), when the brain had been fully repopulated for at least 4 weeks, the body weight of CD11b-TK mice was normal again.
The body weight loss could be due to the lack of microglia, and peripherally-derived myeloid cells were able to rescue it by replacing them. However, this leads to the question of how microglia-depletion induces weight loss in CD11b-TK animals. To answer this question, several parameters were analyzed that are involved in body weight homeostasis.

A reduction in food intake was observed in short-term repopulated CD11b-TK mice which could – at least in part - explain the weight loss. However, there was no difference in food intake at the earlier time point when microglia were depleted in CD11b-TK mice. Thus, this reduction in food intake could be the result of the

repopulation with peripherally-derived myeloid cells, which is accompanied by an increase in pro-inflammatory cytokine expression in the hypothalamus. Pro-inflammatory cytokines have been shown to influence food intake and block NPY action supposed to increase food intake [128, 129]. Furthermore, the reduction in body weight and decrease in food intake of microglia-depleted and short-term repopulated CD11b-TK could also be explained by a general sickness of the animals. However, no serum parameters associated with a general sickness behavior [130, 131] were found to be elevated in the serum of short-term repopulated CD11b-TK mice. Furthermore, increased energy expenditure or increased locomotion might be reasons for weight loss [132, 133] in CD11b-TK mice with short-term repopulation. Yet, no difference was detectable when analyzing these parameters. The same was true for the serum levels of the hormones insulin and leptin, which are also known to influence body weight homeostasis [20, 133].
Finally, the analysis of these parameters cannot satisfyingly explain the body weight loss of microglia-depleted and myeloid cell-repopulated CD11b-TK mice.

6.2.2 Effect of microglia depletion and myeloid cell repopulation on gene expression in the hypothalamus

The hypothalamus plays a key role in regulating body weight homeostasis [26]. Therefore, to evaluate whether changes in hypothalamic gene expression could have induced body weight loss of CD11b-TK mice, gene expression of regulatory (*Pomc*, *Npy* and *Socs3*) as well as inflammatory (*Il1b*, *Tnfa*, *Nfkb* and *Ikkb*) genes was analyzed.
This analysis revealed an increase in *Socs3* expression in the hypothalamus of microglia-depleted and myeloid cell-repopulated CD11b-TK mice. Since the analysis was done in whole tissue it is not possible to determine the cellular source of the increase, making it difficult to deduce the reason for it. The suppressors of cytokine signaling (SOCS) serve as negative feedback inhibitors of cytokine signal transduction [134]. SOCS3 is a key negative regulator of IL-6 signaling [135] and involved in repressing the pro-inflammatory phenotype of macrophages [136]. Therefore, next to other possible cellular sources, *Socs3* upregulation in CD11b-TK mice may be caused by the remaining microglia. In line with this, IL-6 was not detectable in the analyzed tissue (data not shown) as its expression may be suppressed by SOCS3 actions.

Socs3 may also be expressed by astrocytes and neurons [137]. In hypothalamic neurons, *Socs3* expression is induced by leptin and insulin receptor signaling [138]. Thus, this early increase in *Socs3* expression in microglia-depleted CD11b-TK mice could reflect increased leptin or insulin responsiveness of hypothalamic neurons.

Apart from *Socs3, Npy* expression was upregulated in brains of short- and long-term repopulated CD11b-TK mice. Since NPY induces food intake [14], it may be upregulated to compensate the body weight loss observed in the repopulated CD11b-TK mice fed chow. However, this upregulation of mRNA expression did not result in a significant increase in food intake in these mice.

Infiltrating peripherally-derived myeloid cells have been shown to be more reactive than endogenous microglia [139, 140], which is also apparent in the hypothalami of myeloid cell-repopulated CD11b-TK mice, where *Il1b* and *Tnfa* expression were increased compared to wild-type mice harboring endogenous microglia. Although a general sickness was excluded by measuring IL-6, CRP, corticosterone and the liver enzymes AST and ALT in the serum of the mice, increased pro-inflammatory gene expression in the hypothalamus of CD11b-TK mice due to myeloid cell repopulation might also impact on body weight. As Scarlett et al. observed, IL-1β can activate POMC neurons and thus influence energy balance [141].

6.2.3 Effect of microglia depletion and myeloid cell repopulation on gene expression in brown and white adipose tissue

Since body weight homeostasis is regulated by a cross-talk of the CNS with the peripheral organs, white and brown adipose tissue were analyzed to assess the impact of microglia depletion and myeloid cell repopulation in the CNS on the periphery.

The reduction in body weight of CD11b-TK mice could for example also be caused by the induction of metabolic thermogenesis [142], which can be enhanced by UCP1 expression in brown adipose tissue. White adipocytes were recently shown to also be able to express UCP1, a process that was termed ‘browning’ and results in reduction of obesity [143]. No upregulation of UCP1 in brown or white adipose tissue was observed in microglia-depleted and myeloid cell-repopulated CD11b-TK mice. However, PGC-1α, the transcription factor of UCP1 [144], was elevated in white adipose tissue of long-term repopulated CD11b-TK mice. Apart from driving UCP1 expression and thus browning of

white adipose tissue [145, 146], PGC-1α increases lipid oxidation [109, 147]. Together with the reduced fat mass, as measured with the body composition NMR, this could be a reason for the reduced body weight of CD11b-TK animals. PGC-1α was also observed to be upregulated in the muscles of patients that lost weight as a result of gastric bypass surgery [148]. However, for both findings, from this thesis as well as the published paper, it cannot be concluded whether PGC-1α is upregulated due to body weight loss or whether its upregulation is the cause for it.

As mentioned earlier, depletion of microglia in the CD11b-TK mouse model leads to a massive infiltration of peripherally-derived myeloid cells that are twice as numerous as the endogenous microglia cells [101, 102]. Therefore, it can be assumed that an extensive production and mobilization of monocytes takes place in the bone marrow, which might have an impact on whole body weight homeostasis. Similarly, irradiated and bone marrow transplanted mice loose body weight, which they regain with time [149, 150]. Moreover, Ablamuntis et al. observed a reduction in adiposity in irradiated and bone marrow transplanted *ob/ob* mice [151], which supports the assumption that the mobilization of peripheral monocytes to replace endogenous microglia could be the reason for the reduced fat mass and thus the body weight phenotype of microglia-depleted and myeloid cell-repopulated CD11b-TK mice.

Taken together, depletion of microglia and repopulation with peripherally-derived myeloid cell leads to weight loss due to a reduction in fat mass. This reduction appears not to be caused by an increase in energy expenditure or locomotor activity. Furthermore, the animals show no signs of a general sickness behavior. However, pro-inflammatory gene expression was increased in the hypothalamus of CD11b-TK mice due to repopulation with peripherally-derived myeloid cells. In addition, PGC-1α mRNA was upregulated in white adipose tissue of repopulated CD11b-TK, which suggests that lipid oxidation takes place and leads to a reduction in fat mass. All of these changes are probably induced by recruitment and mobilization of bone marrow cells to the brain to replace the depleted microglia, similar to the condition of bone marrow transplantation and might thus mask any effect microglia depletion alone could have on body weight homeostasis.

6.3 Role of microglia in body weight homeostasis in the context of high fat diet

The third aim of this thesis was to determine whether high fat diet feeding has a differential effect in the presence and absence of resident microglia cells. As described in the previous chapter, depletion of microglia is followed by repopulation of the brain with peripherally-derived myeloid cells. In combination with HFD feeding, the difference in Iba1-positive cell number in the hypothalamus of myeloid cell-repopulated mice compared to wild-type mice is not as pronounced as in the hypothalamus of chow-fed mice. This is probably due to the effect of HFD on microglia number in the hypothalamus, as described in 5.1.1 and previously by Thaler et al. [59]. Interestingly, the repopulated myeloid cells also appear to react to the diet specifically in the arcuate nucleus region by appearing morphologically distinct with a 'bushy' appearance.

In respect to body weight, HFD-fed microglia-depleted and short-term repopulated CD11b-TK mice lost weight, though less than the chow-fed CD11b-TK mice. This is likely due to the impact of the high-caloric density of the fatty acids in the diet. Long-term repopulated HFD-fed CD11b-TK mice gained as much weight as wild-type mice treated along the same paradigm. This is also visible when analyzing the fat mass, which at first does not increase in CD11b-TK mice. However, with long-term repopulation, the percentage of fat mass is identical in wild-type and CD11b-TK mice. Thus, also upon HFD conditions microglia-depletion and myeloid cell repopulation has an effect on body weight, as observed in the chow-fed mice. However, in combination with HFD this effect results in a delay in body weight gain of CD11b-TK mice and not so much in body weight loss.

Furthermore, similar to the situation in myeloid cell-repopulated CD11b-TK mice fed chow, no difference in sickness parameters was observed between CD11b-TK and wild-type mice fed HFD. In addition, insulin and leptin levels in the serum of CD11b-TK mice fed HFD were unchanged.

A separate comparison of leptin levels between CD11b-TK mice fed chow and CD11b-TK mice fed HFD reveals a significant difference - chow-fed mice have lower levels, whereas the HFD-fed mice display higher levels of leptin. The low leptin level in the

chow-fed CD11b-TK mice could be explained with the low body and fat mass. The body is in need of nutrients, thus, leptin levels are low to increase food intake and decrease energy expenditure [152]. However, also in short-term repopulated CD11b-TK mice fed HFD, body mass was reduced, whereas serum leptin was elevated. This elevation in leptin levels in CD11b-TK mice fed HFD may already be an indication for a developing leptin resistance in those mice and thus indicate an enhanced reaction to the high fat diet [138]. This could be supported by increased *Socs3* expression in the hypothalamus of short-term repopulated CD11b-TK mice fed HFD, which, similar to elevated leptin levels, might indicate early leptin resistance in these mice [138]. Though, *Socs3* expression was increased in chow-fed CD11b-TK mice as well and thus might also only be a result of the depletion and/or repopulation.

Analysis of the brown adipose tissue revealed a significant increase in PGC-1α (*Ppargc1a)* in microglia-depleted CD11b-TK mice fed HFD. Following this increase, UCP1, which is induced by PGC-1α [144], was significantly increased in short-term repopulated CD11b-TK mice fed HFD. This increase in *Ucp1* mRNA was not detected in brown adipose tissue of chow-fed CD11b-TK mice. Since *Ucp1* mRNA levels have been shown to be increased upon high fat diet intake [142, 153], *Ucp1* increase in CD11b-TK mice fed HFD could, as discussed above, point towards an enhanced response of these mice to the diet.
In the white adipose tissue of CD11b-TK mice fed HFD, *Ppargc1a* was increased, as was observed in CD11b-TK mice fed chow, which may reflect an increase in lipid oxidation [109, 147].

High fat diet feeding and subsequent obesity have been shown to decrease energy expenditure [154]. Therefore, it would be desirable to increase energy expenditure as a measure to decrease body weight. In CD11b-TK mice fed HFD, increased energy expenditure was observed at all time points, which could partly explain the body weight loss. However, CD11b-TK mice fed chow also lost weight, but showed no increase in energy expenditure. Therefore, CD11b-TK mice were treated with aCSF instead of GCV, which does not lead to the depletion of microglia, and fed HFD. Interestingly, also aCSF-treated CD11b-TK mice harboring endogenous microglia displayed a higher energy expenditure than wild-type littermates. This analysis also revealed that the increase in energy expenditure is indeed independent of the change in body weight as

CD11b-TK mice treated with aCSF gained even more weight than wild-type mice fed HFD and treated with aCSF.

These results indicate that there is a specific, intrinsic and so far undetected response of CD11b-TK mice to HFD independent of microglia depletion. In addition, the baseline analysis showed that CD11b-TK mice per se have a higher body weight when compared to their transgene-negative littermates (Figure 13). One explanation for this could be the small litters of CD11b-TK mice, which result in neonatal over nutrition due to less competition for food. Neonatal overnutrition has been shown to lead to increased body weight during adulthood [155, 156]. However, the wild-type control animals used in these experiments were negative littermate controls throughout the study and thus were also exposed to neonatal overnutrition. It is possible that these effects are more pronounced in transgene-positive CD11b-TK mice than mice without the transgene, possibly supported by the fact that the CD11b-TK transgene is integrated somewhere in the genome where it interferes with genes required in the regulation of metabolic process in the context of overnutrition. A second possibility is that the viral thymidine kinase, which is constantly expressed in all CD11b-positive cells in this mouse, constitutively impacts myeloid cell/macrophage survival or function by interfering with endogenous thymidine kinase activity. Since the expansion of adipose tissue caused by high fat diet recruits peripherally-derived myeloid cells and macrophages into the adipose tissue [37] and induces their proliferation [157, 158] these cells may explain the observed HFD-specific phenotype.

Taken together, the analysis of the effect of microglia depletion and myeloid cell repopulation in CD11b-TK mice revealed an intrinsic, so far unknown phenotype of these mice when fed HFD. Apart from the fact that it would be interesting to further investigate the mechanism behind this response; other possibilities to deplete microglia [78, 105] should be taken into consideration to study the role of microglia in body weight homeostasis in the context of HFD.

6.4 Conclusion and Outlook

The presented thesis adds another aspect to the recent findings that microglia respond to nutrient excess. In contrast to what has been concluded from published studies [59,

106], this response was found not to be exclusively pro-inflammatory. Although, a morphological change of microglia can be detected histologically, this phenotype does not coincide with increased pro-inflammatory factors. On the contrary, anti-inflammatory markers were upregulated, while genes involved in microglial sensing of microenvironmental changes were downregulated. In addition, microglia of HFD-fed mice responded normally to LPS stimulation and stimulation with plasma-derived from HFD-fed mice did not induce pro-inflammatory cytokine production in wild-type microglia. The results of the first part of this thesis suggest that microglia may exert neuroprotective rather than neurotoxic functions in the context of prolonged HFD. It is important to keep in mind that microglia might not exclusively be the 'bad guys' after all when devising CNS-targeted treatment strategies for obesity. In line with this, it will be important to elucidate the specific role of microglia in the hypothalamus and thus in the regulation of food intake and energy expenditure. The second and third part of this thesis were aimed at determining whether microglia are important for the hypothalamic regulation of body weight under physiological and high fat diet conditions. However, the mouse model that was used only allows for a short-term depletion of microglia for up to ten days, a time point at which the impact of high fat diet in the diet-induced obesity mouse model is not very pronounced. At the later time points the brain is repopulated with bone marrow derived peripheral myeloid cells, which allows for a functional comparison of endogenous microglia with these peripherally-derived cells. However, the data presented in this thesis reveals that the process of mobilization and recruitment of bone marrow cells to the brain has a tremendous impact on body weight homeostasis. This makes it impossible to independently study the effects of microglia depletion per se. To extend the studies on the role of microglia in body weight homeostasis, other, only recently published, approaches to deplete microglia should be taken into consideration [78, 105]. A promising option is the use of the Csf1-receptor antagonist, with which microglia can be depleted as long as the drug is given, while repopulation of the brain appears to be negligible [105]. Such experimental setting would allow studying long-term effects of high-fat/high-caloric feeding in the absence of microglia.

7 Appendix

7.1 *Abbreviations*

%	Percentage
°C	Degree Celsius
aCSF	artificial Cerebrospinal fluid
ANOVA	Analysis of variance
ALT	Alanine Aminotransferase
AST	Aspartate Aminotransferase
BCA	Bicinchoninc acid
BM	Bone-marrow
BMI	Body mass index
bp	Base pairs
BrdU	Bromodeoxyuridine
CD11b	Cluster of differentiation molecule 11b
CNS	Central nervous system
CO_2	Carbon dioxide
CRP	C-reactive protein
CT	Cycle threshold
CSF-1	Colony-stimulating factor 1
CX3CR1	Fractalkine receptor
CXCL1	Chemokine (C-X-C motif) ligand 1
d	Day
DAB	Diaminobenzidine
ddH_2O	Distilled deionized water
DMEM	Dulbecco's modified eagle medium
DNA	Desoxyribonucleic acid
dNTP	Desoxynucleoside triphosphates
FBS	Fetal bovine serum
G	Gauge
GAPDH	Glycerinaldehyd-3-phosphat-Dehydrogenase
GCV	Ganciclovir
GFAP	Glial fibrillary acidic protein
GFP	Green fluorescent protein
h	Hour
H_2O	Water
H_2O_2	Hydrogen peroxide
HBSS	Hanks balanced salt solution
HCl	Hydrochloric acid
HFD	High fat diet
HSV	Herpes simplex virus
Iba1	Ionized calcium binding protein 1
icv	Intracerebroventricular
IL	Interleukin
i.p.	Intraperitoneal
Ikkb	Inhibitor of nuclear factor kappa-B kinase subunit beta
kg	Kilogram
LPS	Lipopolysaccharide
M	Molar
MACS	Magnetic cell separation
mg	Milligram
min	Minute
mRNA	messenger RNA
MSD	Meso Scale Discovery
NaCl	Sodium chloride
NaOH	Sodium hydroxide
NF-κB	Nuclear factor-κB
NGS	Normal goat serum
NPY	Neuropeptide Y
PBS	Phosphate buffered saline
PBS-TX	PBS with Triton-X100
PCR	Polymerase chain reaction
PenStrep	Penicillin Streptavidin
PFA	Paraformaldehyde
POMC	Proopiomelanocortin
PPARGC1a	Peroxisome Proliferator-Activated Receptor Gamma, Coactivator 1 Alpha
RNA	Ribonucleic acid

ROI	Region of interest	w	Weeks
ROS	Reactive oxygen species		
qRT-PCR	Quantitative real time PCR		
rpm	Rotations per minute		
RT	Room temperature		
RT-PCR	Reverse transcription PCR		
s	Recond		
SDS	Rodium dodecyl sulfate		
SEM	Standard error of the mean		
SOCS3	Suppressor of cytokine signaling 3		
TBS	Tris buffered saline		
TK	Thymidine kinase		
TLR	Toll-like receptor		
Tnfα	Tumor necrosis factor α		
Tris	Tris-(Hydroxymethyl)-aminomethane		
UCP1	Uncoupling Protein 1		
US	United States		

7.2 *Figures*

7.3 *Tables*

8 References

[1] A. Berrington de Gonzalez et al., “Body-mass index and mortality among 1.46 million white adults.,” *N. Engl. J. Med.*, vol. 363, pp. 2211–2219, 2010.

[2] D. A. Boggs et al., “General and abdominal obesity and risk of death among black women,” *N Engl J Med*, vol. 365, no. 10, pp. 901–908, 2011.

[3] W. Zheng et al., “Association between body-mass index and risk of death in more than 1 million Asians,” *N Engl J Med*, vol. 364, no. 8, pp. 719–729, 2011.

[4] Y. C. Wang et al., “Health and economic burden of the projected obesity trends in the USA and the UK.,” *Lancet*, vol. 378, no. 9793, pp. 815–25, Aug. 2011.

[5] V. S. Malik et al., “Global obesity: trends, risk factors and policy implications.,” *Nat. Rev. Endocrinol.*, vol. 9, no. 1, pp. 13–27, 2013.

[6] D. M. Nguyen and H. B. El-Serag, “The epidemiology of obesity.,” *Gastroenterol. Clin. North Am.*, vol. 39, no. 1, pp. 1–7, Mar. 2010.

[7] G. A. Bray and B. M. Popkin, “Dietary fat intake does affect obesity!,” *Am. J. Clin. Nutr.*, vol. 68, no. 6, pp. 1157–73, Dec. 1998.

[8] P. Schrauwen and K. R. Westerterp, “The role of high-fat diets and physical activity in the regulation of body weight.,” *Br. J. Nutr.*, vol. 84, no. 4, pp. 417–27, Oct. 2000.

[9] V. George et al., “Effect of dietary fat content on total and regional adiposity in men and women.,” *Int. J. Obes.*, vol. 14, no. 12, pp. 1085–94, Dec. 1990.

[10] W. H. Saris et al., “Randomized controlled trial of changes in dietary carbohydrate/fat ratio and simple vs complex carbohydrates on body weight and blood lipids: the CARMEN study. The Carbohydrate Ratio Management in European National diets.,” *Int. J. Obes. Relat. Metab. Disord.*, vol. 24, no. 10, pp. 1310–8, Oct. 2000.

[11] L. A. Tucker and M. J. Kano, “Dietary fat and body fat: a multivariate study of 205 adult females.,” *Am. J. Clin. Nutr.*, vol. 56, no. 4, pp. 616–22, Oct. 1992.

[12] T. M. Frayling et al., “A common variant in the FTO gene is associated with body mass index and predisposes to childhood and adult obesity.,” *Science*, vol. 316, no. 5826, pp. 889–94, May 2007.

[13] G. J. Morton et al., “Central nervous system control of food intake and body weight.,” *Nature*, vol. 443, no. 7109, pp. 289–95, Sep. 2006.

[14] M. G. Myers and D. P. Olson, “Central nervous system control of metabolism,” *Nature*, vol. 491, no. 7424, pp. 357–363, Nov. 2012.

[15] M. W. Schwartz et al., “Cerebrospinal fluid leptin levels: relationship to plasma levels and to adiposity in humans.,” *Nat. Med.*, vol. 2, pp. 589–593, 1996.

[16] Y. Zhang et al., “Positional cloning of the mouse obese gene and its human homologue.,” *Nature*, vol. 372. pp. 425–432, 1994.

[17] J. D. Bagdade et al., “The significance of basal insulin levels in the evaluation of the insulin response to glucose in diabetic and nondiabetic subjects,” *J Clin.Invest*, vol. 46, no. 10, pp. 1549–1557, 1967.

[18] K. W. Williams and J. K. Elmquist, “From neuroanatomy to behavior: central integration of peripheral signals regulating feeding behavior.,” *Nat. Neurosci.*, vol. 15, no. 10, pp. 1350–5, Oct. 2012.

[19] G. S. H. Yeo and L. K. Heisler, “Unraveling the brain regulation of appetite: lessons from genetics,” *Nat. Neurosci.*, vol. 15, no. 10, pp. 1343–1349, 2012.

[20] M. a Cowley et al., “Leptin activates anorexigenic POMC neurons through a neural network in the arcuate nucleus.,” *Nature*, vol. 411, no. 6836, pp. 480–4, May 2001.

[21] a. J. Sipols et al., “Effect of intracerebroventricular insulin infusion on diabetic hyperphagia and hypothalamic neuropeptide gene expression,” *Diabetes*, vol. 44, pp. 147–151, 1995.

[22] E. D. Berglund et al., “Direct leptin action on POMC neurons regulates glucose homeostasis and hepatic insulin sensitivity in mice,” vol. 122, no. 3, 2012.

[23] D. L. Coleman and K. P. Hummel, “Effects of parabiosis of normal with genetically diabetic mice.,” *Am. J. Physiol.*, vol. 217, no. 5, pp. 1298–1304, 1969.

[24] J. C. Bruning et al., “Role of Brain Insulin Receptor in Control of Body Weight and Reproduction,” *Science (80-.).*, vol. 289, no. September, pp. 2122–2125, 2000.

[25] N. Balthasar et al., “Leptin receptor signaling in POMC neurons is required for normal body weight homeostasis.,” *Neuron*, vol. 42, no. 6, pp. 983–91, Jun. 2004.

[26] L. Varela and T. L. Horvath, “Leptin and insulin pathways in POMC and AgRP neurons that modulate energy balance and glucose homeostasis.,” *EMBO Rep.*, vol. 13, no. 12, pp. 1079–1086, Nov. 2012.

[27] C. Bjorbak et al., “SOCS3 mediates feedback inhibition of the leptin receptor via Tyr985.,” *J. Biol. Chem.*, vol. 275, no. 51, pp. 40649–57, Dec. 2000.

[28] H. Mori et al., “Socs3 deficiency in the brain elevates leptin sensitivity and confers resistance to diet-induced obesity.,” *Nat. Med.*, vol. 10, no. 7, pp. 739–43, Jul. 2004.

[29] S. B. Heymsfield et al., “Recombinant leptin for weight loss in obese and lean adults: a randomized, controlled, dose-escalation trial.,” *JAMA*, vol. 282, no. 16, pp. 1568–1575, 1999.

[30] C. T. De Souza et al., “Consumption of a fat-rich diet activates a proinflammatory response and induces insulin resistance in the hypothalamus,” *Endocrinology*, vol. 146, no. 10, pp. 4192–4199, 2005.

[31] H. Munzberg et al., “Region-specific leptin resistance within the hypothalamus of diet-induced obese mice,” *Endocrinology*, vol. 145, no. 11, pp. 4880–4889, 2004.

[32] M. B. Ernst et al., “Enhanced Stat3 activation in POMC neurons provokes negative feedback inhibition of leptin and insulin signaling in obesity.,” *J. Neurosci.*, vol. 29, no. 37, pp. 11582–93, Sep. 2009.

[33] X. Zhang et al., “Hypothalamic IKKbeta/NF-kappaB and ER stress link overnutrition to energy imbalance and obesity,” *Cell*, vol. 135, no. 1, pp. 61–73, Oct. 2008.

[34] J. P. Thaler and M. W. Schwartz, “Minireview: Inflammation and obesity pathogenesis: the hypothalamus heats up,” *Endocrinology*, vol. 151, no. 9, pp. 4109–4115, 2010.

[35] F. P. de Heredia et al., “Obesity, inflammation and the immune system,” *Proc Nutr Soc*, no. April 2011, pp. 1–7, Mar. 2012.

[36] a. W. Ferrante and A. W. Ferrante Jr., “Obesity-induced inflammation: a metabolic dialogue in the language of inflammation,” *J Intern Med*, vol. 262, no. 4, pp. 408–414, 2007.

[37] K. E. Wellen and G. S. Hotamisligil, “Obesity-induced inflammatory changes in adipose tissue,” *J Clin Invest*, vol. 112, no. 12, pp. 1785–1788, 2003.

[38] G. S. Hotamisligil, “Inflammation and metabolic disorders,” *Nature*, vol. 444, no. 7121, pp. 860–867, Dec. 2006.

[39] K. E. Wellen and G. S. Hotamisligil, “Inflammation, stress, and diabetes,” *J Clin Invest*, vol. 115, no. 5, pp. 1111–1119, May 2005.

[40] S. E. Shoelson et al., “Inflammation and insulin resistance,” *J Clin Invest*, vol. 116, no. 7, pp. 1793–1801, 2006.

[41] A. Aguilar-Valles et al., “Obesity, adipokines and neuroinflammation,” *Neuropharmacology*, 2015.

[42] M. Mraz and M. Haluzik, “The role of adipose tissue immune cells in obesity and low-grade inflammation.,” *J. Endocrinol.*, no. Bluher 2009, pp. 1–35, 2014.

[43] S. P. Weisberg et al., “Obesity is associated with macrophage accumulation in adipose tissue,” *J Clin Invest*, vol. 112, no. 12, pp. 1796–1808, 2003.

[44] H. Xu et al., “Chronic inflammation in fat plays a crucial role in the development of obesity-related insulin resistance,” *J Clin Invest*, vol. 112, no. 12, pp. 1821–1830, 2003.

[45] A. Chawla et al., “Macrophage-mediated inflammation in metabolic disease.,” *Nat. Rev. Immunol.*, vol. 11, no. 11, pp. 738–49, Nov. 2011.

[46] C. N. Lumeng et al., “Obesity induces a phenotypic switch in adipose tissue macrophage polarization,” *J. Clin. Invest.*, vol. 117, no. 1, pp. 175–184, 2007.

[47] J. I. Odegaard et al., “Macrophage-specific PPARgamma controls alternative activation and improves insulin resistance.,” *Nature*, vol. 447, no. 7148, pp. 1116–20, Jun. 2007.

[48] M. T. A. Nguyen et al., “A subpopulation of macrophages infiltrates hypertrophic adipose tissue and is activated by free fatty acids via Toll-like receptors 2 and 4 and JNK-dependent pathways.,” *J. Biol. Chem.*, vol. 282, no. 48, pp. 35279–92, Nov. 2007.

[49] R. Cancello et al., “Reduction of Macrophage Infiltration and Chemoattractant Gene Expression Changes in White Adipose Tissue of Morbidly Obese Subjects After Surgery-Induced Weight Loss,” *Diabetes*, vol. 54, no. 8, pp. 2277–2286, Jul. 2005.

[50] J. P. Thaler et al., “Hypothalamic inflammation and energy homeostasis: resolving the paradox.,” *Front. Neuroendocrinol.*, vol. 31, no. 1, pp. 79–84, Jan. 2010.

[51] H.-R. Berthoud, “The neurobiology of food intake in an obesogenic environment.,” *Proc. Nutr. Soc.*, vol. 71, no. 4, pp. 478–87, Nov. 2012.

[52] L. M. Ignacio-Souza et al., “Defective regulation of the ubiquitin/proteasome system in the hypothalamus of obese male mice.,” *Endocrinology*, vol. 155, no. 8, pp. 2831–44, Aug. 2014.

[53] D. Cai, “NFkappaB-mediated metabolic inflammation in peripheral tissues versus central nervous system.,” *Cell Cycle*, vol. 8, no. 16, pp. 2542–8, Aug. 2009.

[54] A. Kleinridders et al., “MyD88 signaling in the CNS is required for development of fatty acid-induced leptin resistance and diet-induced obesity,” *Cell Metab*, vol. 10, no. 4, pp. 249–259, Oct. 2009.

[55] M. Milanski et al., “Saturated fatty acids produce an inflammatory response predominantly through the activation of TLR4 signaling in hypothalamus: implications for the pathogenesis of obesity,” *J Neurosci*, vol. 29, no. 2, pp. 359–370, Jan. 2009.

[56] S. Purkayastha and D. Cai, “Disruption of neurogenesis by hypothalamic inflammation in obesity or aging.,” *Rev. Endocr. Metab. Disord.*, vol. 14, no. 4, pp. 351–6, Dec. 2013.

[57] K. A. Posey et al., “Hypothalamic proinflammatory lipid accumulation, inflammation, and insulin resistance in rats fed a high-fat diet,” *Am J Physiol Endocrinol Metab*, vol. 296, no. 5, pp. E1003–12, 2009.

[58] J. C. Moraes et al., “High-fat diet induces apoptosis of hypothalamic neurons,” *PLoS One*, vol. 4, no. 4, p. e5045, Jan. 2009.

[59] J. P. Thaler et al., “Obesity is associated with hypothalamic injury in rodents and humans,” *J Clin Invest*, vol. 122, no. 1, pp. 153–162, 2012.

[60] D. Cai, “Neuroinflammation and neurodegeneration in overnutrition-induced diseases.,” *Trends Endocrinol. Metab.*, vol. 24, no. 1, pp. 40–7, Jan. 2013.

[61] A. N. Verkhratsky and A. Butt, *Glial neurobiology: a textbook*. John Wiley & Sons, 2007.

[62] B. Ajami et al., “Local self-renewal can sustain CNS microglia maintenance and function throughout adult life,” *Nat Neurosci*, vol. 10, no. 12, pp. 1538–1543, 2007.

[63] H. Kettenmann et al., “Physiology of microglia,” *Physiol Rev*, vol. 91, no. 2, pp. 461–553, 2011.

[64] M. Prinz and J. Priller, “Microglia and brain macrophages in the molecular age: from origin to neuropsychiatric disease.,” *Nat. Rev. Neurosci.*, vol. 15, no. 5, pp. 300–12, May 2014.

[65] M. Prinz et al., “Microglia: unique and common features with other tissue macrophages.,” *Acta Neuropathol.*, vol. 128, no. 3, pp. 319–31, Sep. 2014.

[66] K. Kierdorf et al., “Microglia emerge from erythromyeloid precursors via Pu.1- and Irf8-dependent pathways.,” *Nat. Neurosci.*, vol. 16, no. 3, pp. 273–80, Mar. 2013.

[67] F. Alliot et al., “Microglia derive from progenitors, originating from the yolk sac, and which proliferate in the brain.,” *Brain Res. Dev. Brain Res.*, vol. 117, no. 2, pp. 145–52, Nov. 1999.

[68] F. Ginhoux et al., “Fate mapping analysis reveals that adult microglia derive from primitive macrophages.,” *Science*, vol. 330, no. 6005, pp. 841–5, Nov. 2010.

[69] B. Ajami et al., “Infiltrating monocytes trigger EAE progression, but do not contribute to the resident microglia pool.,” *Nat. Neurosci.*, vol. 14, no. 9, pp. 1142–1149, Jul. 2011.

[70] M. G. Frank et al., “Glucocorticoids mediate stress-induced priming of microglial pro-inflammatory responses.,” *Brain. Behav. Immun.*, vol. 26, no. 2, pp. 337–45, Mar. 2012.

[71] W. J. Streit et al., “Role of microglia in the central nervous system ’ s immune response,” *Neurol. Res.*, vol. 27, pp. 685–691, 2005.

[72] O. Butovsky et al., “Identification of a unique TGF-β-dependent molecular and functional signature in microglia.,” *Nat. Neurosci.*, vol. 17, no. 1, pp. 131–43, 2014.

[73] O. Butovsky et al., “Targeting miR-155 restores abnormal microglia and attenuates disease in SOD1 mice.,” *Ann. Neurol.*, 2014.

[74] F. L. Heppner et al., “Immune attack: the role of inflammation in Alzheimer disease,” *Nat Rev Neurosci*, vol. 16, no. 6, pp. 358–372, 2015.

[75] A. Galoyan et al., *Handbook of Neurochemistry and Molecular Neurobiology: Neuroimmunology*, no. Bd. 12. Springer, 2007.

[76] M. A. Cuadros et al., “The origin and differentiation of microglial cells during development.,” *Prog. Neurobiol.*, vol. 56, no. 2, pp. 173–89, Oct. 1998.

[77] C. L. Cunningham et al., “Microglia regulate the number of neural precursor cells in the developing cerebral cortex.,” *J. Neurosci.*, vol. 33, no. 10, pp. 4216–33, Mar. 2013.

[78] C. N. Parkhurst et al., “Microglia promote learning-dependent synapse formation through brain-derived neurotrophic factor.,” *Cell*, vol. 155, no. 7, pp. 1596–609, Dec. 2013.

[79] A. Nehlig and A. Pereira de Vasconcelos, “Glucose and ketone body utilization by the brain of neonatal rats.,” *Prog. Neurobiol.*, vol. 40, no. 2, pp. 163–221, Feb. 1993.

[80] J. Edmond, “Energy metabolism in developing brain cells.,” *Can. J. Physiol. Pharmacol.*, vol. 70 Suppl, pp. S118–29, Jan. 1992.

[81] C.-X. Yi et al., “A role for astrocytes in the central control of metabolism.,” *Neuroendocrinology*, vol. 93, no. 3, pp. 143–9, Jan. 2011.

[82] E. Fuente-Martín et al., “Leptin regulates glutamate and glucose transporters in hypothalamic astrocytes.,” *J. Clin. Invest.*, vol. 122, no. 11, pp. 3900–13, Nov. 2012.

[83] C.-H. Tang et al., “Leptin-induced IL-6 production is mediated by leptin receptor, insulin receptor substrate-1, phosphatidylinositol 3-kinase, Akt, NF-kappaB, and p300 pathway in microglia.,” *J. Immunol.*, vol. 179, no. 2, pp. 1292–302, Jul. 2007.

[84] V. Lafrance et al., “Leptin modulates cell morphology and cytokine release in microglia.,” *Brain. Behav. Immun.*, vol. 24, no. 3, pp. 358–65, Mar. 2010.

[85] H. Hsuchou et al., “Blood-borne metabolic factors in obesity exacerbate injury-induced gliosis,” *J Mol Neurosci*, vol. 47, no. 2, pp. 267–277, Jun. 2012.

[86] S. S. Gupta et al., “Saturated long-chain fatty acids activate inflammatory signaling in astrocytes,” *J Neurochem*, vol. 120, no. 6, pp. 1060–1071, Mar. 2012.

[87] C. García-Cáceres et al., “Differential acute and chronic effects of leptin on hypothalamic astrocyte morphology and synaptic protein levels.,” *Endocrinology*, vol. 152, no. 5, pp. 1809–18, May 2011.

[88] E. Fuente-Martín et al., “Hypothalamic inflammation without astrogliosis in response to high sucrose intake is modulated by neonatal nutrition in male rats.,” *Endocrinology*, vol. 154, no. 7, pp. 2318–30, Jul. 2013.

[89] Y. Gao et al., “Hormones and diet, but not body weight, control hypothalamic microglial activity.,” *Glia*, vol. 62, no. 1, pp. 17–25, Jan. 2014.

[90] E. Pinteaux et al., “Leptin induces interleukin-1beta release from rat microglial cells through a caspase 1 independent mechanism.,” *J. Neurochem.*, vol. 102, no. 3, pp. 826–33, Aug. 2007.

[91] C.-X. X. Yi et al., “Exercise protects against high-fat diet-induced hypothalamic inflammation,” *Physiol Behav*, vol. 106, no. 4, pp. 485–490, Jun. 2012.

[92] K. E. Berkseth et al., “Hypothalamic gliosis associated with high-fat diet feeding is reversible in mice: A combined immunohistochemical and magnetic resonance imaging study,” *Endocrinology*, vol. 155, no. 8, pp. 2858–2867, 2014.

[93] C. T. Ekdahl et al., “Inflammation is detrimental for neurogenesis in adult brain.,” *Proc. Natl. Acad. Sci. U. S. A.*, vol. 100, no. 23, pp. 13632–7, Nov. 2003.

[94] M. V Kokoeva et al., “Neurogenesis in the hypothalamus of adult mice: potential role in energy balance.,” *Science*, vol. 310, no. 5748, pp. 679–83, Oct. 2005.

[95] D. E. McNay et al., “Remodeling of the arcuate nucleus energy-balance circuit is inhibited in obese mice,” *J Clin Invest*, vol. 122, no. 1, pp. 142–152, 2012.

[96] W. V. Brown et al., “Obesity: why be concerned?,” *Am. J. Med.*, vol. 122, no. 4 Suppl 1, pp. S4–11, Apr. 2009.

[97] K. Kanasaki and D. Koya, “Biology of obesity: lessons from animal models of obesity.,” *J. Biomed. Biotechnol.*, vol. 2011, p. 197636, 2011.

[98] A. M. Ingalls et al., “Obese, a new mutation in the house mouse.,” *J. Hered.*, vol. 41, no. 12, pp. 317–8, Dec. 1950.

[99] C.-X. X. Yi et al., “High-fat-diet exposure induces IgG accumulation in hypothalamic microglia,” *Dis Model Mech*, vol. 5, no. 5, pp. 686–90, Sep. 2012.

[100] F. L. Heppner et al., “Experimental autoimmune encephalomyelitis repressed by microglial paralysis,” *Nat Med*, vol. 11, no. 2, pp. 146–152, 2005.

[101] N. H. Varvel et al., “Microglial repopulation model reveals a robust homeostatic process for replacing CNS myeloid cells.,” *Proc. Natl. Acad. Sci. U. S. A.*, vol. 109, no. 44, pp. 18150–5, Oct. 2012.

[102] S. Prokop et al., “Impact of peripheral myeloid cells on amyloid- pathology in Alzheimer’s disease-like mice,” *J. Exp. Med.*, vol. 212, no. 11, pp. 1811–1818, 2015.

[103] S. A. Grathwohl et al., “Formation and maintenance of Alzheimer’s disease beta-amyloid plaques in the absence of microglia,” *Nat Neurosci*, vol. 12, no. 11, pp. 1361–1363, 2009.

[104] U. C. Schneider et al., “Microglia inflict delayed brain injury after subarachnoid hemorrhage.,” *Acta Neuropathol.*, May 2015.

[105] M. R. P. Elmore et al., “Colony-stimulating factor 1 receptor signaling is necessary for microglia viability, unmasking a microglia progenitor cell in the adult brain.,” *Neuron*, vol. 82, no. 2, pp. 380–97, Apr. 2014.

[106] M. Valdearcos et al., “Microglia dictate the impact of saturated fat consumption on hypothalamic inflammation and neuronal function.,” *Cell Rep.*, vol. 9, no. 6, pp. 2124–38, Dec. 2014.

[107] T. L. Horvath et al., “Synaptic input organization of the melanocortin system predicts diet-induced hypothalamic reactive gliosis and obesity.,” *Proc. Natl. Acad. Sci. U. S. A.*, vol. 107, no. 33, pp. 14875–80, Aug. 2010.

[108] A. J. Newton et al., “AgRP Innervation onto POMC Neurons Increases with Age and Is Accelerated with Chronic High-Fat Feeding in Male Mice,” vol. 154, no. January 2013, pp. 172–183, Nov. 2014.

[109] A. L. Birkenfeld et al., “Deletion of the mammalian INDY homolog mimics aspects of dietary restriction and protects against adiposity and insulin resistance in mice.,” *Cell Metab.*, vol. 14, no. 2, pp. 184–95, Aug. 2011.

[110] J. Vom Berg et al., “Inhibition of IL-12/IL-23 signaling reduces Alzheimer’s disease-like pathology and cognitive decline.,” *Nat. Med.*, vol. 18, no. 12, pp. 1812–9, Dec. 2012.

[111] J. H. Schefe et al., “Quantitative real-time RT-PCR data analysis: current concepts and the novel ‘gene expression’s CT difference’ formula.,” *J. Mol. Med. (Berl).*, vol. 84, no. 11, pp. 901–10, Nov. 2006.

[112] M. B. Lemus et al., “A stereological analysis of NPY, POMC, orexin, GFAP astrocyte and Iba1 microglia cell number and volume in diet-induced obese male mice,” *Endocrinology*, vol. i, no. March, pp. en.2014–1961, 2015.

[113] T. Romanatto et al., “Deletion of tumor necrosis factor-alpha receptor 1 (TNFR1) protects against diet-induced obesity by means of increased thermogenesis.,” *J. Biol. Chem.*, vol. 284, no. 52, pp. 36213–22, Dec. 2009.

[114] S. E. Hickman et al., “The microglial sensome revealed by direct RNA sequencing,” *Nat. Neurosci.*, vol. 16, no. 12, pp. 1896–1905, Dec. 2013.

[115] D. M. Norden and J. P. Godbout, “Review: microglia of the aged brain: primed to be activated and resistant to regulation.,” *Neuropathol. Appl. Neurobiol.*, vol. 39, no. 1, pp. 19–34, Feb. 2013.

[116] V. H. Perry and C. Holmes, “Microglial priming in neurodegenerative disease.,” *Nat. Rev. Neurol.*, vol. 10, no. 4, pp. 217–24, Apr. 2014.

[117] R. C. Paolicelli et al., “Synaptic pruning by microglia is necessary for normal brain development.,” *Science*, vol. 333, no. 6048, pp. 1456–8, Sep. 2011.

[118] A. S. Reed et al., “Functional role of suppressor of cytokine signaling 3 upregulation in hypothalamic leptin resistance and long-term energy homeostasis.,” *Diabetes*, vol. 59, no. 4, pp. 894–906, Apr. 2010.

[119] E. Baquedano et al., “The Absence of GH Signaling Affects the Susceptibility to High-Fat Diet-Induced Hypothalamic Inflammation in Male Mice.,” *Endocrinology*, vol. 155, no. 12, pp. 4856–67, Dec. 2014.

[120] M. A. Ajmone-Cat et al., “Microglial polarization and plasticity: evidence from organotypic hippocampal slice cultures.,” *Glia*, vol. 61, no. 10, pp. 1698–711, Oct. 2013.

[121] M. A. Ajmone-Cat et al., “Prolonged exposure of microglia to lipopolysaccharide modifies the intracellular signaling pathways and selectively promotes prostaglandin E2 synthesis,” *J. Neurochem.*, vol. 87, no. 5, pp. 1193–1203, Oct. 2003.

[122] A. Lampron et al., “Migration of bone marrow-derived cells into the central nervous system in models of neurodegeneration.,” *J. Comp. Neurol.*, vol. 521, no. 17, pp. 3863–76, Dec. 2013.

[123] L. B. Buckman et al., “Obesity induced by a high-fat diet is associated with increased immune cell entry into the central nervous system.,” *Brain. Behav. Immun.*, vol. 35, pp. 33–42, Jan. 2014.

[124] a. Mildner et al., “Distinct and Non-Redundant Roles of Microglia and Myeloid Subsets in Mouse Models of Alzheimer’s Disease,” *J. Neurosci.*, vol. 31, no. 31, pp. 11159–11171, 2011.

[125] D. J. Mahad and R. M. Ransohoff, “The role of MCP-1 (CCL2) and CCR2 in multiple sclerosis and experimental autoimmune encephalomyelitis (EAE),” *Semin. Immunol.*, vol. 15, no. 1, pp. 23–32, Feb. 2003.

[126] K. Fjeldborg et al., “Human adipose tissue macrophages are enhanced but changed to an anti-inflammatory profile in obesity.,” *J. Immunol. Res.*, vol. 2014, p. 309548, Jan. 2014.

[127] J. R. Erion et al., “Obesity elicits interleukin 1-mediated deficits in hippocampal synaptic plasticity.,” *J. Neurosci.*, vol. 34, no. 7, pp. 2618–31, Feb. 2014.

[128] G. Sonti et al., “Neuropeptide Y blocks and reverses interleukin-1 beta-induced anorexia in rats.,” *Peptides*, vol. 17, no. 3, pp. 517–20, Jan. 1996.

[129] C. R. Plata-Salamán, “Cytokine-induced anorexia. Behavioral, cellular, and molecular mechanisms.,” *Ann. N. Y. Acad. Sci.*, vol. 856, pp. 160–70, Sep. 1998.

[130] C. A. Hunter and S. A. Jones, “IL-6 as a keystone cytokine in health and disease.,” *Nat. Immunol.*, vol. 16, no. 5, pp. 448–457, Apr. 2015.

[131] R. Dantzer, “Cytokine, sickness behavior, and depression.,” *Immunol. Allergy Clin. North Am.*, vol. 29, no. 2, pp. 247–64, May 2009.

[132] N. E. Cyr et al., “Central Sirt1 regulates body weight and energy expenditure along with the POMC-derived peptide α-MSH and the processing enzyme CPE production in diet-induced obese male rats.,” *Endocrinology*, vol. 155, no. 7, pp. 2423–35, Jul. 2014.

[133] G. T. Dodd et al., “Leptin and Insulin Act on POMC Neurons to Promote the Browning of White Fat,” *Cell*, vol. 160, no. 1–2, pp. 88–104, Jan. 2015.

[134] R. Starr et al., “A family of cytokine-inducible inhibitors of signalling.,” *Nature*, vol. 387, no. 6636, pp. 917–21, Jun. 1997.

[135] J. L. Sarvas et al., “The IL-6 Paradox: Context Dependent Interplay of SOCS3 and AMPK.,” *J. Diabetes Metab.*, vol. Suppl 13, 2013.

[136] H. Qin et al., “SOCS3 deficiency promotes M1 macrophage polarization and inflammation.,” *J. Immunol.*, vol. 189, no. 7, pp. 3439–3448, 2012.

[137] B. J. Baker et al., “SOCS1 and SOCS3 in the control of CNS immunity,” *Trends Immunol.*, vol. 30, no. 8, pp. 392–400, 2009.

[138] J. K. Howard and J. S. Flier, “Attenuation of leptin and insulin signaling by SOCS proteins,” *Trends Endocrinol. Metab.*, vol. 17, no. 9, pp. 365–371, 2006.

[139] K. Biber et al., “Neuronal ‘On’ and ‘Off’ signals control microglia.,” *Trends Neurosci.*, vol. 30, no. 11, pp. 596–602, Nov. 2007.

[140] H. Neumann, “Control of glial immune function by neurons.,” *Glia*, vol. 36, no. 2, pp. 191–9, Nov. 2001.

[141] J. M. Scarlett et al., “Regulation of central melanocortin signaling by interleukin-1 beta.,” *Endocrinology*, vol. 148, no. 9, pp. 4217–25, Sep. 2007.

[142] T. Fromme and M. Klingenspor, “Uncoupling protein 1 expression and high-fat diets.,” *Am. J. Physiol. Regul. Integr. Comp. Physiol.*, vol. 300, no. 1, pp. R1–8, Jan. 2011.

[143] J. Nedergaard and B. Cannon, “The Browning of White Adipose Tissue: Some Burning Issues,” *Cell Metab.*, vol. 20, no. 3, pp. 396–407, Aug. 2014.

[144] B. M. Spiegelman and J. S. Flier, “Obesity and the Regulation of Energy Balance,” *Cell*, vol. 104, no. 4, pp. 531–543, Feb. 2001.

[145] P. Boström et al., “A PGC1-α-dependent myokine that drives brown-fat-like development of white fat and thermogenesis.,” *Nature*, vol. 481, no. 7382, pp. 463–8, Jan. 2012.

[146] F. M. Fisher et al., “FGF21 regulates PGC-1α and browning of white adipose tissues in adaptive thermogenesis.,” *Genes Dev.*, vol. 26, no. 3, pp. 271–81, Feb. 2012.

[147] J. S. Flier, “Obesity wars: molecular progress confronts an expanding epidemic,” *Cell*, vol. 116, no. 2, pp. 337–350, 2004.

[148] G. Gastaldi et al., “Upregulation of peroxisome proliferator-activated receptor gamma coactivator gene (PGC1A) during weight loss is related to insulin sensitivity but not to energy expenditure,” *Diabetologia*, vol. 50, no. 11, pp. 2348–2355, 2007.

[149] M. E. Gove et al., “Generation of leptin receptor bone marrow chimeras: recovery from irradiation, immune cellularity, cytokine expression, and metabolic parameters.,” *Obesity (Silver Spring).*, vol. 18, no. 12, pp. 2274–81, Dec. 2010.

[150] R. Duran-Struuck and R. C. Dysko, “Principles of bone marrow transplantation (BMT): providing optimal veterinary and husbandry care to irradiated mice in BMT studies.,” *J. Am. Assoc. Lab. Anim. Sci.*, vol. 48, no. 1, pp. 11–22, Jan. 2009.

[151] V. Ablamunits et al., “Reduced adiposity in ob/ob mice following total body irradiation and bone marrow transplantation.,” *Obesity (Silver Spring).*, vol. 15, no. 6, pp. 1419–29, Jun. 2007.

[152] M. G. Myers et al., “Mechanisms of leptin action and leptin resistance.,” *Annu. Rev. Physiol.*, vol. 70, pp. 537–56, Jan. 2008.

[153] P. Oliver et al., “The intake of a high-fat diet triggers higher brown adipose tissue UCP1 levels in male rats but not in females.,” *Genes Nutr.*, vol. 2, no. 1, pp. 125–6, Oct. 2007.

[154] L. H. Storlien et al., “Fat feeding causes widespread in vivo insulin resistance, decreased energy expenditure, and obesity in rats.,” *Am. J. Physiol.*, vol. 251, no. 5 Pt 1, pp. E576–83, Nov. 1986.

[155] Z. Liu et al., “Neonatal overnutrition in mice exacerbates high-fat diet-induced metabolic perturbations.,” *J. Endocrinol.*, vol. 219, no. 2, pp. 131–43, Nov. 2013.

[156] B. D. Kayser et al., “Perinatal overnutrition exacerbates adipose tissue inflammation caused by high-fat feeding in C57BL/6J mice.,” *PLoS One*, vol. 10, no. 3, p. e0121954, Jan. 2015.

[157] P. R. Nagareddy et al., “Adipose tissue macrophages promote myelopoiesis and monocytosis in obesity.,” *Cell Metab.*, vol. 19, no. 5, pp. 821–35, May 2014.

[158] S. U. Amano et al., “Local proliferation of macrophages contributes to obesity-associated adipose tissue inflammation.,” *Cell Metab.*, vol. 19, no. 1, pp. 162–71, Jan. 2014.

9 Eidesstattliche Versicherung

„Ich, Caroline Baufeld, versichere an Eides statt durch meine eigenhändige Unterschrift, dass ich die vorgelegte Dissertation mit dem Thema: „Characterization of the nature and consequence of the microglia response to high fat diet“ selbstständig und ohne nicht offengelegte Hilfe Dritter verfasst und keine anderen als die angegebenen Quellen und Hilfsmittel genutzt habe.
Alle Stellen, die wörtlich oder dem Sinne nach auf Publikationen oder Vorträgen anderer Autoren beruhen, sind als solche in korrekter Zitierung (siehe „Uniform Requirements for Manuscripts (URM)“ des ICMJE -*www.**icmje**.org*) kenntlich gemacht. Die Abschnitte zu Methodik (insbesondere praktische Arbeiten, Laborbestimmungen, statistische Aufarbeitung) und Resultaten (insbesondere Abbildungen, Graphiken und Tabellen) entsprechen den URM (s.o) und werden von mir verantwortet.
Meine Anteile an etwaigen Publikationen zu dieser Dissertation entsprechen denen, die in der untenstehenden gemeinsamen Erklärung mit dem/der Betreuer/in, angegeben sind. Sämtliche Publikationen, die aus dieser Dissertation hervorgegangen sind und bei denen ich Autor bin, entsprechen den URM (s.o) und werden von mir verantwortet.

Die Bedeutung dieser eidesstattlichen Versicherung und die strafrechtlichen Folgen einer unwahren eidesstattlichen Versicherung (§156,161 des Strafgesetzbuches) sind mir bekannt und bewusst.“

Datum Unterschrift

10 Curriculum Vitae

Mein Lebenslauf wird aus datenschutzrechtlichen Gründen in der elektronischen Version meiner Arbeit nicht veröffentlicht.

11 Publications

Baufeld, C., Miller, K.R., Heppner, F.L. “High fat diet-induced brain region-specific phenotypic spectrum of CNS resident microglia” Manuscript in preparation.

Miller, K.R., **Baufeld, C**. et al. “Microglia regulate adult-born neuroblast development and survival” Manuscript in preparation.

Schweiger, D., **Baufeld, C.**, Drescher, P., Oltrogge, B., Höpfner, S., Mess, A., Lüttke, J., Rippke, F., Filbry, A., Max, H. “Efficacy of a new tonic containing urea, lactate, polidocanol, and glycyrrhiza inflata root extract in the treatment of a dry, itchy, and subclinically inflamed scalp.” Skin Pharmacol Physiol. 2013; 26(2):108-18

12 Acknowledgements

At this point I want to thank a group of people, without whom the realization of this thesis would not have been possible.

First of all, I want to thank Prof. Heppner for giving me the opportunity to pursue my PhD in his institute. Thank you for your guidance and support.

A very special and sincere thank you to Kelly Miller for not just being a supervisor, but a friend who shared and encouraged my scientific passion and enthusiasm.

I want to thank all the members of the department for neuropathology; especially the doctors for their help with the collection of the human tissue and the diagnostic technicians as well as the lab technicians for their help and assistance whenever problems or questions came up.

I also thank the colleagues of the department for endocrinology, diabetes and nutrition and the center of cardiovascular research, who made it possible for me to use the metabolic cages and the body composition NMR, who answered my topic-related questions and helped me with every issue that came up.

Without Lisa, Natalia, Juliane and Claudia the time would not have been anywhere near as good.

Last, but not least, I want to thank my family for their unconditional support and my boyfriend for being able to tolerate a scientist's 'life style'.